New directions in seismology - **numerical earthquake dynamic rupture modelling**

Alice-Agnes Gabriel

Lecture, WS 21/22, LMU Munich

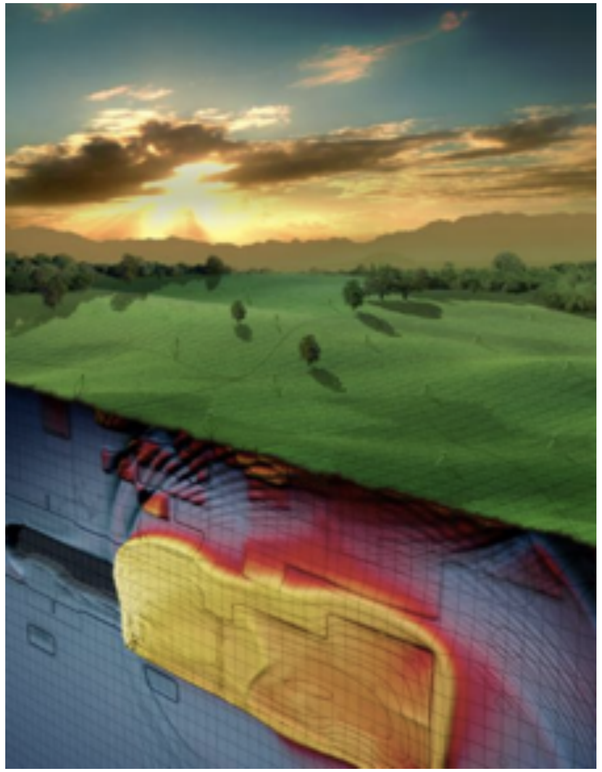

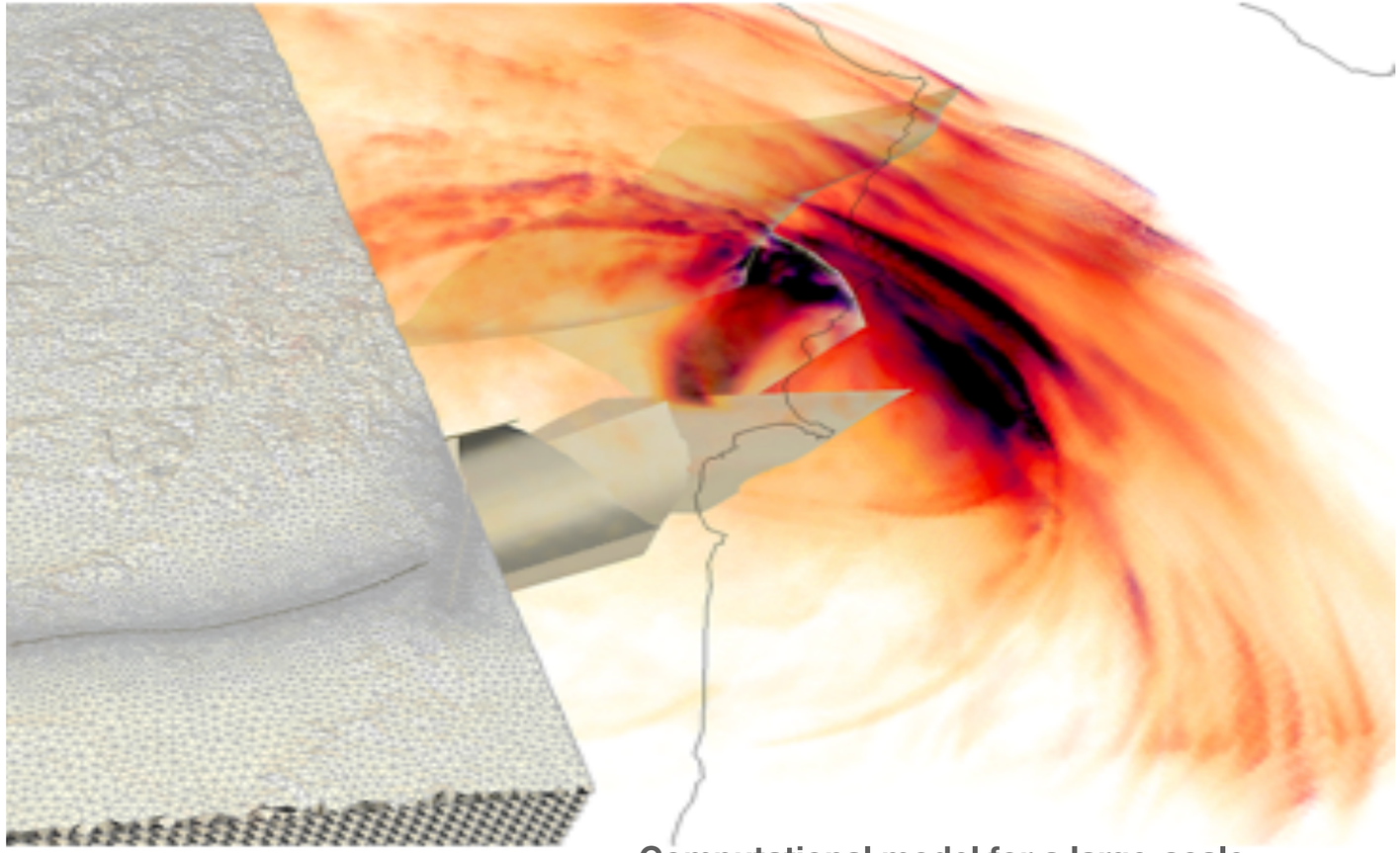

Computational model for a large-scale scenario of the 2016 Kaikoura, New Zealand earthquake (Ulrich et al., Nat. Comm., 2018)

Earthquake seismology

Recent well-recorded earthquakes and laboratory experiments reveal **striking variability**

- Slip reactivation
- Nucleation with/without slow-slip pre-cursors
- Variability of rupture style (pulses vs cracks)
- Rupture cascading and “jumping”
- Propagation along both locked and creeping fault sections during the same earthquake
- Supershear propagation

Source inversion model of Tohoku-Oki event (Japan) 2011, from combined local ground motion, teleseismics, GPS & multiple time window parametrization of slip rate. (Lee & Wang, 2011)

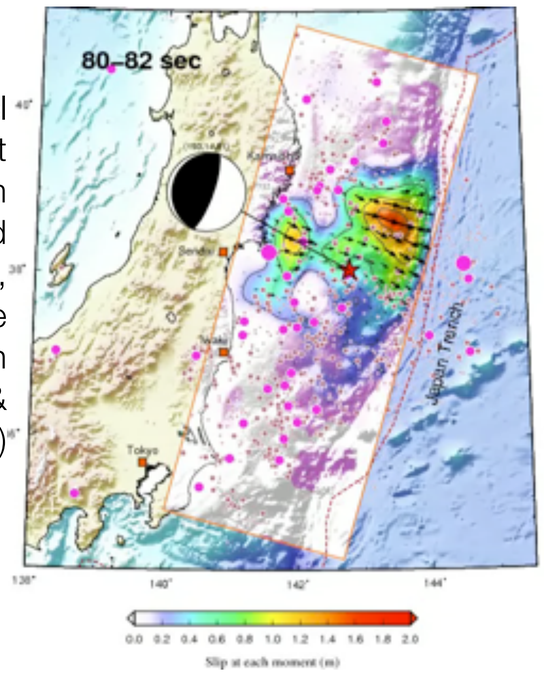

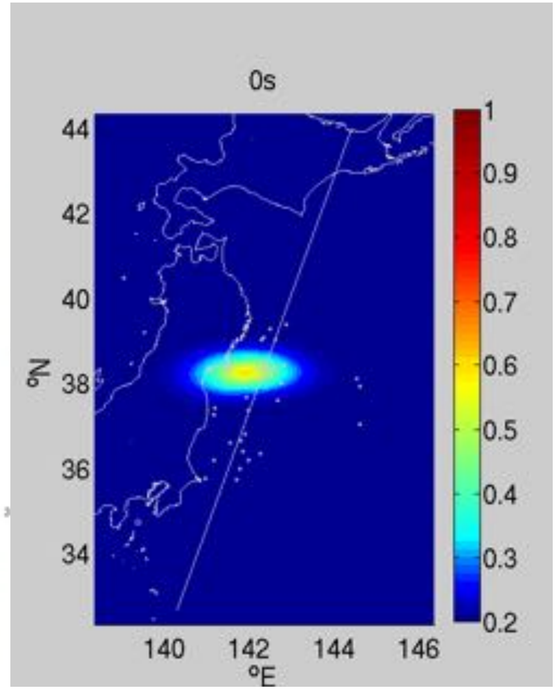

Back projection: Indicating major areas of high-frequency radiation on the fault (Meng et al., 2012)

“The most useful thing seismologists could do – understand (predict) earthquakes - is what they are least able to”
(P. Shearer)

Sub-Rayleigh vs **supershear** rupture in the laboratory. Mach cone emanating from rupture tip (courtesy of L. Bruhat)

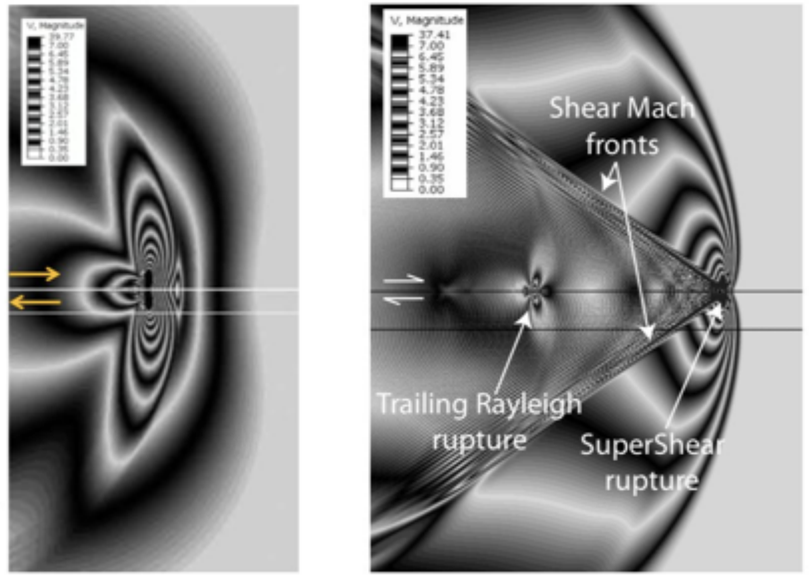

Earthquake seismology

- **increasingly data-rich** (machine-learning enhanced seismic catalogues, space geodesy, seismic arrays, Distributed Acoustic Sensing)

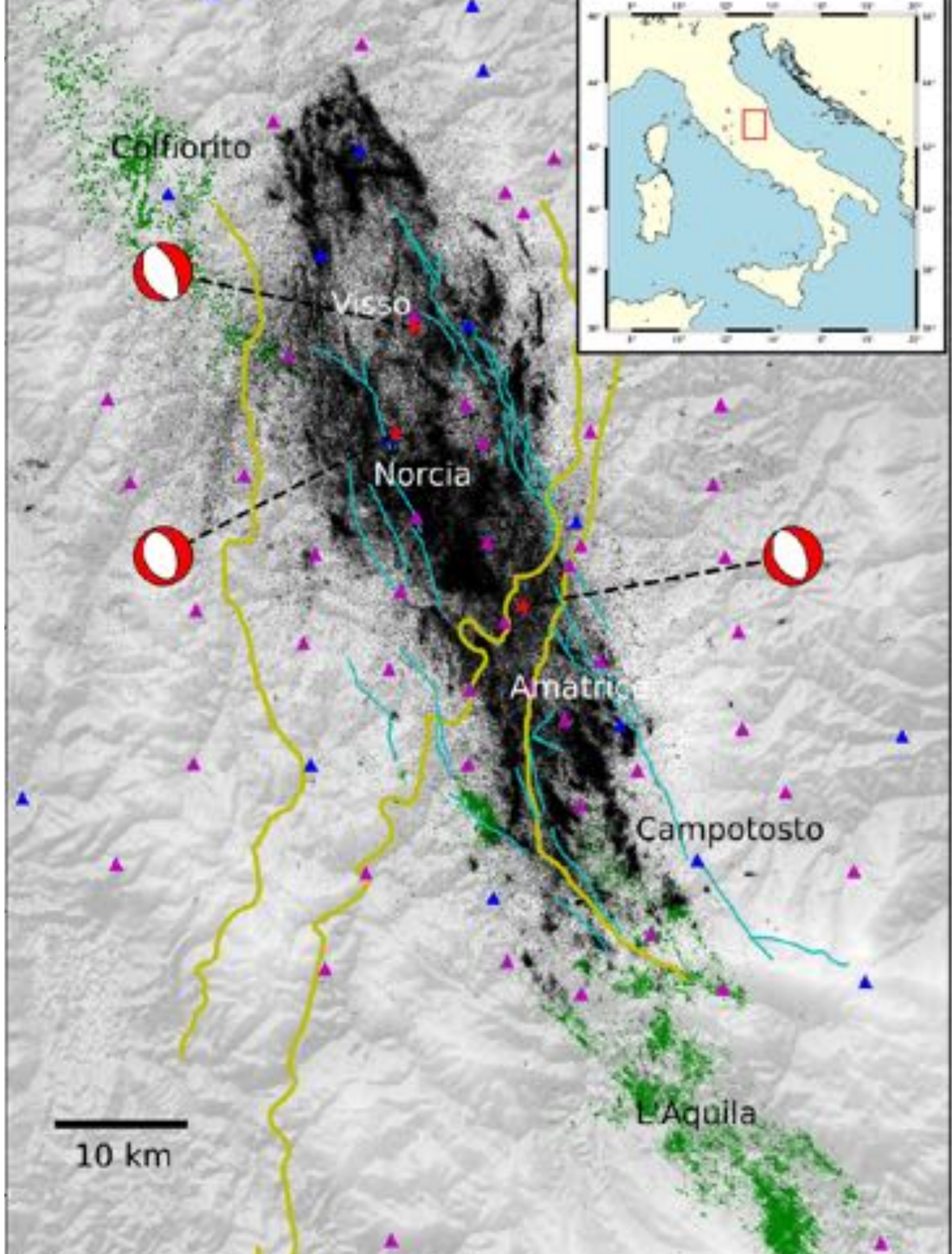

Machine-Learning-Based High-Resolution Earthquake Catalog Reveals How Complex Fault Structures Were Activated during the 2016–2017 Central Italy Sequence. Tan et al., TSR, 2021

Earthquake seismology

- **increasingly data-rich** (machine-learning enhanced seismic catalogues, space geodesy, seismic arrays, Distributed Acoustic Sensing)

- **data-driven imaging methods hint on complex earthquake dynamics**

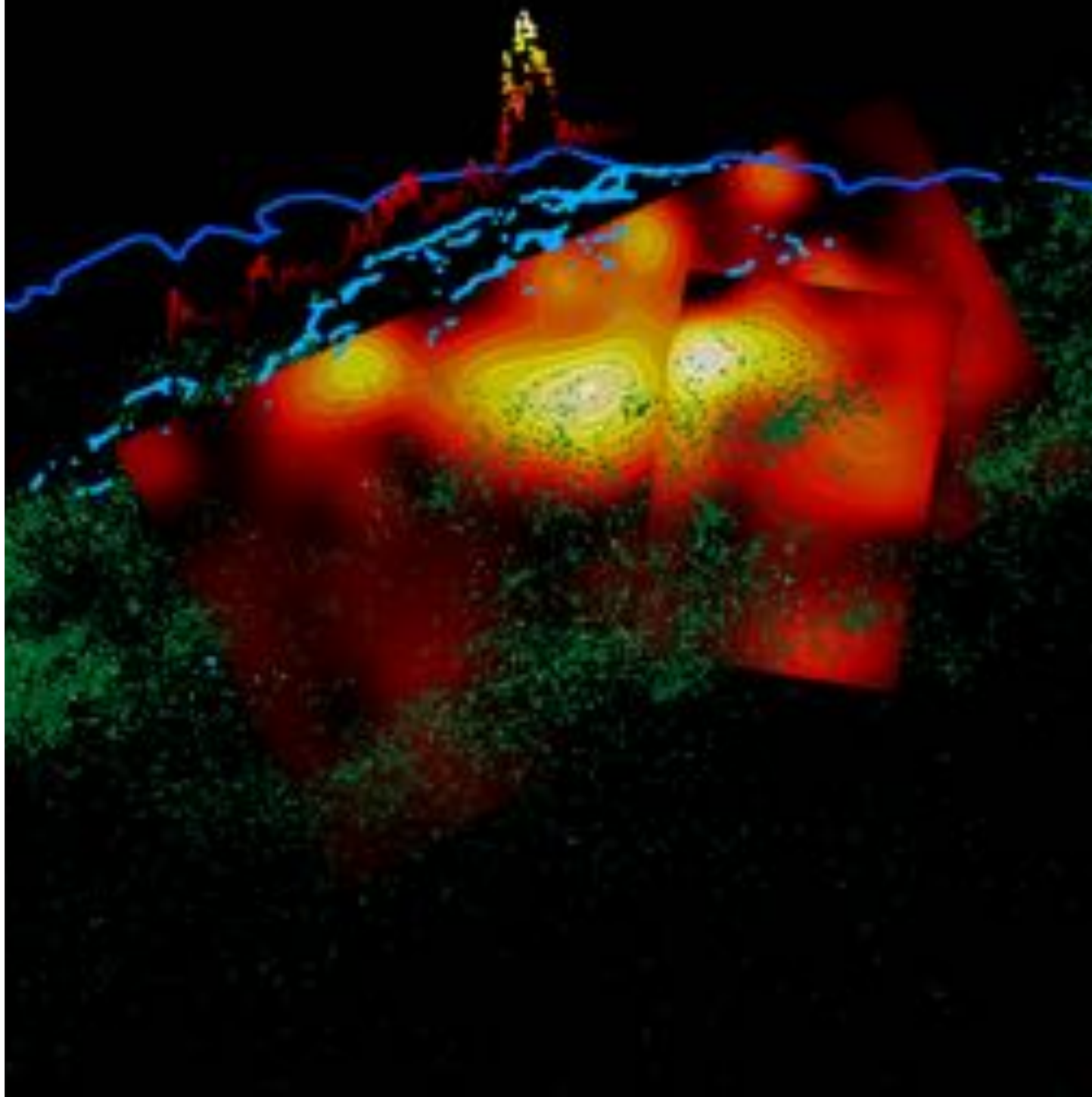

Kinematic source inversion of the 2016 M6.5 Norcia earthquake, suggesting that two fault planes slipped simultaneously, Scognamiglio et al., 2018

Earthquake seismology

- **increasingly data-rich** (machine-learning enhanced seismic catalogues, space geodesy, seismic arrays, Distributed Acoustic Sensing)

- **data-driven imaging methods hint on complex earthquake dynamics**

- integrated synergistically with **multi-physics forward modeling empowered by high-performance computing**

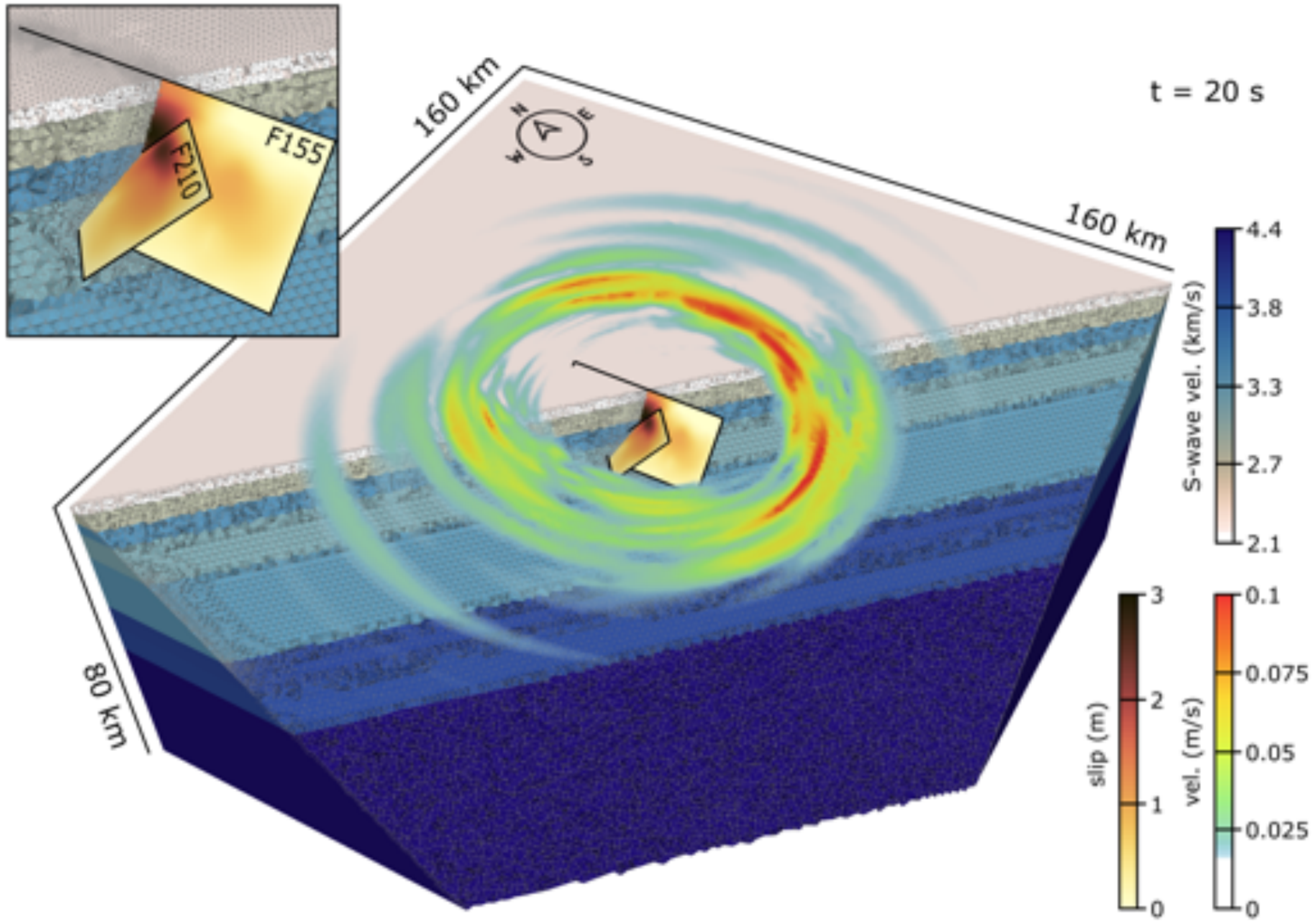

Dynamic rupture simulation probing the mechanical viability of Scognamiglio et al 2018's kinematic model.
Tinti et al., preprint https://eartharxiv.org/repository/view/2441/

Computational earthquake seismology

- **Physics-based:** solving for spontaneous dynamic earthquake rupture as non-linear interaction of frictional failure and seismic wave propagation

- **Earthquakes:** frictional shear failure of brittle solids under compression along preexisting weak interfaces

- "**Bootstrapping**": on methods originally not developed for earthquake source modelling

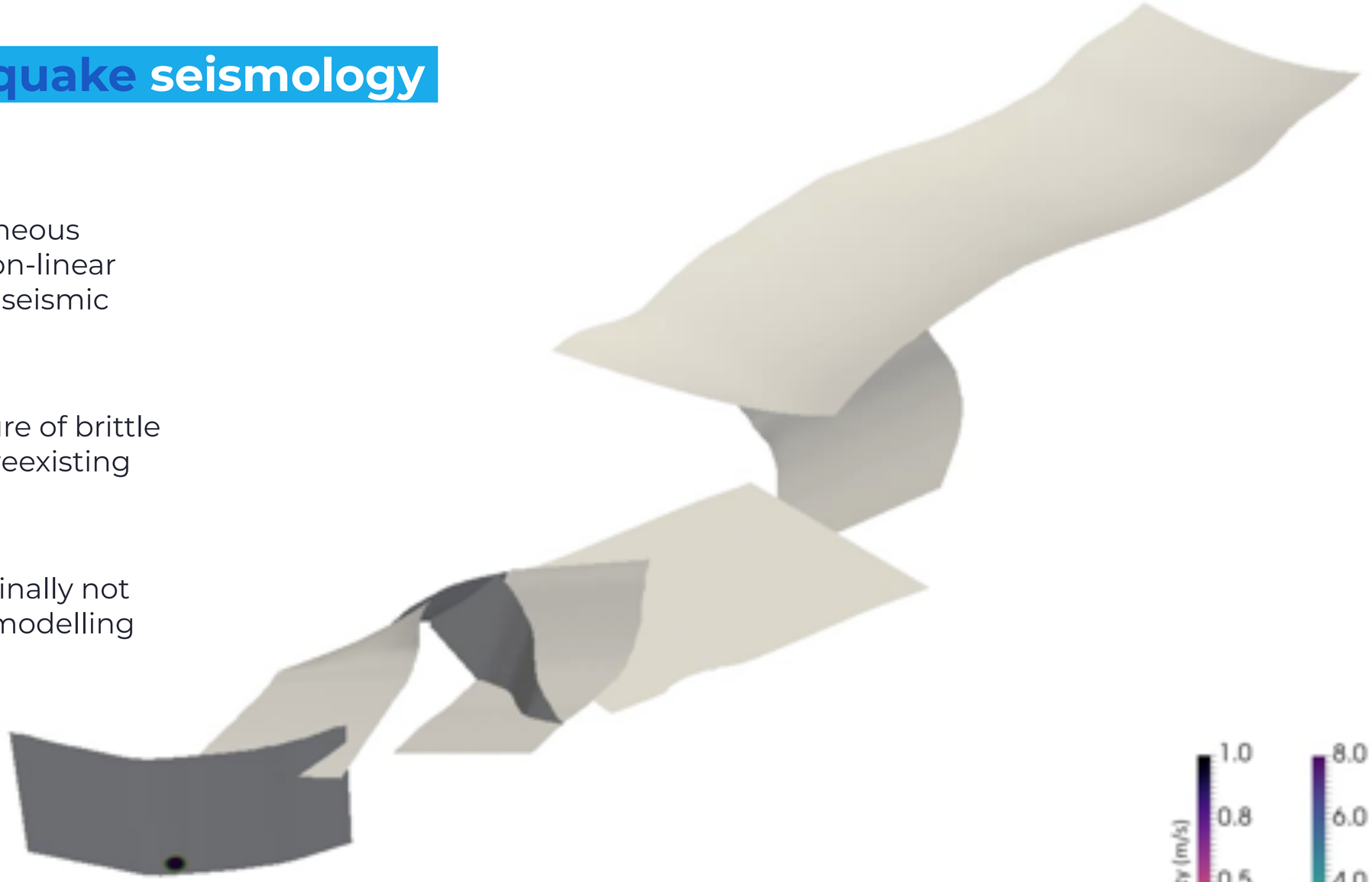

Observationally constrained 3D dynamic rupture scenario of the 2016, Kaikōura Earthquake (Ulrich et al., 2019, Nat. Comm.)

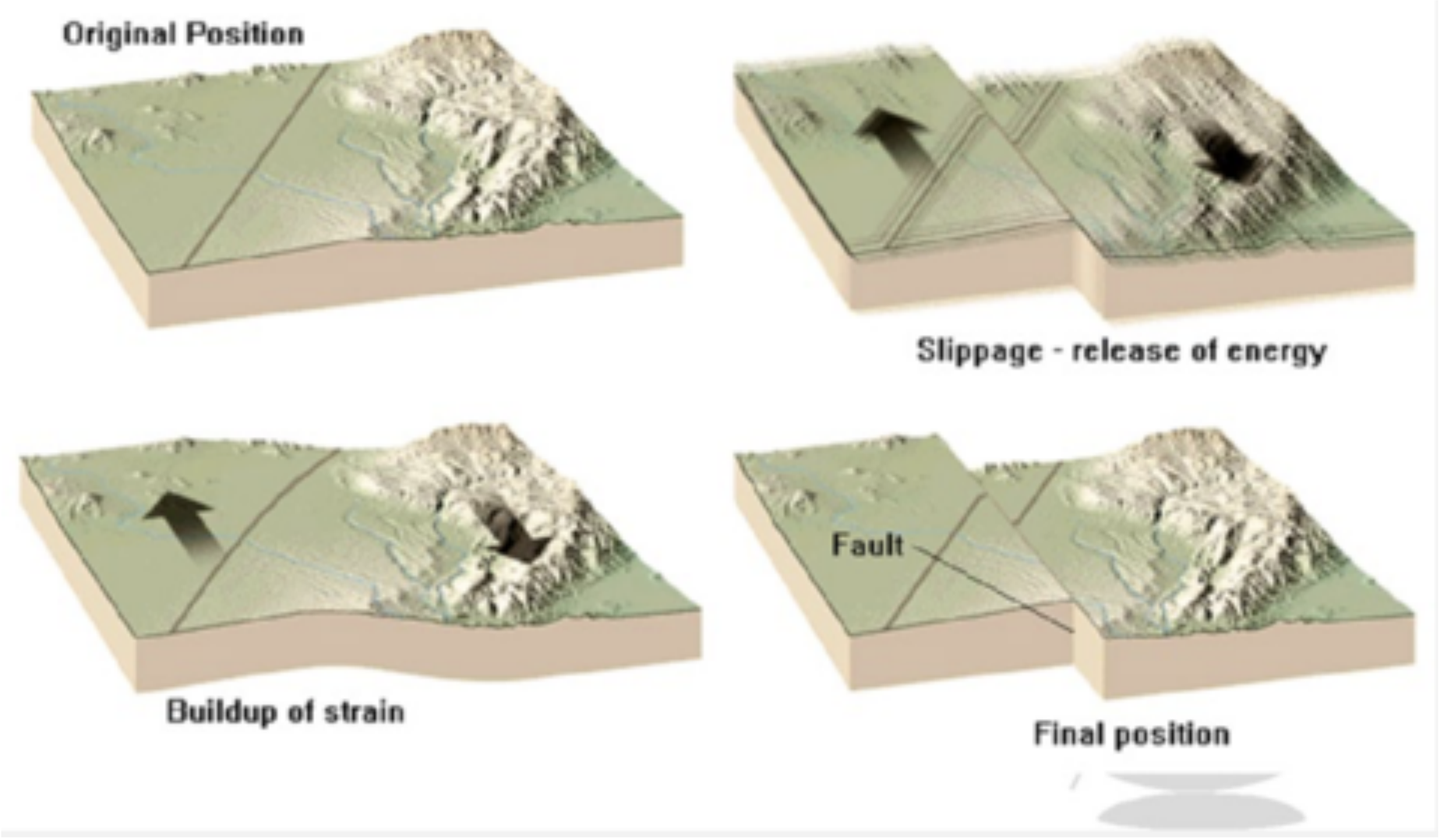
Original Position
Slippage - release of energy
Buildup of strain
Fault
Final position

Seismo-tectonic simulations: current capabilities

physical time

	Dynamic simulation	Kinematic simulation	Dynamic boundary integral method	Quasi-dynamic integral method	Short-term tectonics, fully numerical	Long-term tectonics, fully numerical
Dimension	3D	3D	2D/3D	2D/3D	2D	2D
Rupture	Spontaneous	Prescribed	Spontaneous	Spontaneous	Spontaneous	Spontaneous
Inertia	Yes	Yes	Yes	Radiation damping	Yes	Limited
Seismic cycle	Single	Single	Multiple	Multiple	Multiple	Simplified
Fault morphology	Complex	Complex	Planar	Fault network	Planar	Complex and emergent
Distributed deformation	Limited	Limited	None	Viscoelastic	Viscoplastic	Viscoplastic
Material heterogeneity	Fine-grain	Fine-grain	None	Simplest cases	Fine-grain	Fine-grain
Fault evolution	None	None	None	None	Allowed	Emergent
Fluid effects	Thermal Press.	None	Poroelastic	Poroelastic	Poroelastic	Poroelastic & metamorphism
Large strain	None	None	None	None	None	Yes

THE SPECTRUM OF FAULT SLIP BEHAVIORS

Discrete & Fast: m/s

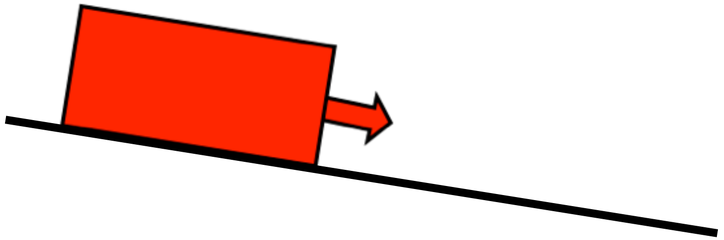

Continuous & Slow: cm/yr

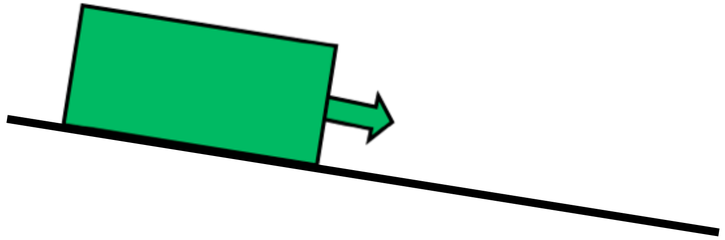

Seismic: earthquake

The *Anime Sante* church (1713)
after the M_W = 6.3 L'Aquila earthquake (2009)

Aseismic: fault creep

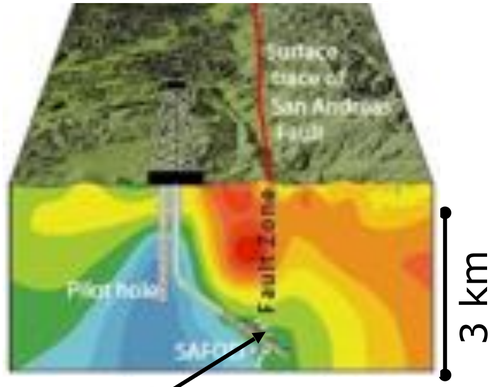

Borehole casing deformation along the San Andreas

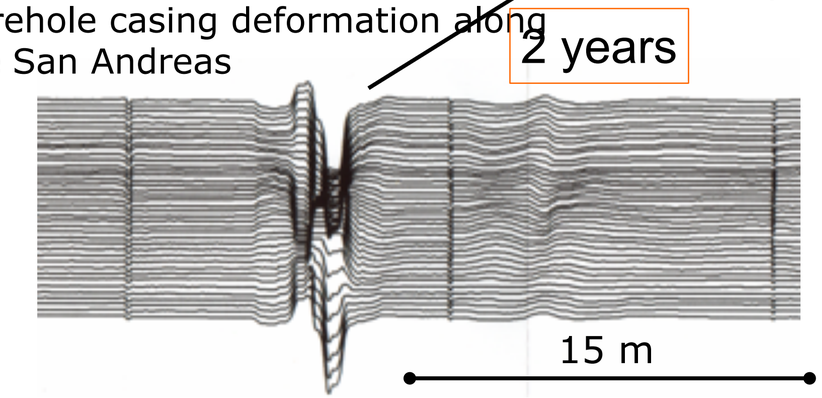

After Collettini, 2010

THE SPECTRUM OF FAULT SLIP BEHAVIORS

Tremor, Slow Slip, Swarms, Low frequency earthquakes, Creep, Geodetic transients, Dynamic triggering, Postseismic slip

Stick Slip vs. Stable Sliding

THE SPECTRUM OF FAULT SLIP BEHAVIORS

Tremor, Slow Slip, Swarms, Low frequency earthquakes, Creep, Geodetic transients, Dynamic triggering, Postseismic slip

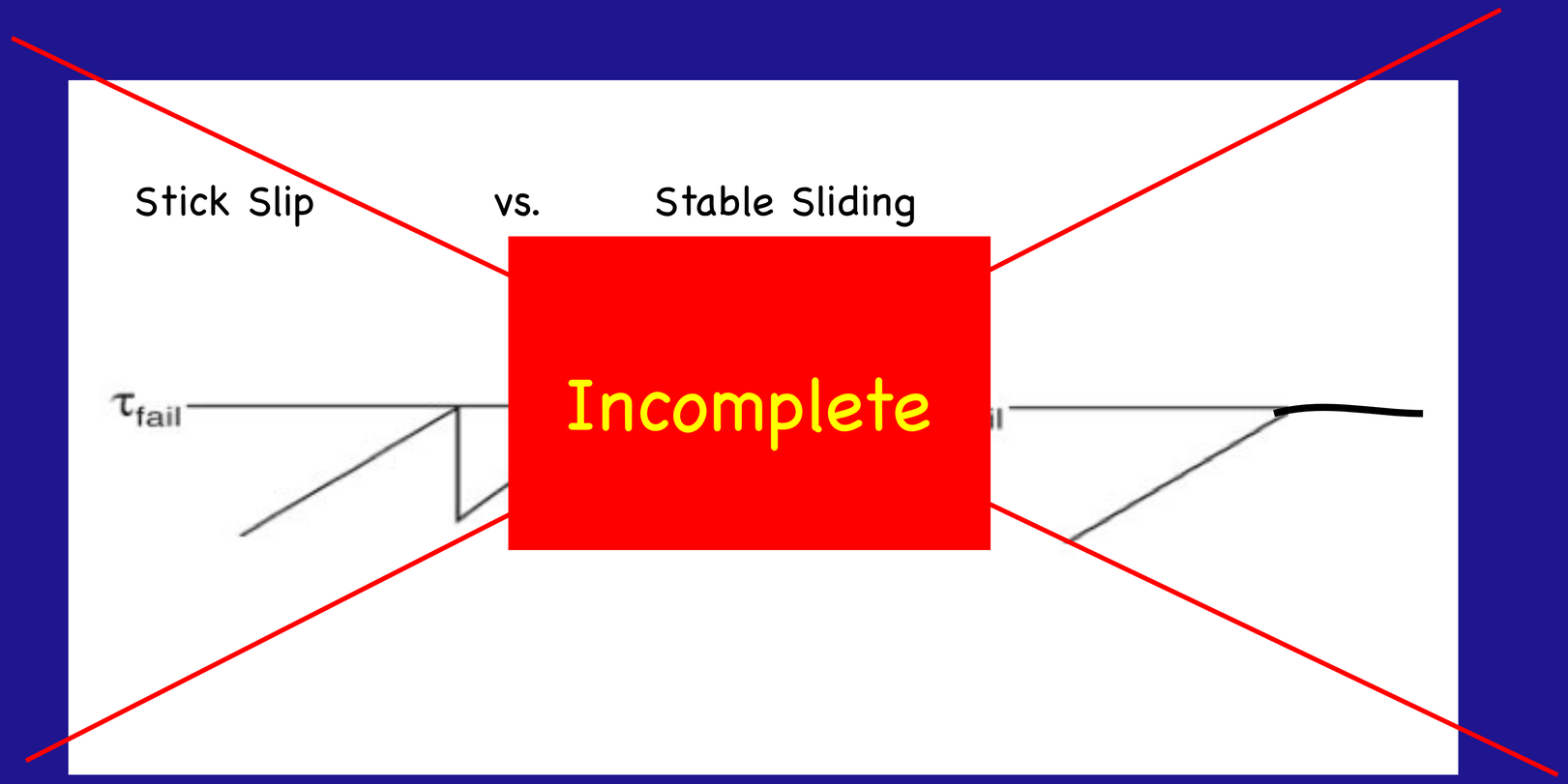

Fault Mechanics & Earthquake Physics

- Aseismic slip
- Creep events
- Strain transients
- Slow earthquakes
- Episodic tremor
- Silent earthquakes
- Afterslip and transient postseismic deformation
- Slow precursors to “normal” earthquak
- Earthquakes with a distinct nucleation phase
- Normal (fast) earthquakes
- Earthquakes with supersonic rupture velocity

Seismic slip and aseismic faulting
are **end members**
of a
continuous spectrum
of behaviors

A single fault, and perhaps even a single fault patch, may exhibit both seismic and aseismic slip

Earthquake source physics

? **Which physics ? On which scale ? Relevance ? Cost ?**

Kinematics

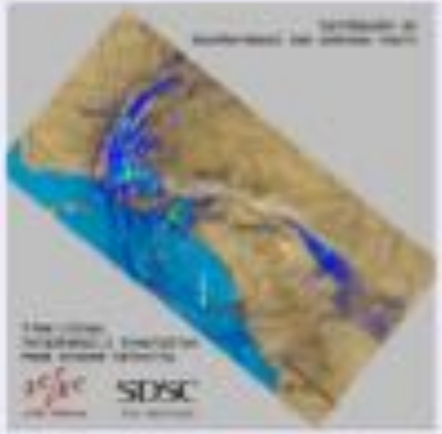

Wave propagation, velocity structure, prescribed sources

Dynamics

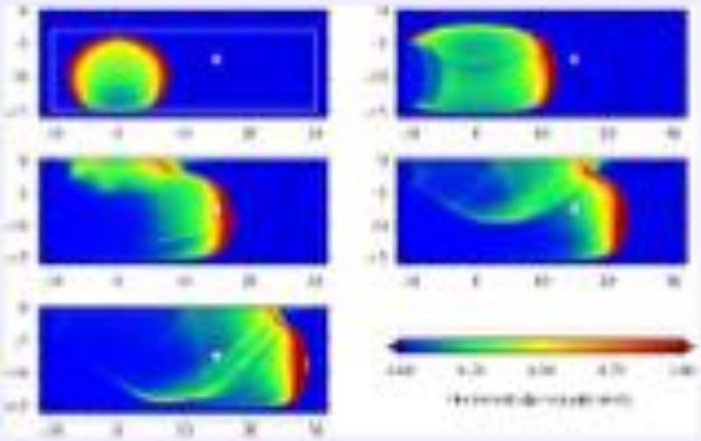

Friction law, non-linearities, initial conditions

Molecular Dynamics

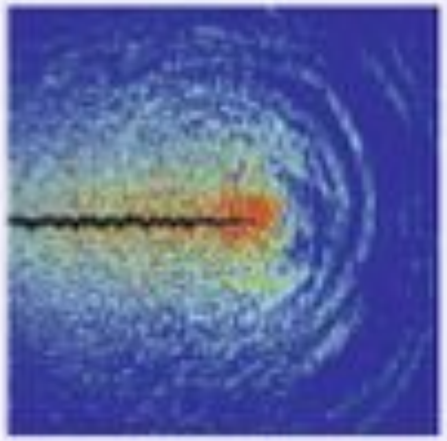

Atomic forces,electronic forces, quantum mechanics

Natural fault zones

What is a fault?

→ A fault zone may be several hundreds of meters wide, with a very thin internal zone/plane of deformation, surrounded by a different rock units at different stages of deformation, different rock/mineral content and different degree of fracturing

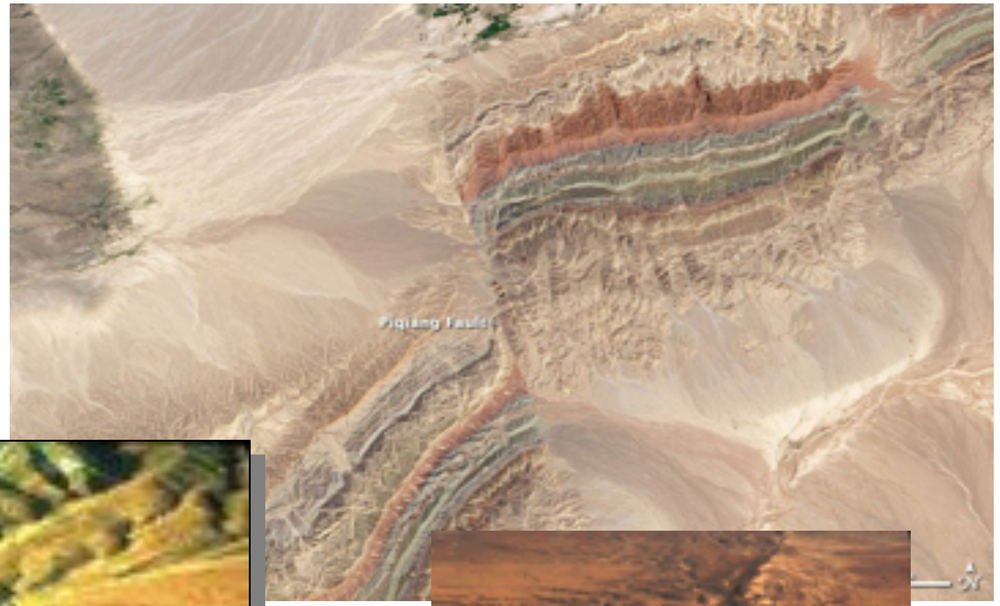

Natural fault zones

What is a fault **zone**?

→ **zone of weakness along which previous earthquakes have occurred**

→ **zone of complex deformation surrounding a thin fault plane**

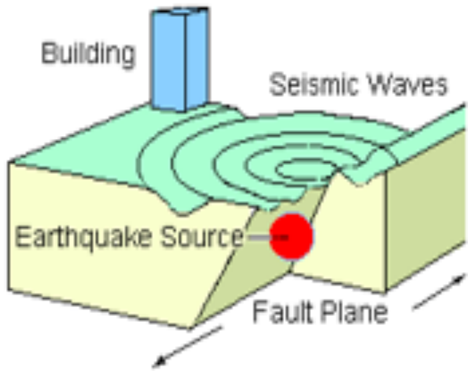

SCEC Community Fault Model

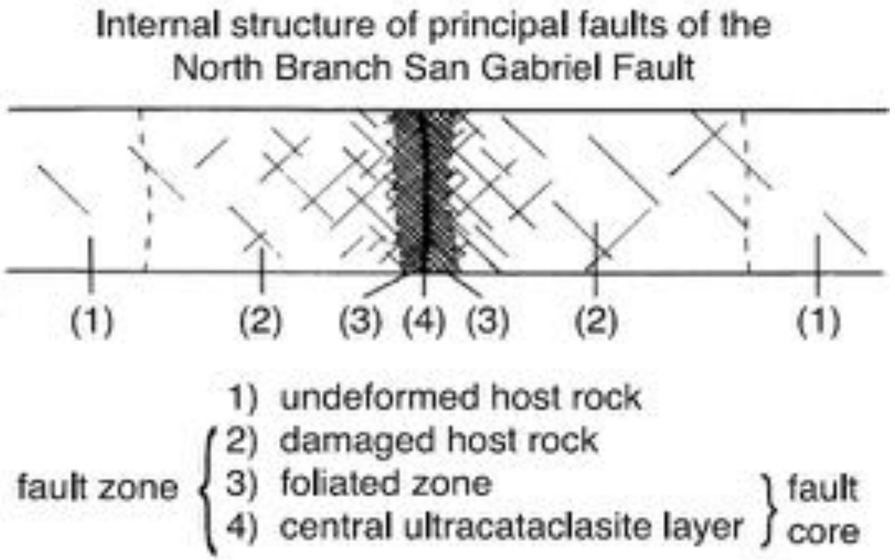

Chester et al. 1998

Natural fault zones

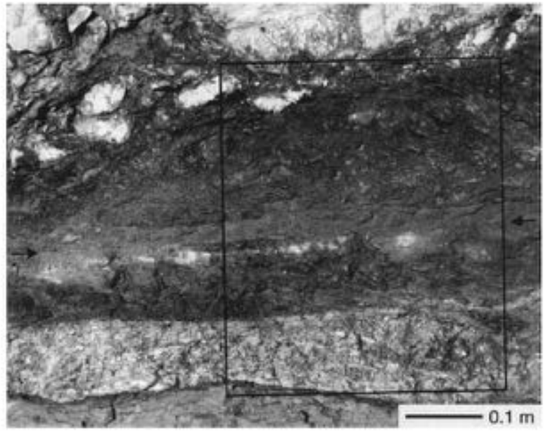

Figure 2. Ultracataclasite zone with the prominent slip surface (marked by the black arrow) along the Punchbowl fault.

Chester&Chester, 1998

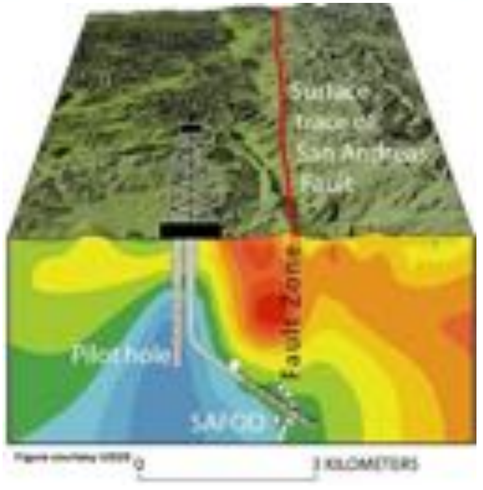

SAFOD drilling project

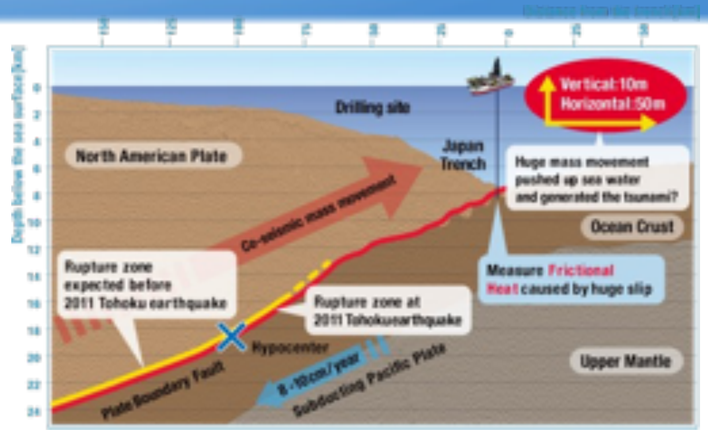

JAMSTEC Drilling Project: Single major plate-boundary (less than 5 meters) of pelagic clay

- ***Geological and borehole studies***

Characterization of natural fault zones as ultracataclastic, gougerich, and possibly clayey zone surrounded by a cataclastic damage zone; plus potential presence of gel, decarbonation products, nanopowders, melts, fluids

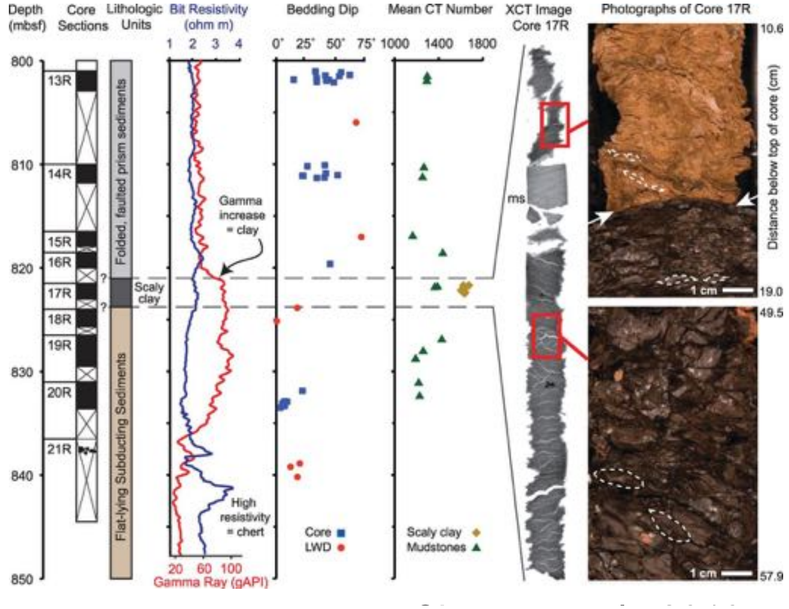

Geometrical complexity of fault zones

- Faults are only **idealized** as planes, or a collection of planar surfaces. Detailed geological mapping reveals that fault traces exhibit geometrical complexities at all scales

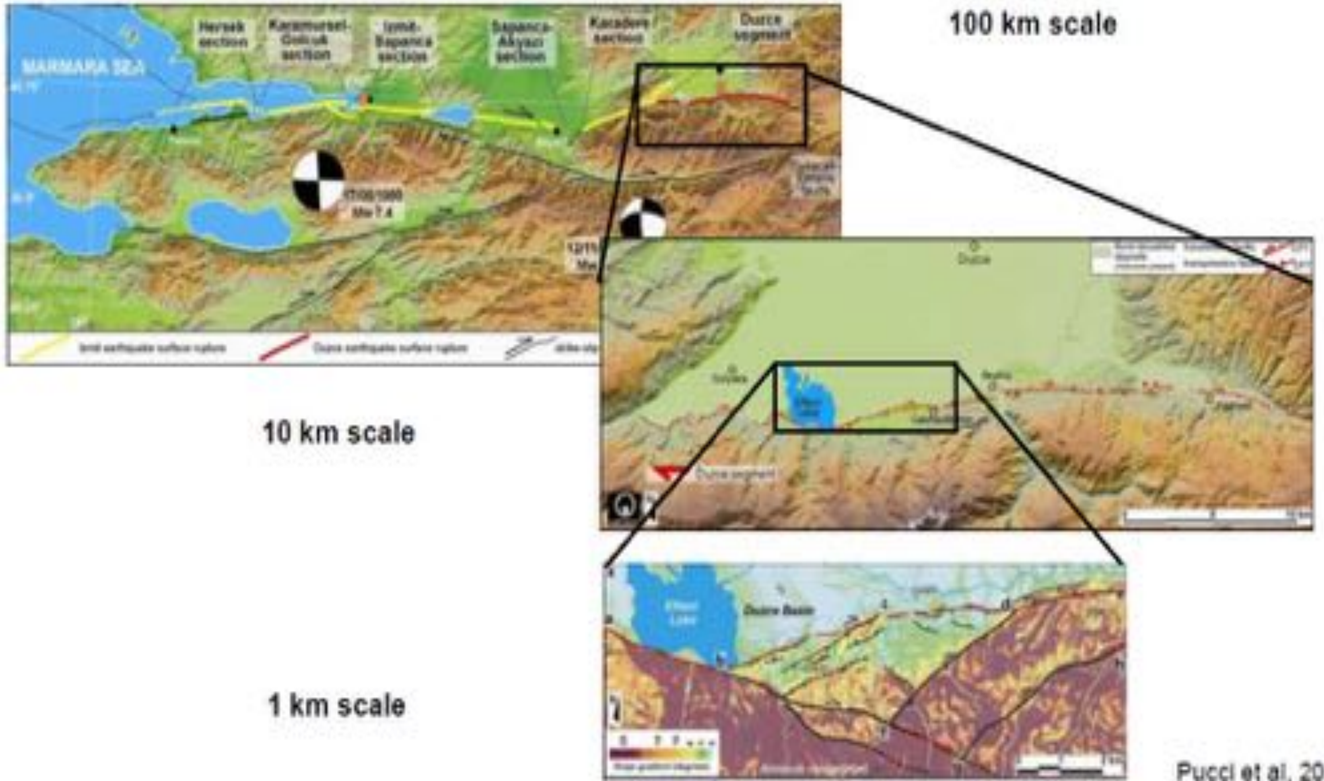

Pucci et al. 2006

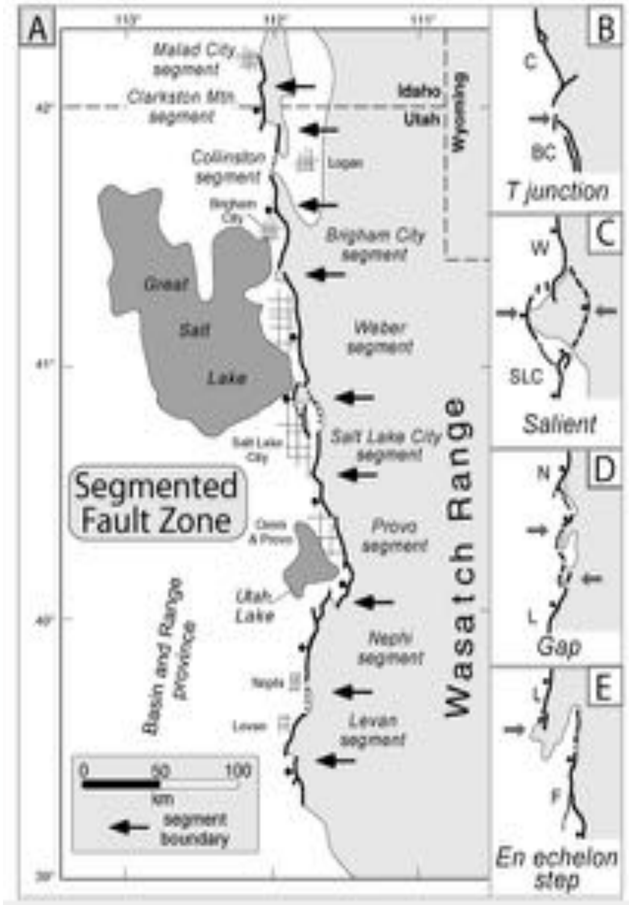

Segmentation of range-front faults

Geometrical complexity of fault zones

- Faults are only **idealized** as planes, or a collection of planar surfaces. Detailed geological mapping reveals that fault traces exhibit geometrical complexities at all scales

- Fault complexity as mapped on the surface shows irregularities at all scales. The structure of fault networks has been quantified in terms of fractals.

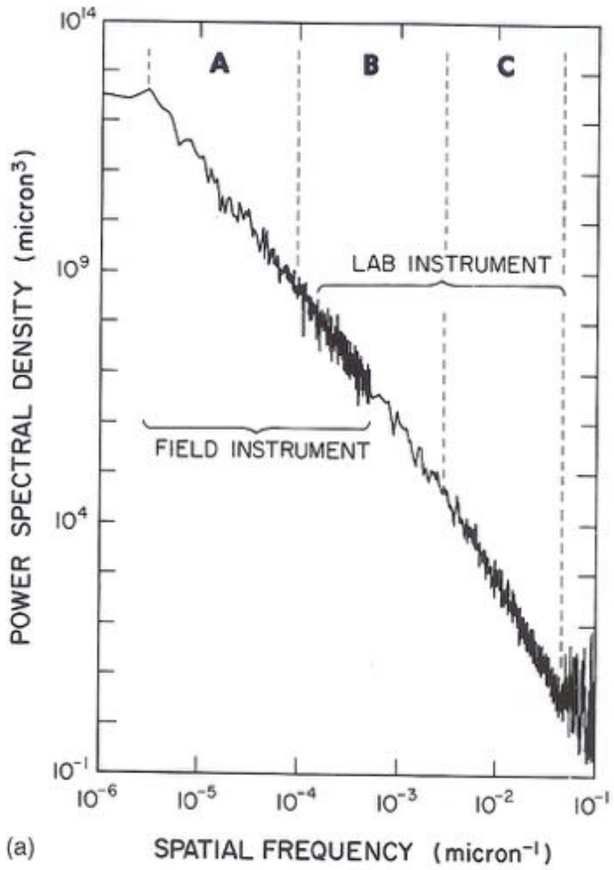

Fig. 2.3. Power spectra of the topography of rock surfaces: (a) spectrum from 1 m to 10 mm of a natural joint surface; (b) spectra (1 cm to 10 mm) of ground surfaces of various roughnesses. (After Brown and Scholz, 1985b.) In (a) the fractal dimension, proportional to the slope of the curve, is found to be different over different scale ranges, denoted A, B, and C. In (b) the corner in the spectra is a result of grinding and occurs approximately at the dimension of the grit size of the grinding wheel.

Rock friction

What is an earthquake ?

→ Frictional failure of brittle solids under compression

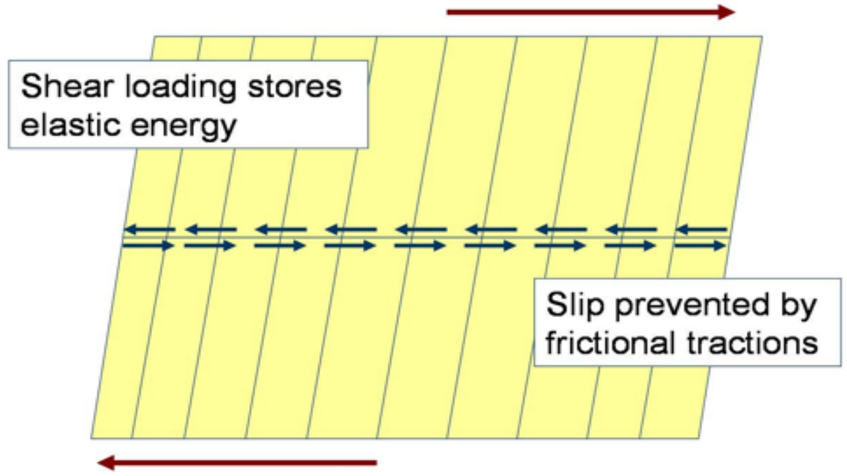

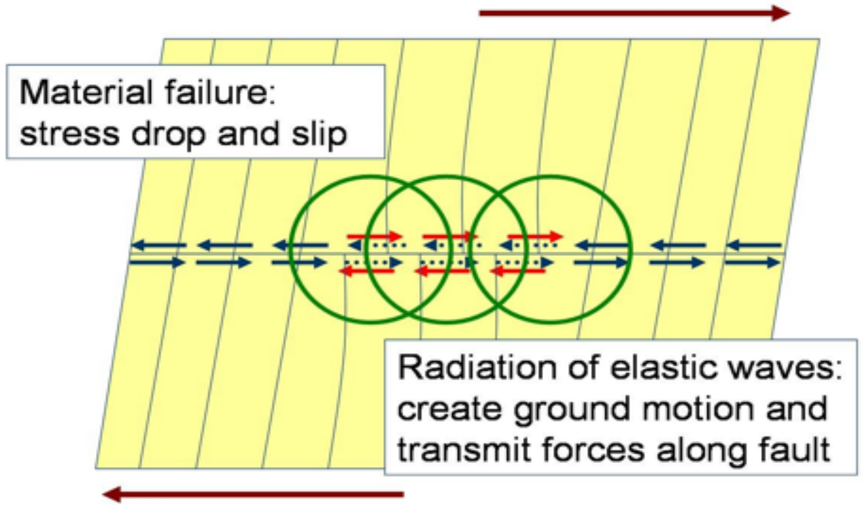

Rock friction

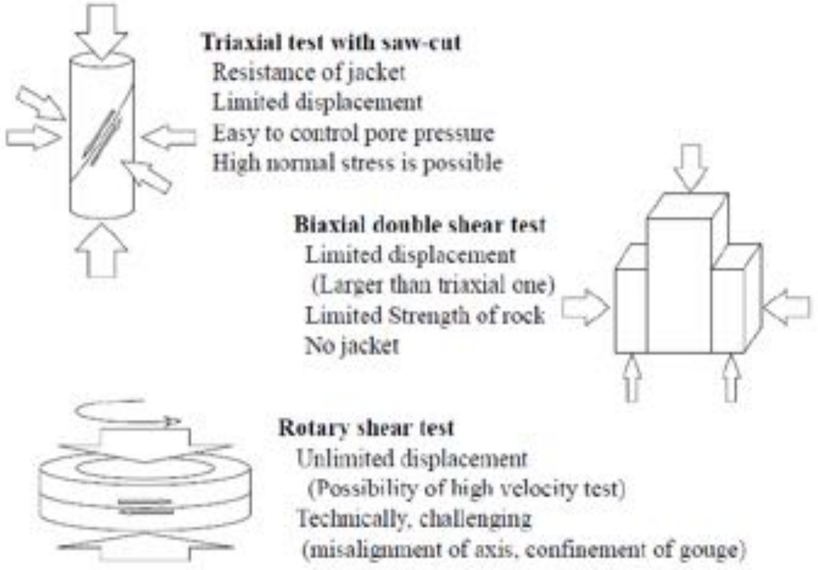

Laboratory setups for rock friction analysis

DiToro et al.

→ How and when does rock break?

- ***Laboratory experiments***

  Frictional behavior of rock (+ fluids, gouge, ..) under co-seismic conditions

  → Relations of frictional properties to slip, slip rate and material state

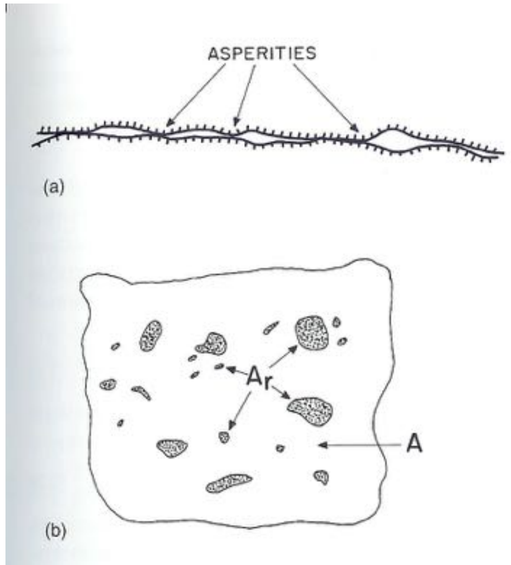

Fig. 2.1. Schematic diagram, in section and plan view, of contacting surface. The stippled regions in plan view represent the areas of asperity contact, which together comprise the real contact area A_r.

Rock friction

Linear slip-weakening friction

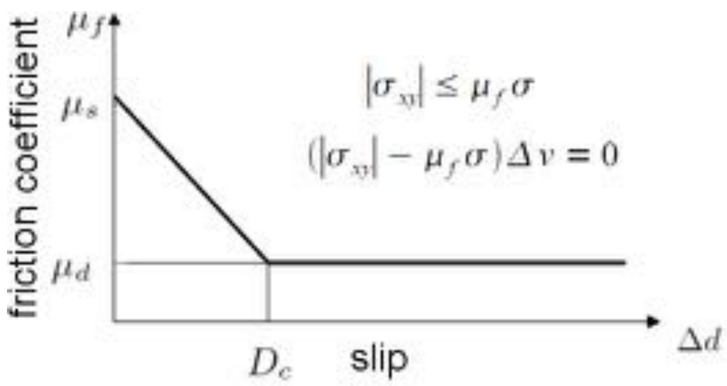

$$\mu_f = \begin{cases} \mu_s - \dfrac{\mu_s - \mu_d}{D_c}\Delta d & \text{if } \Delta d < D_c\,, \\ \mu_d & \text{if } \Delta d \ge D_c\,. \end{cases}$$

σ_{xy}	shear strength	Δd	slip
μ_f	friction coefficent	Δv	slip rate
σ	normal stress	D_c	critical slip distance

Rate-and-state dependent friction

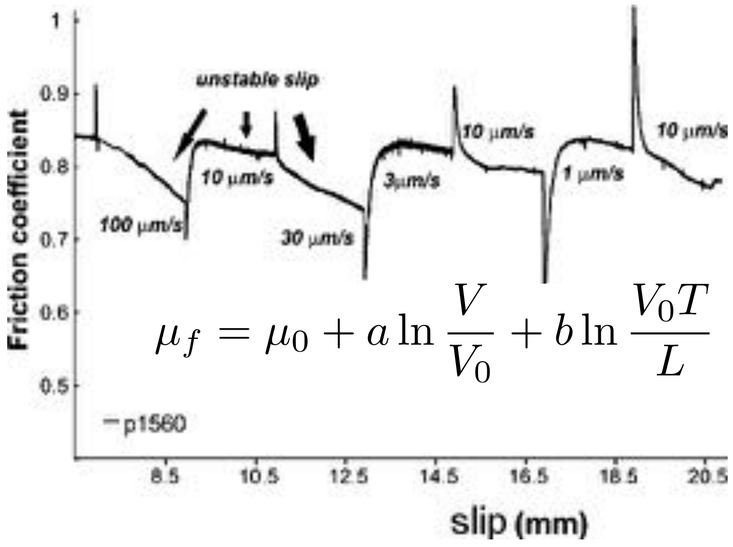

→ Rock friction as a non- linear relation between fault stress and slip (Coulomb failure criterion, empirical friction laws from laboratory experiments)

Earthquake dynamic rupture modeling

Adapted from Harris et al., SRL 2011, 2018

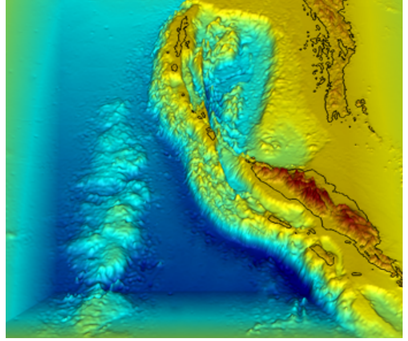

Geology

Physics-based approach

- Solving for spontaneous dynamic earthquake rupture as non-linear interaction of frictional failure and seismic wave propagation
- Earthquake = frictional shear failure of brittle solids under compression along preexisting weak interfaces

"Input"

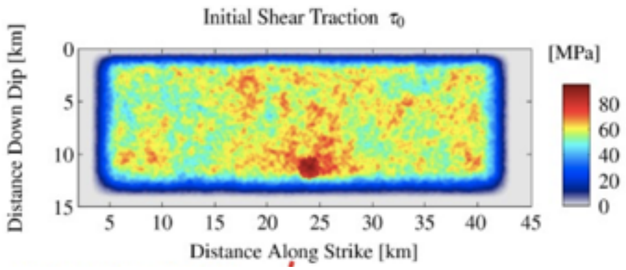

Initial fault stresses

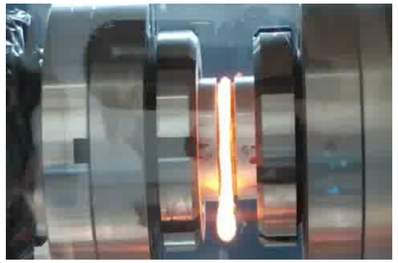

Friction experiments

Earthquake dynamic rupture modeling

Adapted from Harris et al., SRL 2011, 2018

Physics-based approach

- Solving for spontaneous dynamic earthquake rupture as non-linear interaction of frictional failure and seismic wave propagation
- Earthquake = frictional shear failure of brittle solids under compression along preexisting weak interfaces

"Input"

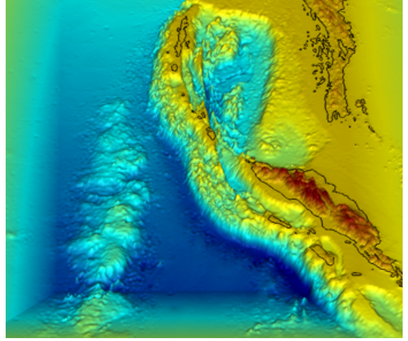

Geology

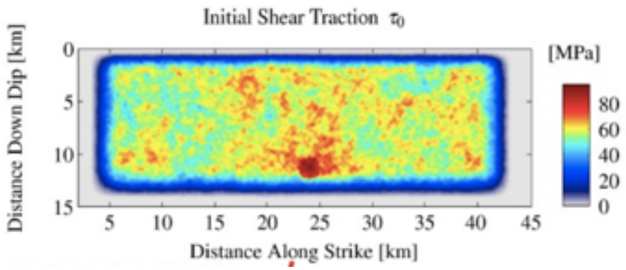

Initial fault stresses

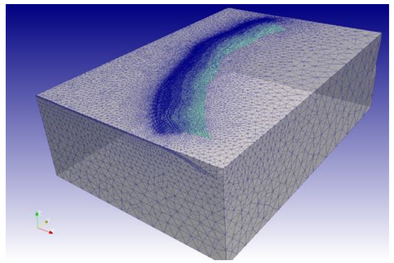

Mesh generation

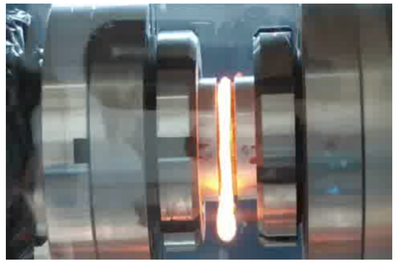

Friction experiments

SOLVER

"Output"

Rupture dynamics

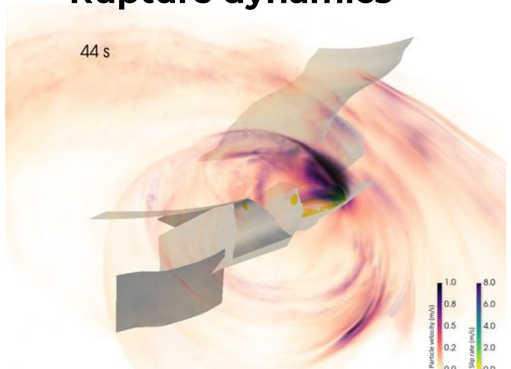

Ground deformation

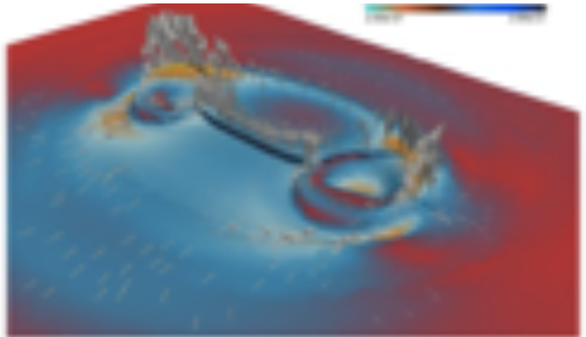

Synthetic observables

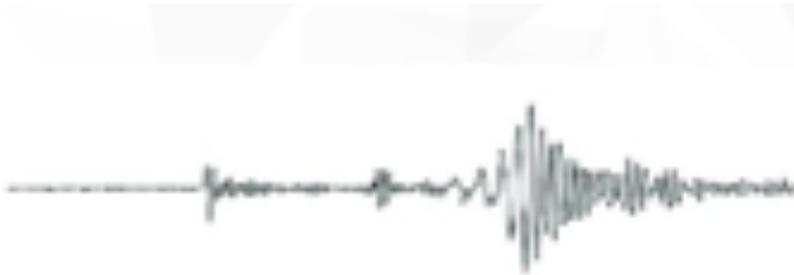

Dynamic rupture modeling

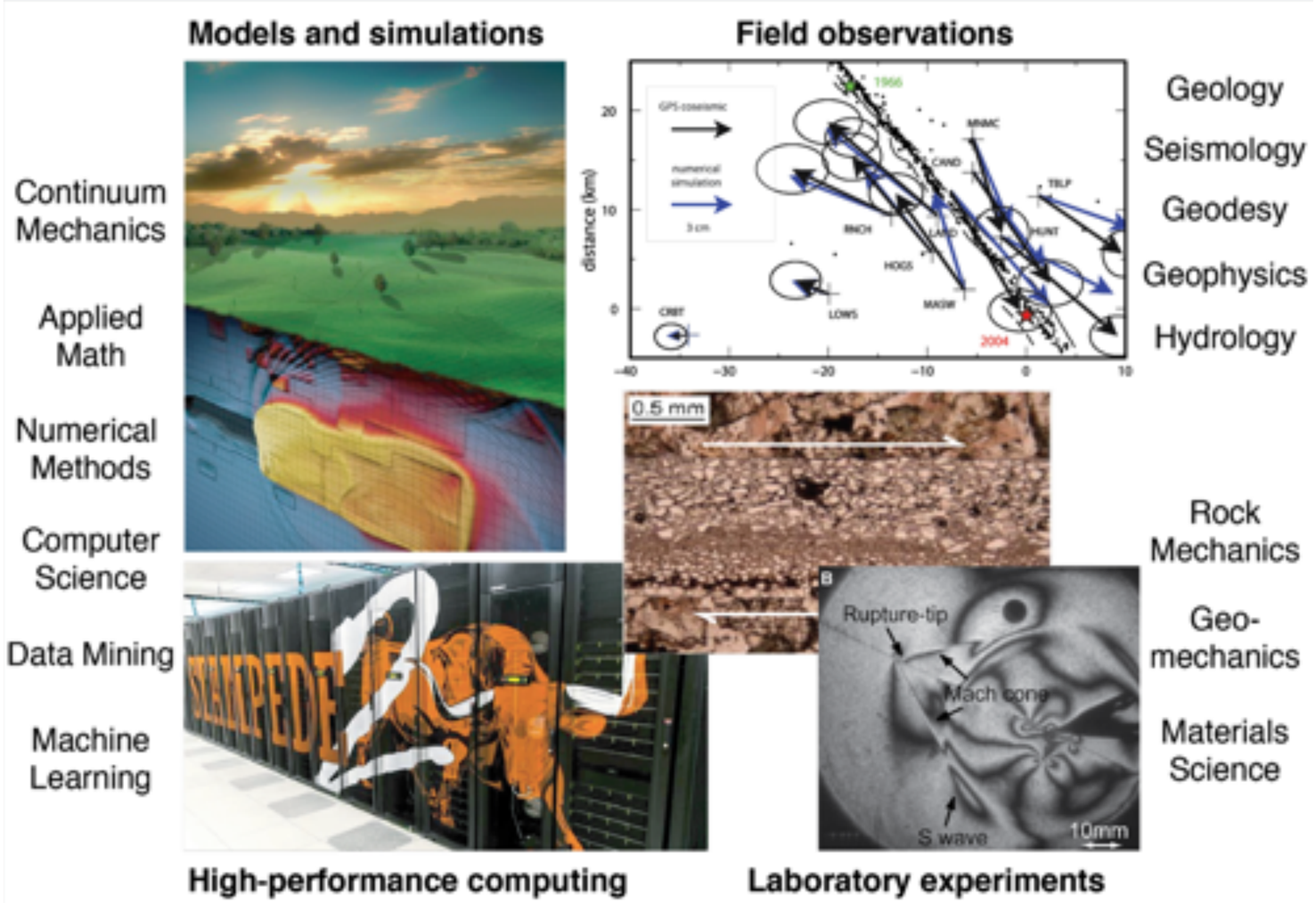

Challenge 1: Earthquake source processes are (very) **ill-constrained** and **highly non-linear.**

Challenge 2: Which **physical processes** are **dominant and relevant** at a given spatio-temporal scale (and in real earthquakes)? Can we justify the "cost" of their inclusion?

Challenge 3: How to **assimilate all available knowledge** in a suitable manner for **software** (numerical discretisation, solvers, equations solved) and **hardware** (heterogeneous HPC systems, energy concerns)?

white paper "Modeling earthquake source processes: from tectonics to dynamic rupture", Lapusta et al., 2019

Heinecke et al., Gordon Bell Prize Finalist, SC'14

Wollherr et al., JGR 2019

Empowered by supercomputing

- We exploit unstructured tetrahedral meshes and high-order accuracy in space and time based on an **ADER-DG method** handling **geometric complexity and highly varying element sizes in open source software, e.g., SeisSol (www.seissol.org)**

- **Data-fused forward modeling using big geo-data-sets and community models**

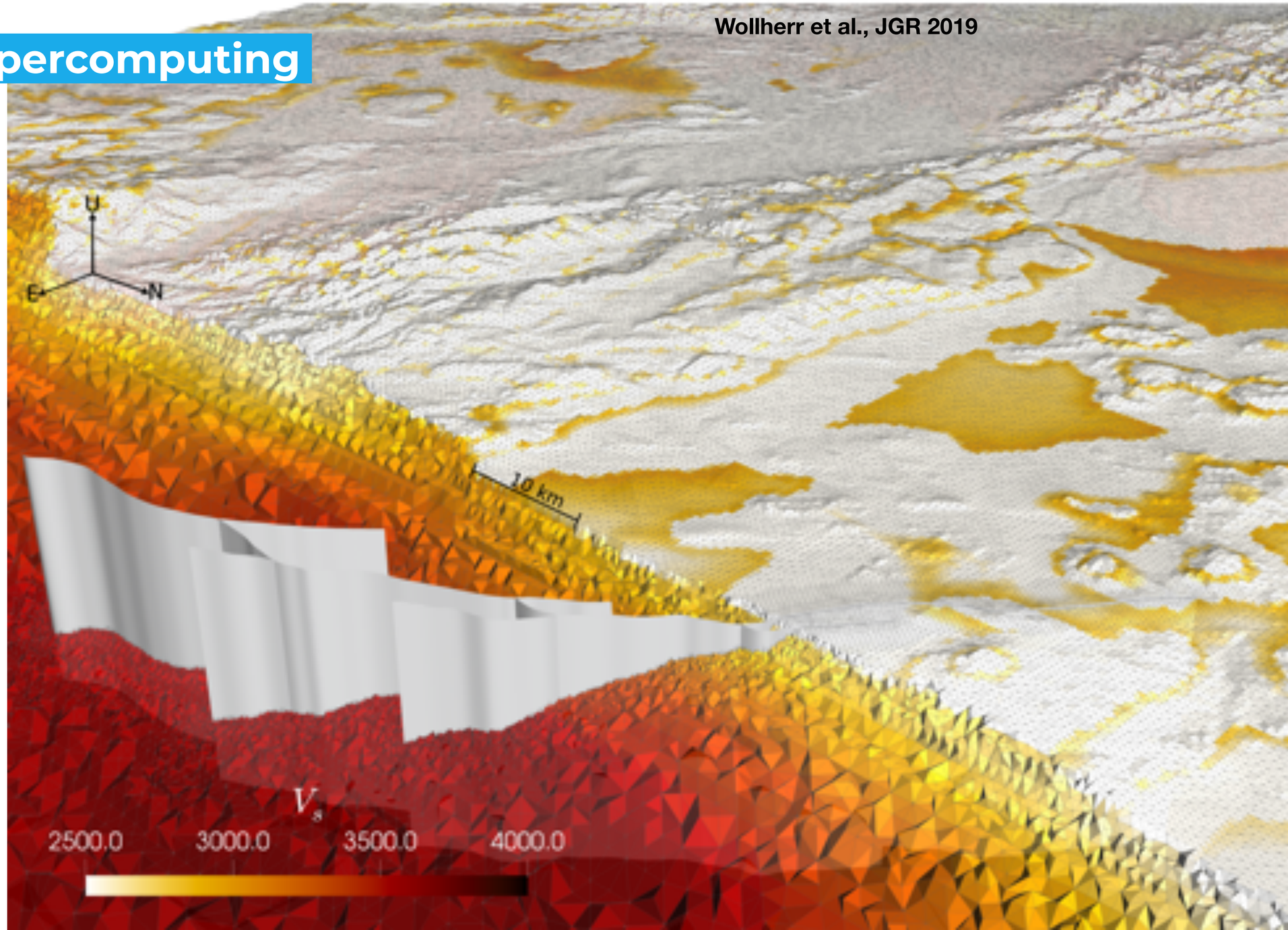

Data-fused dynamic rupture modelling of multi-fault earthquakes

- **data-driven methods** hint on **complex earthquake dynamics** which can be integrated synergistically with **multi-physics forward modeling empowered by high-performance computing**

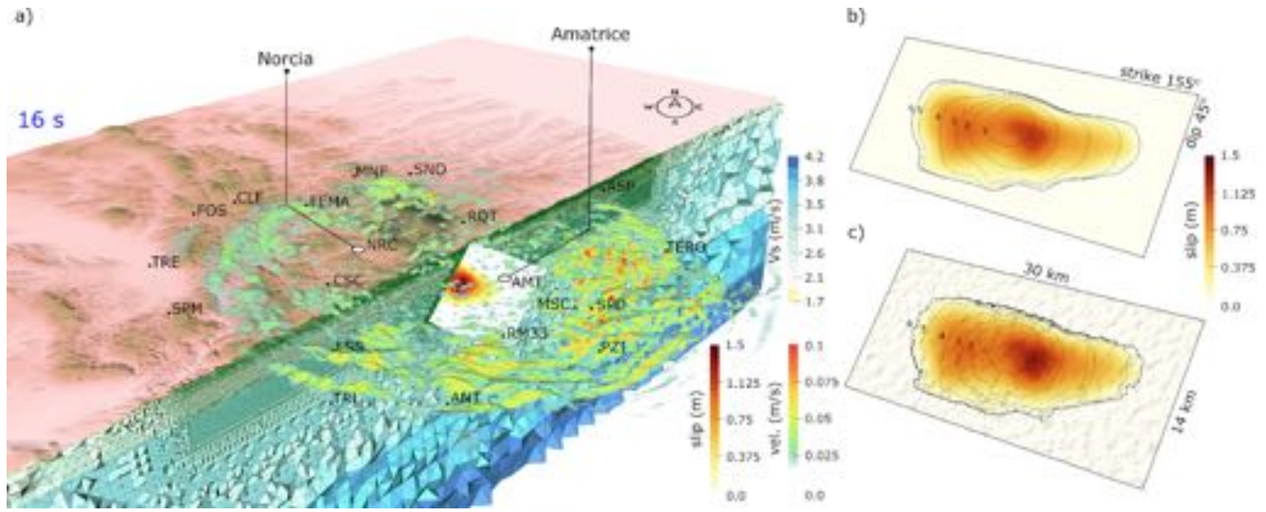

Broadband dynamic rupture simulation (>5 Hz) of the 2016 Amatrice earthquake combining fault roughness and topography with Bayesian dynamic inversion

Taufiqurrahman et al., AGU'21, S55D-0167

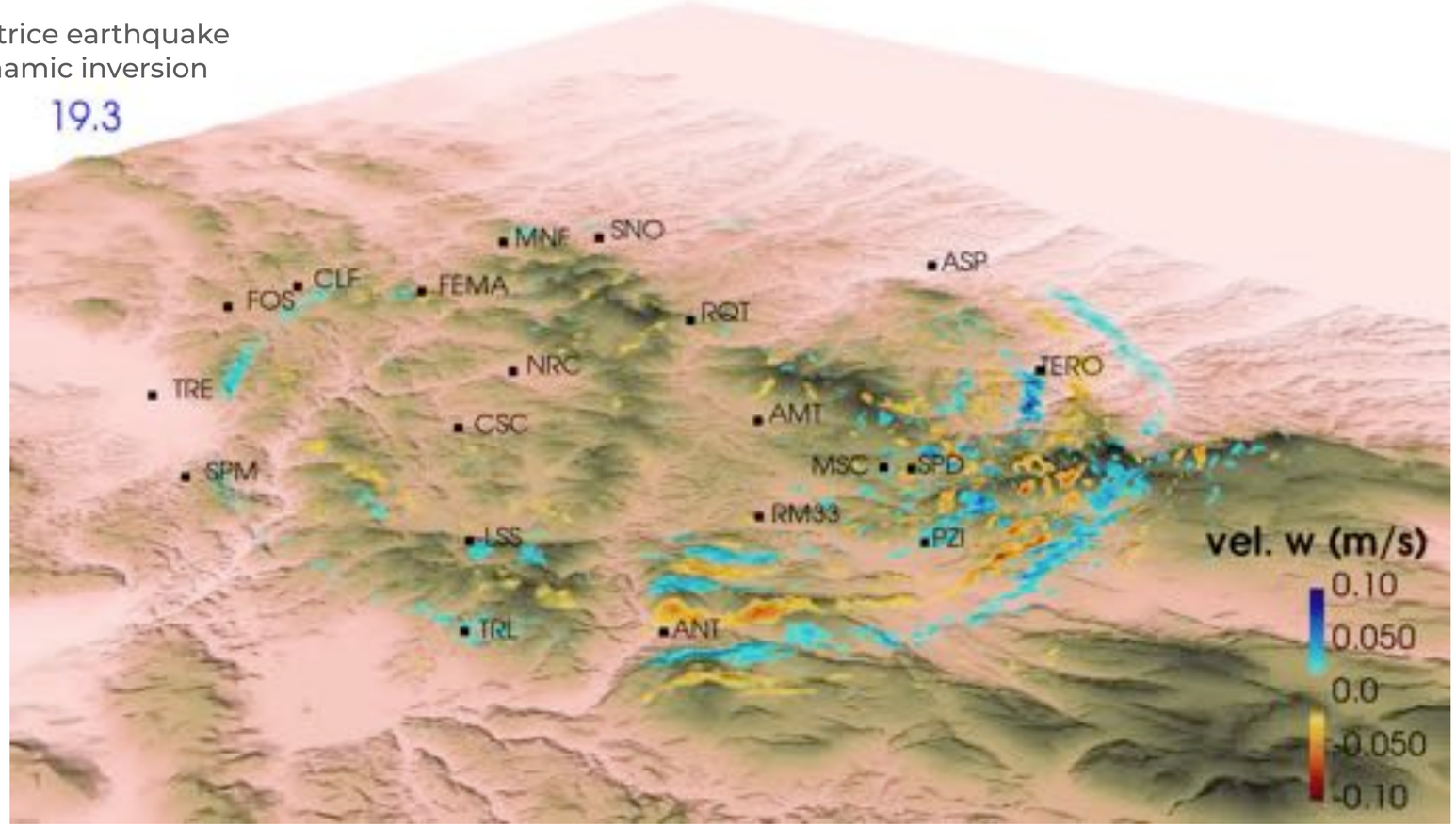

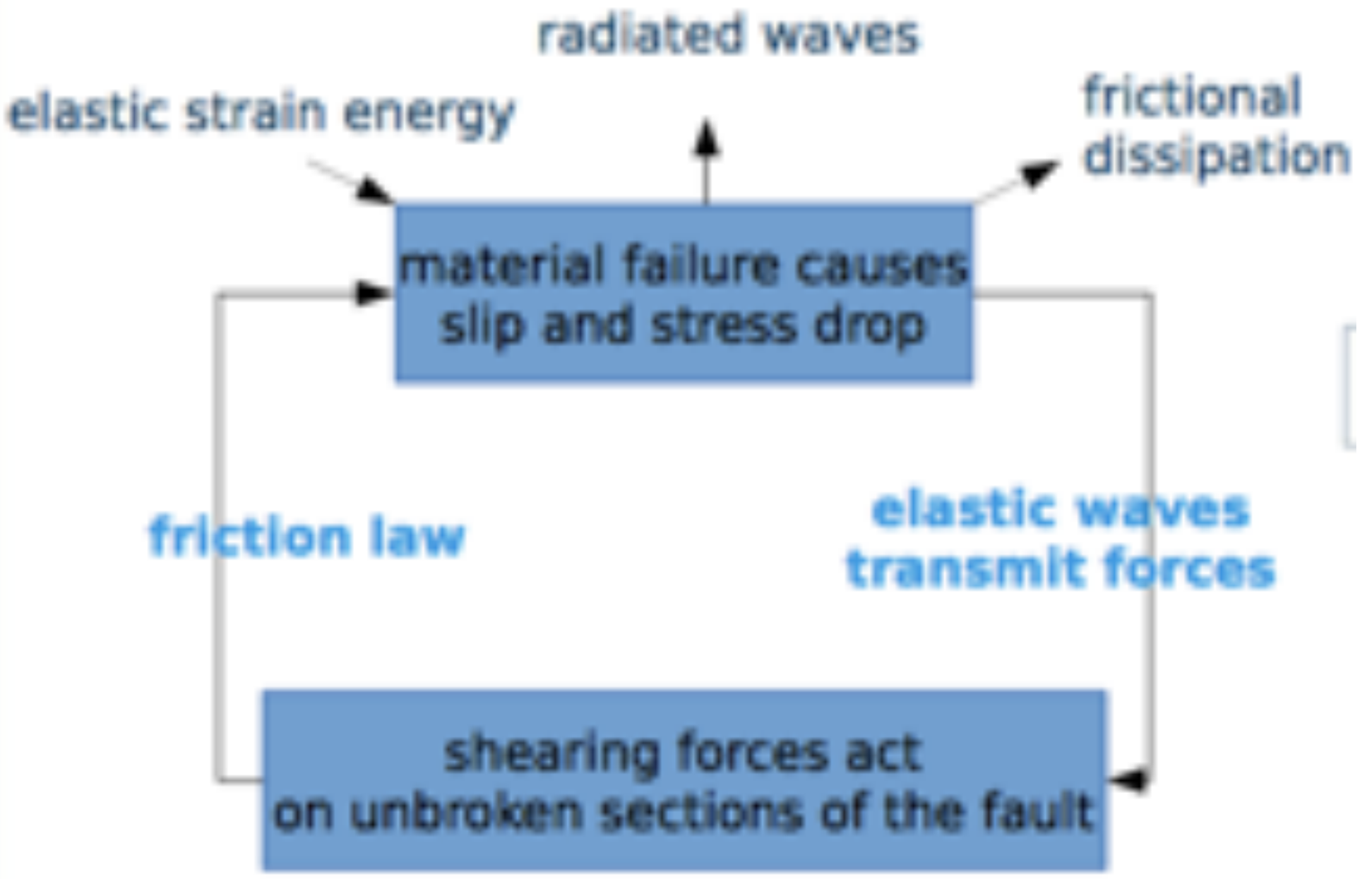
radiated waves
elastic strain energy
frictional dissipation
material failure causes slip and stress drop
friction law
elastic waves transmit forces
shearing forces act on unbroken sections of the fault

3D dynamic rupture modeling

- Earthquake dynamic rupture is treated as a boundary condition in terms of **contact and friction**
- **Thin fault without 'opening'** - two matching fault surfaces are in unilateral contact
- **Displacement discontinuity** across the fault = **slip**
- Much complexity lives in the definition of **friction** (shear traction is bounded by the fault strength), and **fault geometry** and **intersections**

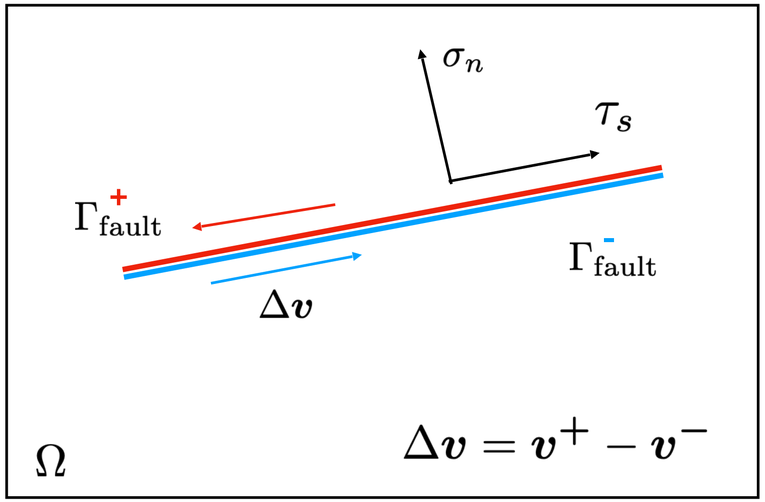

Earthquake dynamics are not predetermined: but evolve as a consequence of the model's initial conditions and the way the fault yields and slides controlled by an assigned friction law relating shear and normal traction on frictional interfaces

3D dynamic rupture modeling

- Earthquake dynamic rupture is treated as a boundary condition in terms of **contact and friction**
- **Thin fault without 'opening'** - two matching fault surfaces are in unilateral contact
- **Displacement discontinuity** across the fault = **slip**
- Much complexity lives in the definition of **friction** (shear traction is bounded by the fault strength), and **fault geometry** and **intersections**
- Can be implemented by **splitting the fault interface**
- FD, FEM, SEM methods suffer from **spurious oscillations** - which have to be damped (e.g., by a thin layer of Kelvin-Voigt-Damping cells, Day et al., 2005), DG methods carefully choose numerical fluxes

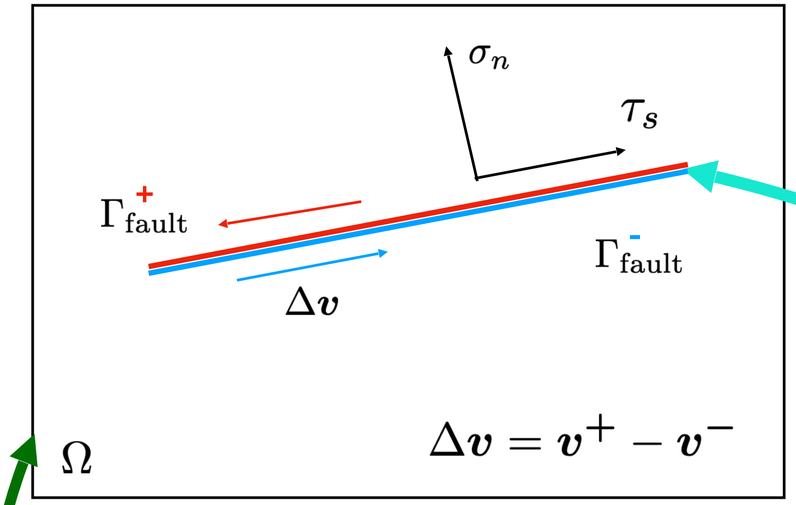

constitutive law (volume)

$$\frac{\partial}{\partial t}\sigma_{xx} - (\lambda + 2\mu)\frac{\partial}{\partial x}u - \lambda\frac{\partial}{\partial y}v - \lambda\frac{\partial}{\partial z}w = 0,$$
$$\frac{\partial}{\partial t}\sigma_{yy} - \lambda\frac{\partial}{\partial x}u - (\lambda + 2\mu)\frac{\partial}{\partial y}v - \lambda\frac{\partial}{\partial z}w = 0,$$
$$\frac{\partial}{\partial t}\sigma_{zz} - \lambda\frac{\partial}{\partial x}u - \lambda\frac{\partial}{\partial y}v - (\lambda + 2\mu)\frac{\partial}{\partial z}w = 0,$$

constitutive law (surfaces)

$$\tau_s = \mu_f \sigma_n.$$
$$|\boldsymbol{\tau}| \leq \tau_s,$$
$$(|\boldsymbol{\tau}| - \tau_s)|\Delta \mathbf{v}| = 0,$$
$$\Delta \mathbf{v}|\boldsymbol{\tau}| + |\Delta \mathbf{v}|\boldsymbol{\tau} = 0.$$

SIMPLE 2D MODELS + ANALYTICS

REVEAL A 'ZOO OF RUPTURE STYLES'

the ideal world

- **Fracture mechanics**: Frictional failure of brittle solids under compression initiates earthquakes as propagating shear fracture; mostly unsolvable analytically

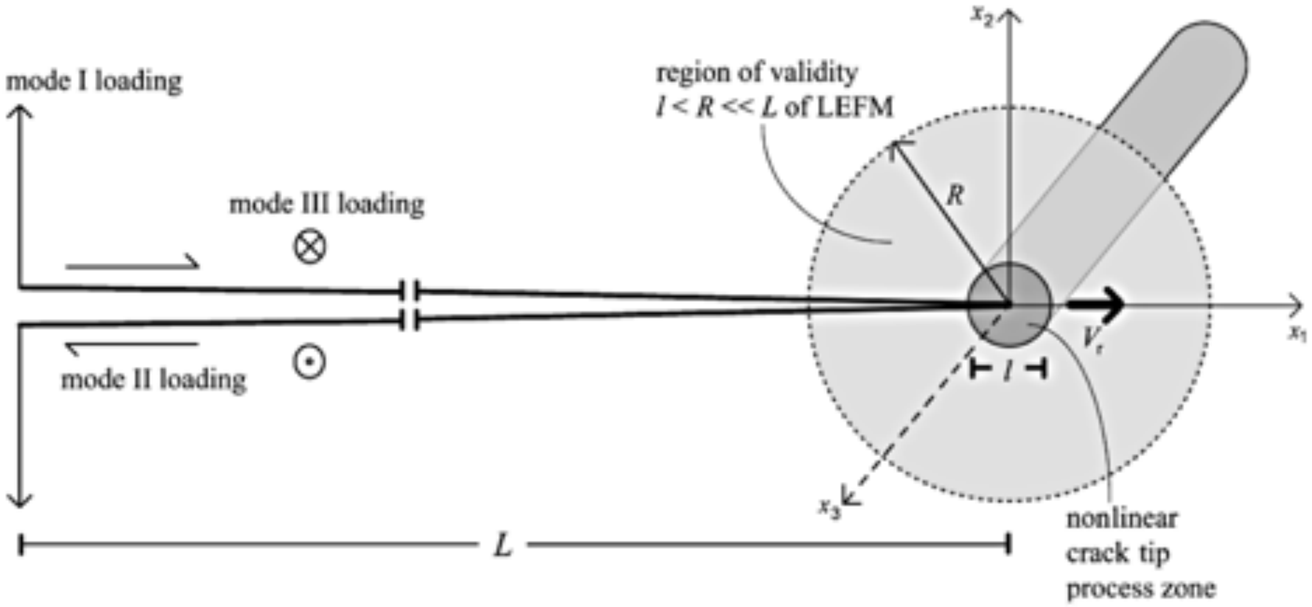

A schematic of a 2D crack illustrating the region of validity for linear elastic fracture mechanics and modes I, II and III of rupture extending along the x_1 axis with velocity v_r (Ben-Zion, 2003).

Gabriel et al., JGR 2012; Gabriel et al., JGR 2013

SIMPLE 2D MODELS + ANALYTICS

REVEAL A 'ZOO OF RUPTURE STYLES'

the ideal world

- **Fracture mechanics**: Frictional failure of brittle solids under compression initiates earthquakes as propagating shear fracture; mostly unsolvable analytically
- **Dynamic rupture modelling**: Seismic wave propagation coupled to dynamically running shear fracture on a frictional interface embedded in a rheological continuum (elastic, visco-plastic, ...)

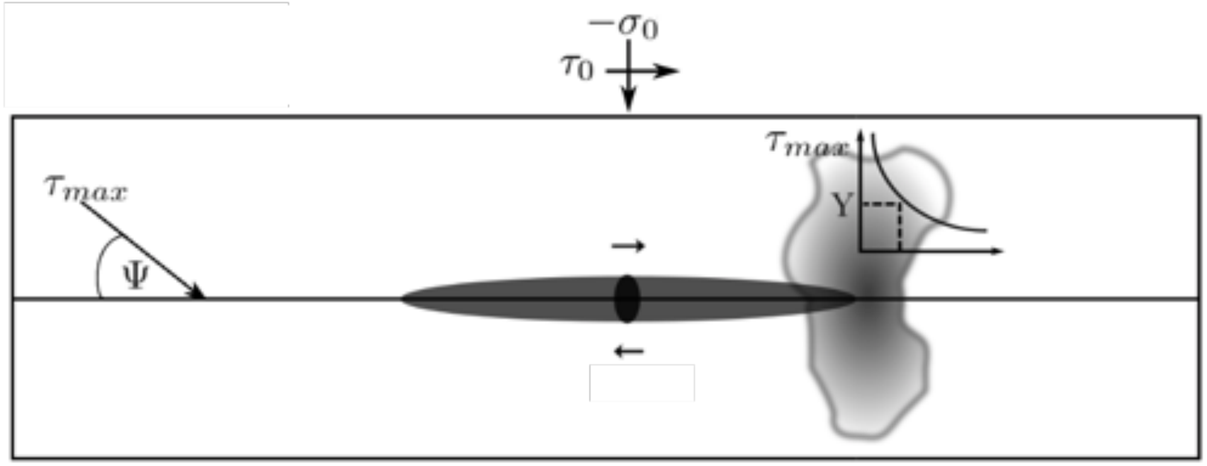

2D plane strain model. The fault is a linear interface across which displacement discontinuity is allowed, embedded in an unbounded, isotropic, elasto-visco-plastic medium. We adopt a cohesionless Coulomb yield function (Andrews, 2005) of internal friction μs.

SIMPLE 2D MODELS + ANALYTICS

REVEAL A 'ZOO OF RUPTURE STYLES'

the ideal world

Gabriel et al., JGR 2012; Gabriel et al., JGR 2013

- **Fracture mechanics**: Frictional failure of brittle solids under compression initiates earthquakes as propagating shear fracture; mostly unsolvable analytically
- **Dynamic rupture modelling**: Seismic wave propagation coupled to dynamically running shear fracture on a frictional interface embedded in a rheological continuum (elastic, visco-plastic, ...)
- **Frictional constitutive law:** Laboratory derived non-linear relation between fault stress and slip, slip-rate, material state

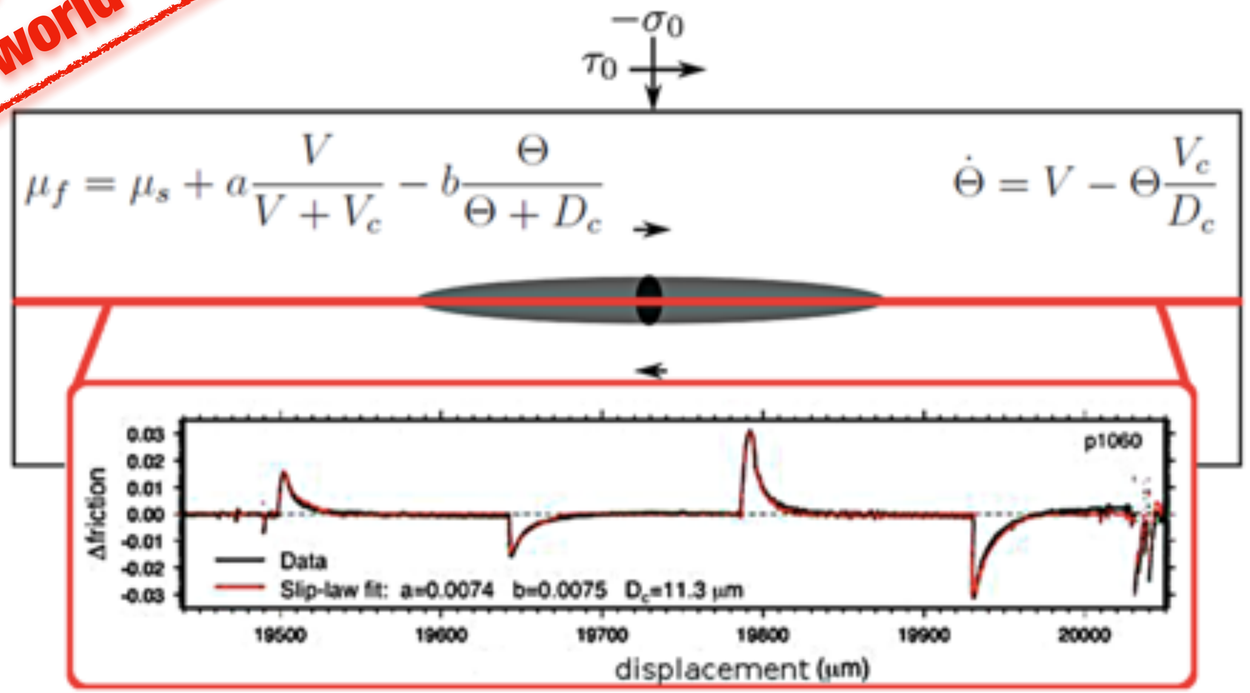

Rate- and state-dependent friction law with fast velocity-weakening

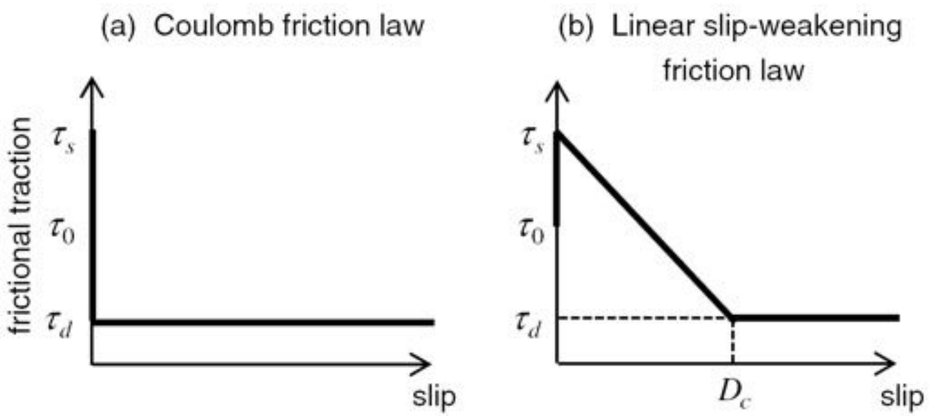

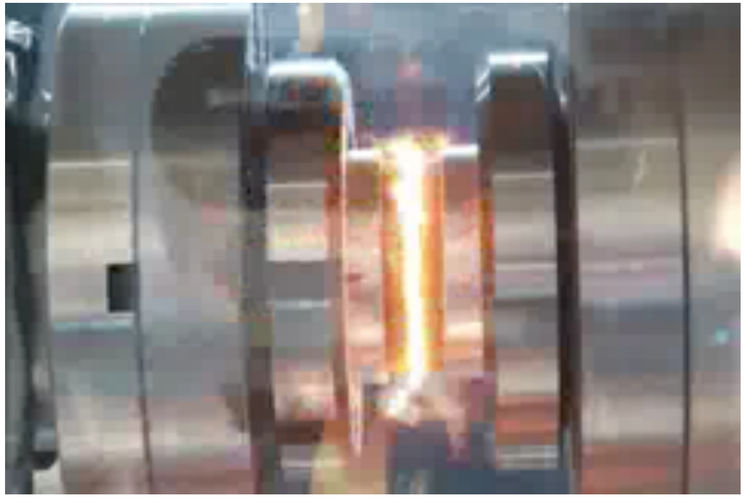

High-speed friction experiment (courtesy of Giulio di Toro)

SIMPLE 2D MODELS + ANALYTICS

REVEAL A 'ZOO OF RUPTURE STYLES'

the ideal world

- **Fracture mechanics**: Frictional failure of brittle solids under compression initiates earthquakes as propagating shear fracture; mostly unsolvable analytically
- **Dynamic rupture modelling**: Seismic wave propagation coupled to dynamically running shear fracture on a frictional interface embedded in a rheological continuum (elastic, visco-plastic, ...)
- **Frictional constitutive law:** Laboratory derived non-linear relation between fault stress and slip, slip-rate, material state
- **A zoo of rupture styles:** Slow and fast ruptures, sub-shear and super-shear, cracks and pulses under varying relative strength of the fault and nucleation size

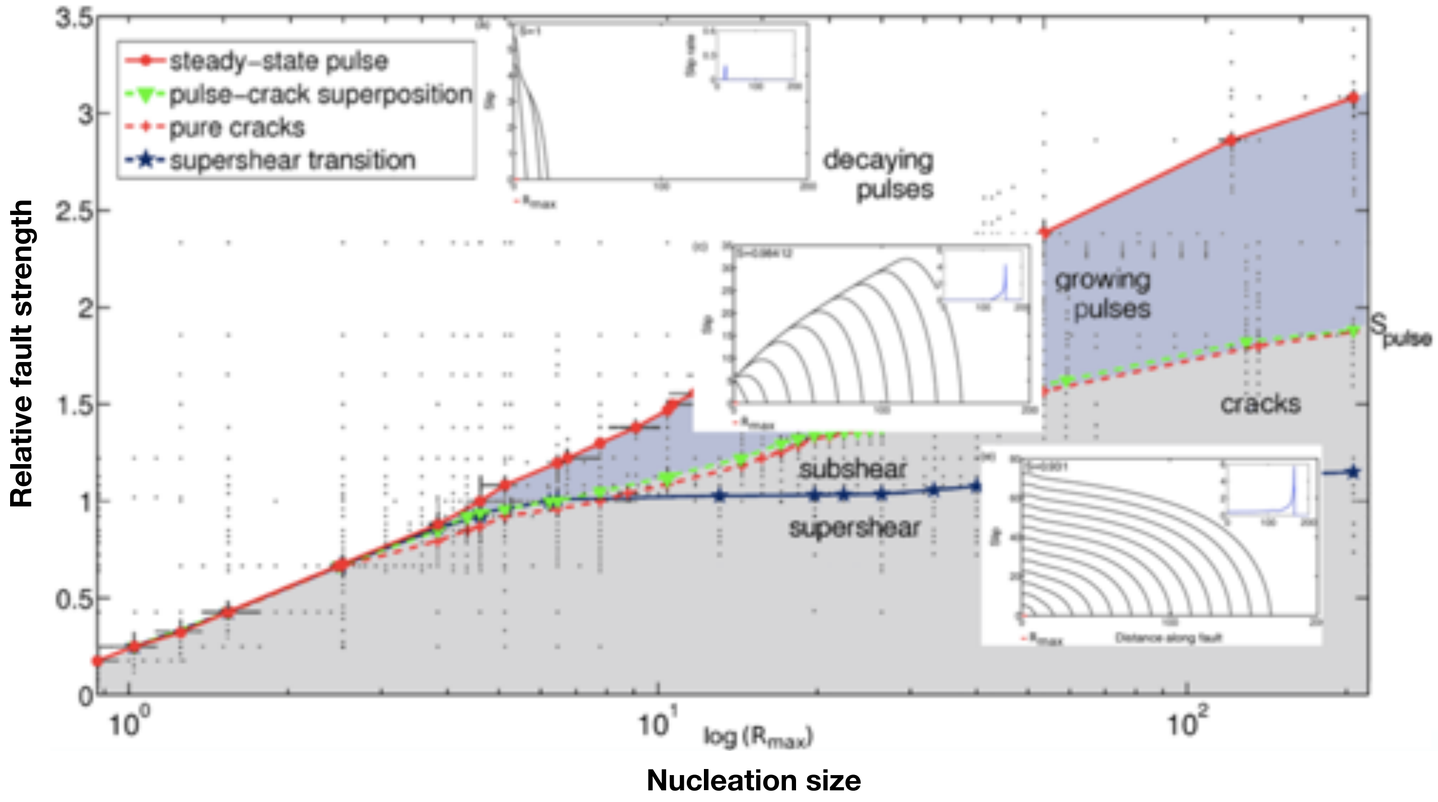

Gabriel et al., JGR 2012; Gabriel et al., JGR 2013

SIMPLE 2D MODELS + ANALYTICS

REVEAL A 'ZOO OF RUPTURE STYLES'

- **Slip re-activation**: Growing pulses gradually concentrate stress in their hypo-central region, as analytically predicted (Nielsen & Madariaga, 2003), may trigger secondary rupture

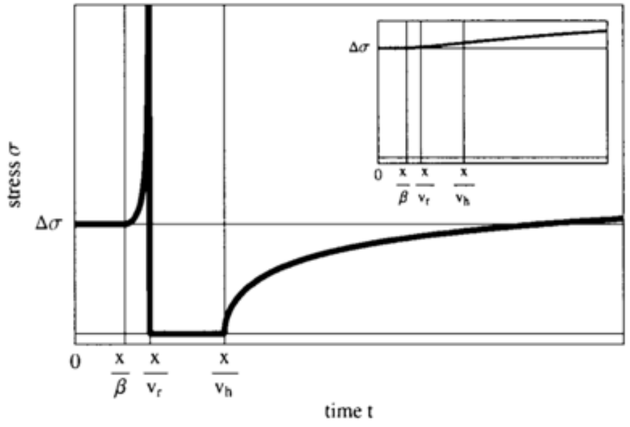

Figure 2. Stress as a function of t/x, for the unilateral, self-similar pulse. In the example the rupture and healing velocities are $v_r = 2\beta/3$ and $v_h = \beta/3$. Note that on the healed portion, the stress continuously increases, as long as the pulse continues to propagate, eventually reaching and surpassing the initial level. The persistence of such an increase toward the limit $t/x \to \infty$ corresponds to a stress singularity located at $x = 0$, represented in Figure 3. The incerpt represents the stress trend on a point along the negative x axis (unbroken side), with an increase slowly starting at the arrival of the first shear waves from the nucleation point.

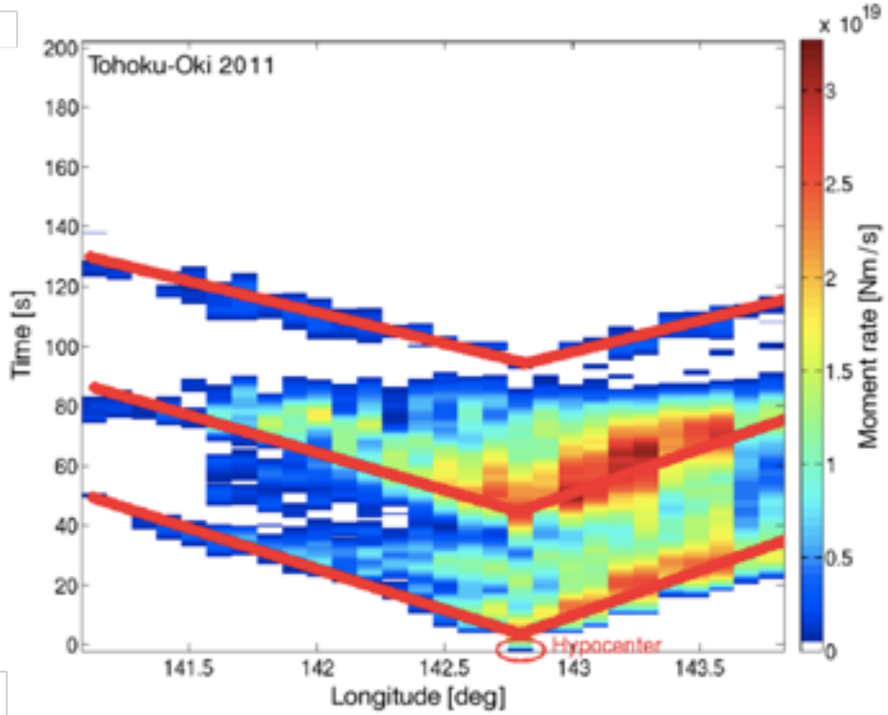

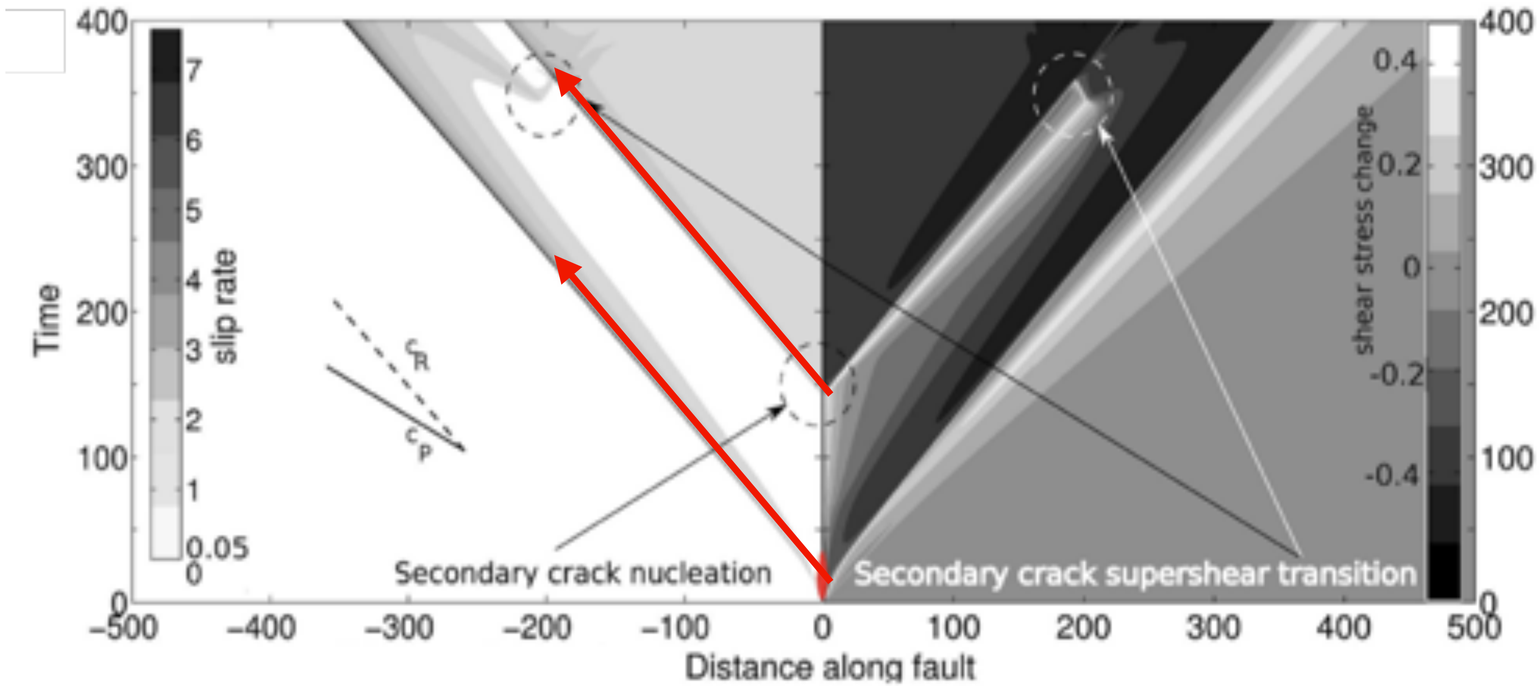

Multi-Scale and Multi-Physics
Dynamic rupture simulations

➡ Few methods support all modelling requirements

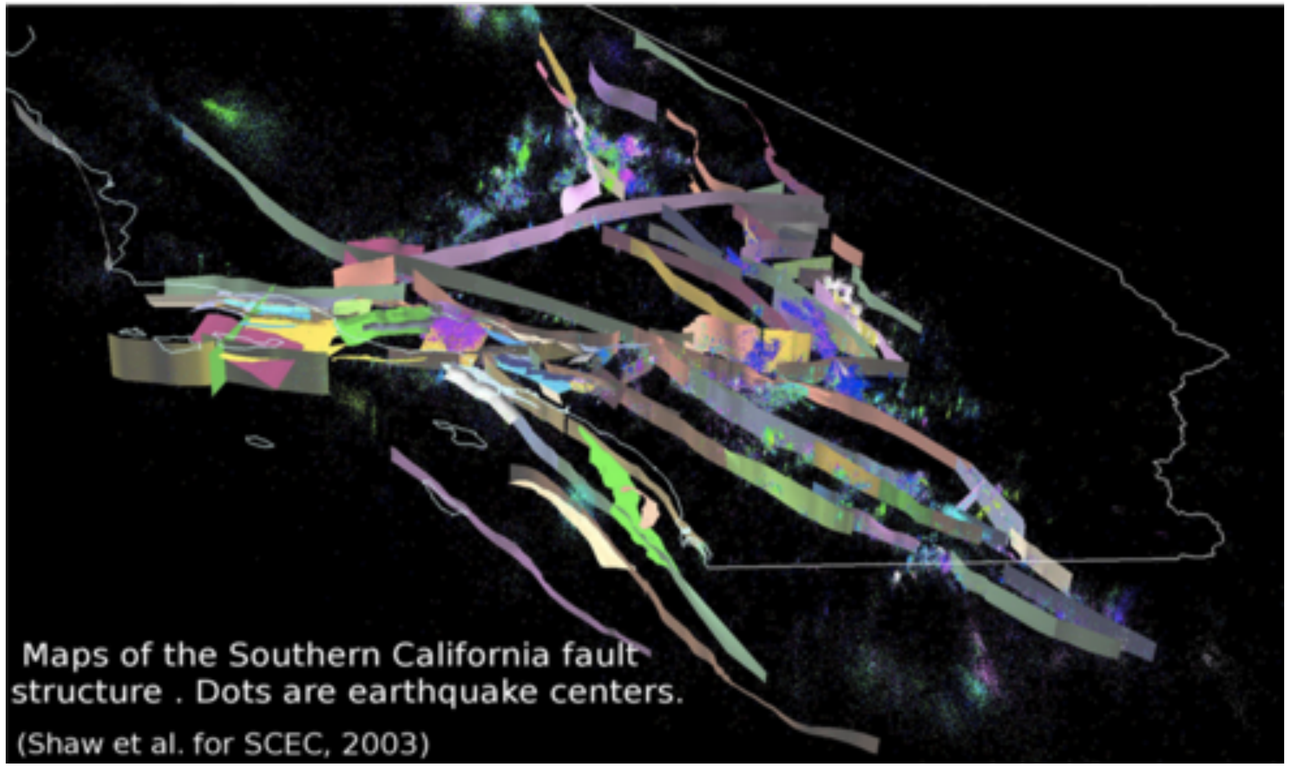

Multitude of spatio-temporal scales: fault geometry spans hundreds of km; frictional process zone size is m (or even cm) scale, tectonic loading (seismic cycle) 10-10000 years; rise time on second scale

the real world

- Non-planar, intersecting faults
- Non-linear friction
- Heterogeneities in stress and strength
- Dynamic damage around the fault
- Fault roughness and segmentation on all scales
- Bi-material effects
- Low velocity zones surrounding faults
- Thermal pressurization of fault zone fluids
- Thermal decomposition
- Dilatancy of the fault gouge
- Flash heating, melting, lubrication
- Feedback mechanisms across time scales

… this list grows continuously

Governing **equations**

linear hyperbolic system

- **Elastic wave equation** in velocity stress formulation

$$\frac{\partial Q_p}{\partial t} + A_{pq}\frac{\partial Q_q}{\partial x} + B_{pq}\frac{\partial Q_q}{\partial y} + C_{pq}\frac{\partial Q_q}{\partial z} = S_p$$

$$Q = (\sigma_{xx}, \sigma_{yy}, \sigma_{zz}, \sigma_{xy}, \sigma_{yz}, \sigma_{xz}, u, v, w)^T$$

Governing **equations**

linear hyperbolic system

- **Elastic wave equation** in velocity stress formulation

$$\frac{\partial Q_p}{\partial t} + A_{pq}\frac{\partial Q_q}{\partial x} + B_{pq}\frac{\partial Q_q}{\partial y} + C_{pq}\frac{\partial Q_q}{\partial z} = S_p$$

$$Q = (\sigma_{xx}, \sigma_{yy}, \sigma_{zz}, \sigma_{xy}, \sigma_{yz}, \sigma_{xz}, u, v, w)^T$$

constitutive relationships in terms of velocity

$$\frac{\partial}{\partial t}\sigma_{xx} - (\lambda + 2\mu)\frac{\partial}{\partial x}u - \lambda\frac{\partial}{\partial y}v - \lambda\frac{\partial}{\partial z}w = 0,$$

$$\frac{\partial}{\partial t}\sigma_{yy} - \lambda\frac{\partial}{\partial x}u - (\lambda + 2\mu)\frac{\partial}{\partial y}v - \lambda\frac{\partial}{\partial z}w = 0,$$

$$\frac{\partial}{\partial t}\sigma_{zz} - \lambda\frac{\partial}{\partial x}u - \lambda\frac{\partial}{\partial y}v - (\lambda + 2\mu)\frac{\partial}{\partial z}w = 0,$$

$$\frac{\partial}{\partial t}\sigma_{xy} - \mu\left(\frac{\partial}{\partial x}v + \frac{\partial}{\partial y}u\right) = 0,$$

$$\frac{\partial}{\partial t}\sigma_{yz} - \mu\left(\frac{\partial}{\partial z}v + \frac{\partial}{\partial y}w\right) = 0,$$

$$\frac{\partial}{\partial t}\sigma_{xz} - \mu\left(\frac{\partial}{\partial z}u + \frac{\partial}{\partial x}w\right) = 0,$$

conservation of momentum

$$\rho\frac{\partial}{\partial t}u - \frac{\partial}{\partial x}\sigma_{xx} - \frac{\partial}{\partial y}\sigma_{xy} - \frac{\partial}{\partial z}\sigma_{xz} = 0,$$

$$\rho\frac{\partial}{\partial t}v - \frac{\partial}{\partial x}\sigma_{xy} - \frac{\partial}{\partial y}\sigma_{yy} - \frac{\partial}{\partial z}\sigma_{yz} = 0,$$

$$\rho\frac{\partial}{\partial t}w - \frac{\partial}{\partial x}\sigma_{xz} - \frac{\partial}{\partial y}\sigma_{yz} - \frac{\partial}{\partial z}\sigma_{zz} = 0,$$

Governing **equations**

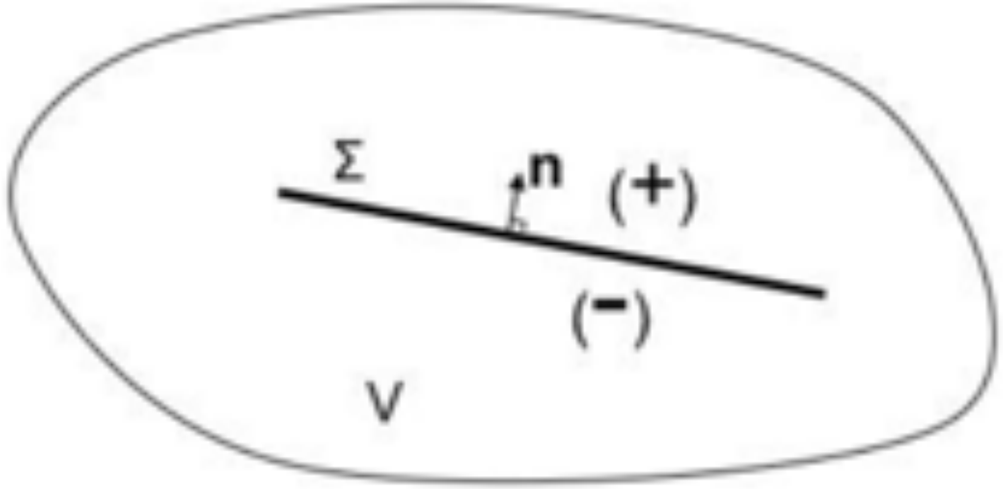

Figure 1. Schematic representation of an space of volume V containing a fault surface $\sum$ with normal unit vector **n** directed from negative side toward positive side of the fault.

Governing **equations**

- Earthquake dynamic rupture is typically implemented as a interface condition in terms of **contact and friction**

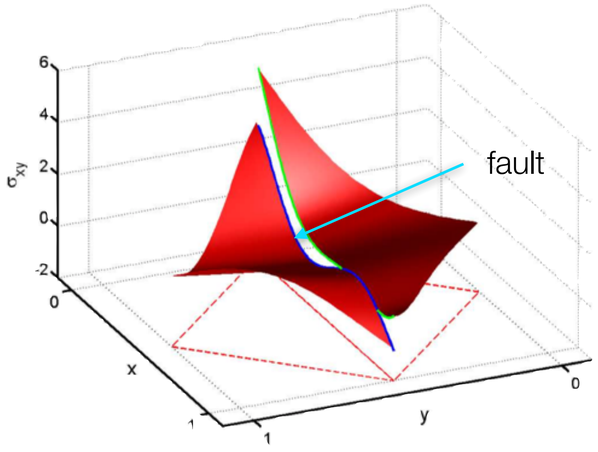

Representation of the shear stress discontinuity across the fault interface. Spontaneous rupture = internal boundary condition of flux term.

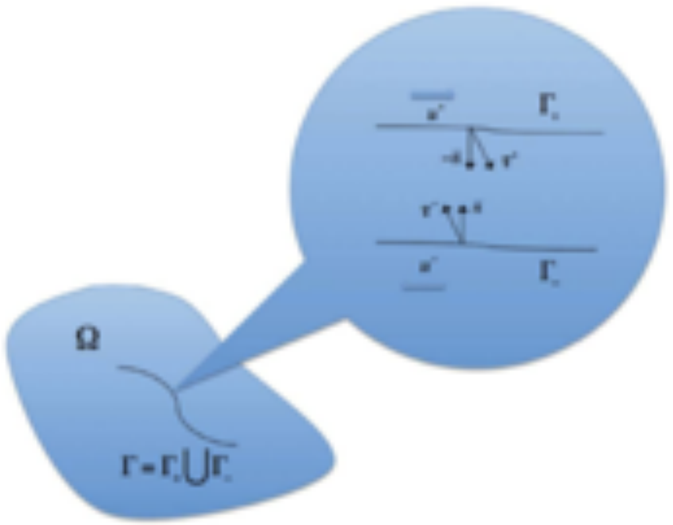

Thin fault: Two matching surfaces in contact

$$\Gamma = \Gamma_+ \bigcup \Gamma_-$$

Fault normal vector:

$$n = n_- = -n_+$$

Displacement discontinuity allowed across the fault:

Slip = $s = u_+ - u_-$

Fault tractions: $T = \sigma \cdot n$

Galvez et al (2014)

Boundary conditions:

- Unilateral contact:

$$T^N \leq 0$$
$$s^N \geq 0$$
$$T^N s^N = 0$$

- Friction

$$|T^T| + \mu T^N < 0$$
$$|\dot{s}|\,(|T^T| + \mu T^N) = 0$$
$$\dot{s}|T^T| - |\dot{s}|T^T = 0$$

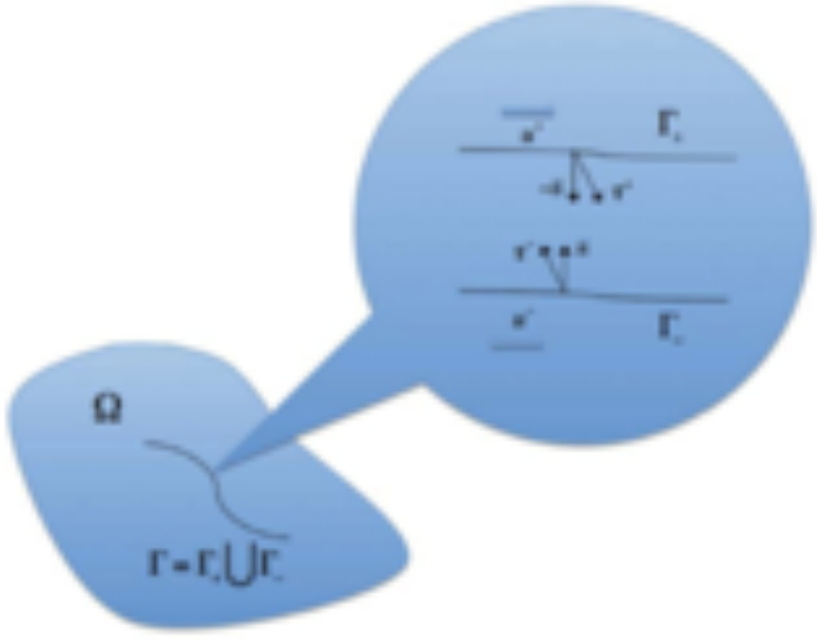

- Friction law, e.g. slip-weakening:

$$\mu(\delta) = \mu_s - (\mu_s - \mu_d)\,\mathrm{min}\left(\frac{\delta}{D_c}, 1\right)$$
$$\dot{\delta} = |\dot{s}|$$

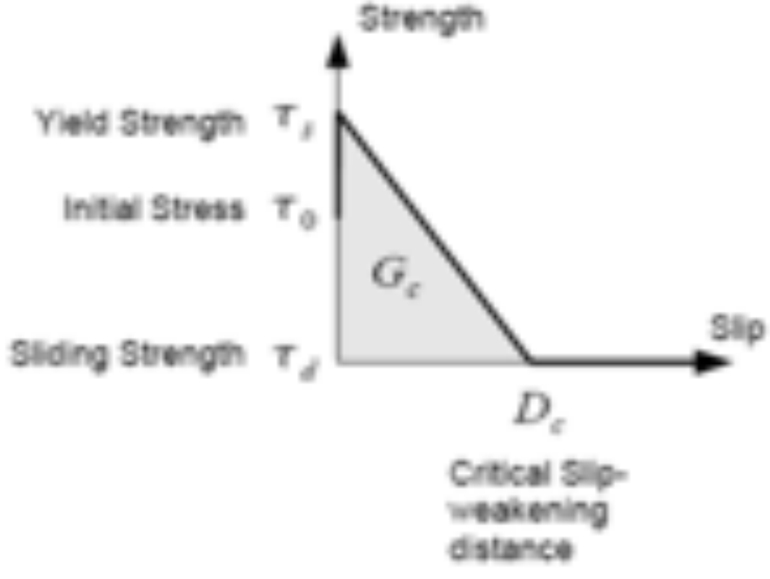

Galvez et al (2014)

The “grand challenge” of meshing

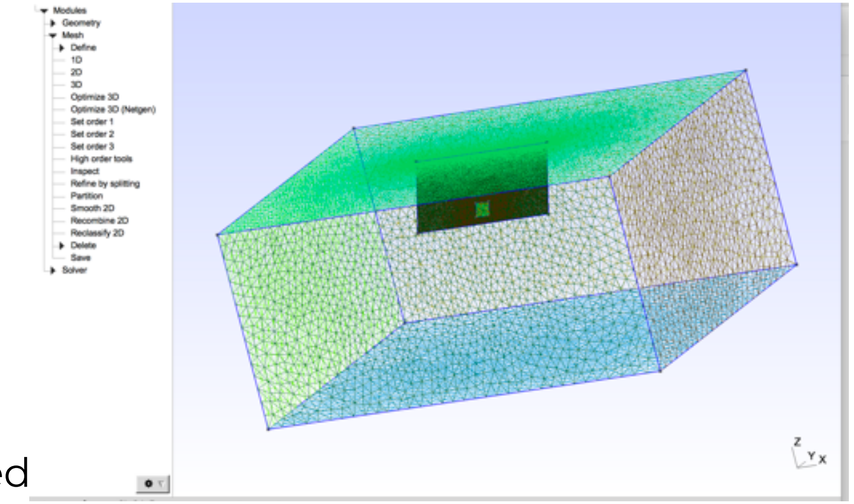

- Community standard 1) **Hexahedral** meshes - may consume weeks in mesh generation, **limited** for complex geometries (external / internal boundary conditions), common tool: TRELIS
- Community standard 2) **Unstructured tetrahedral** meshes - allows automatised meshing and complex internal/external boundary conditions, however are numerically challenging (sliver elements), our tools: GMSH, SIMMODELER

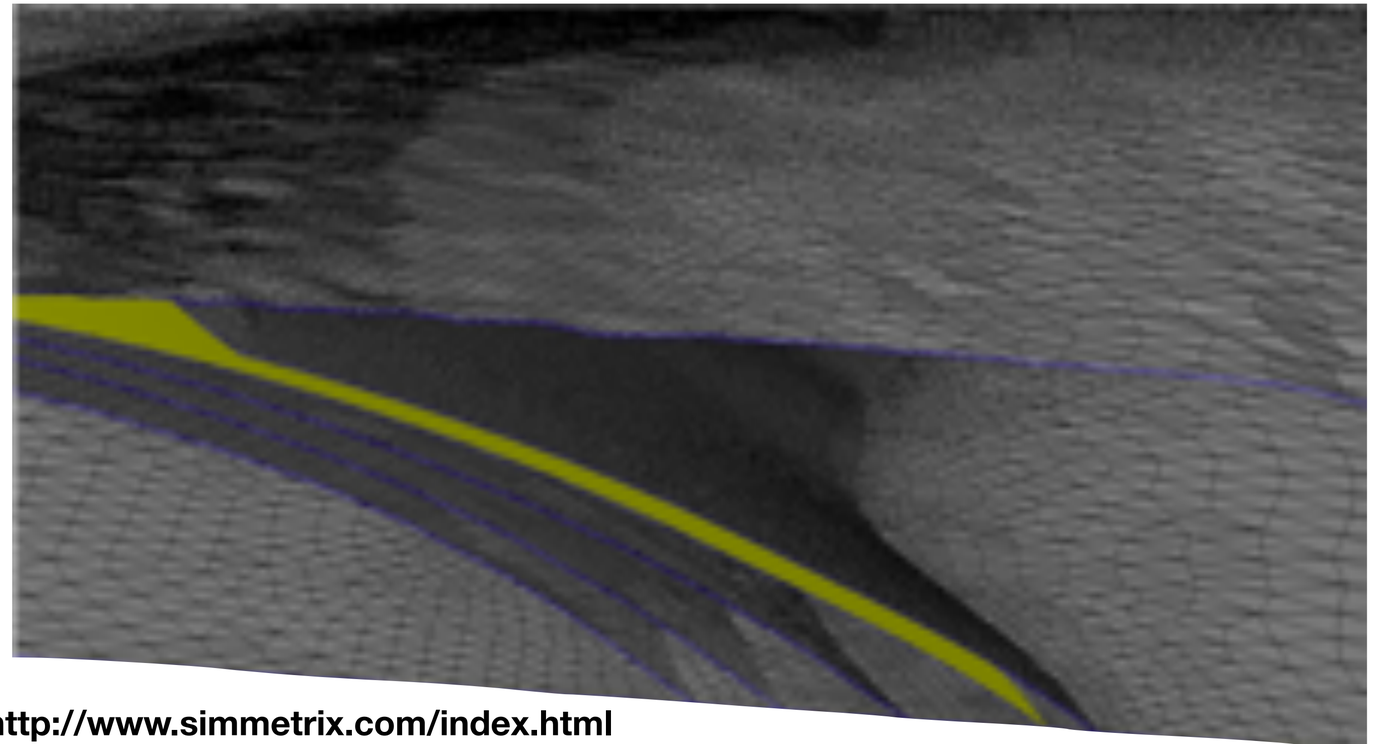

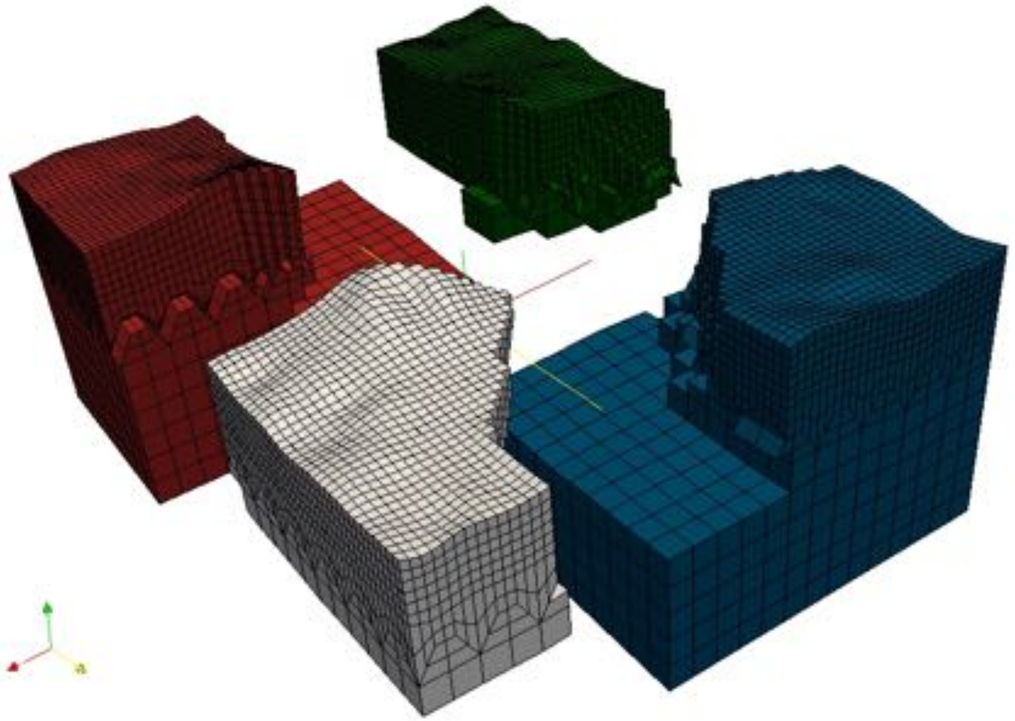

http://www.simmetrix.com/index.html

The “grand challenge” of meshing

- Emerging: **Diffuse interface** and **curvilinear mesh** approaches

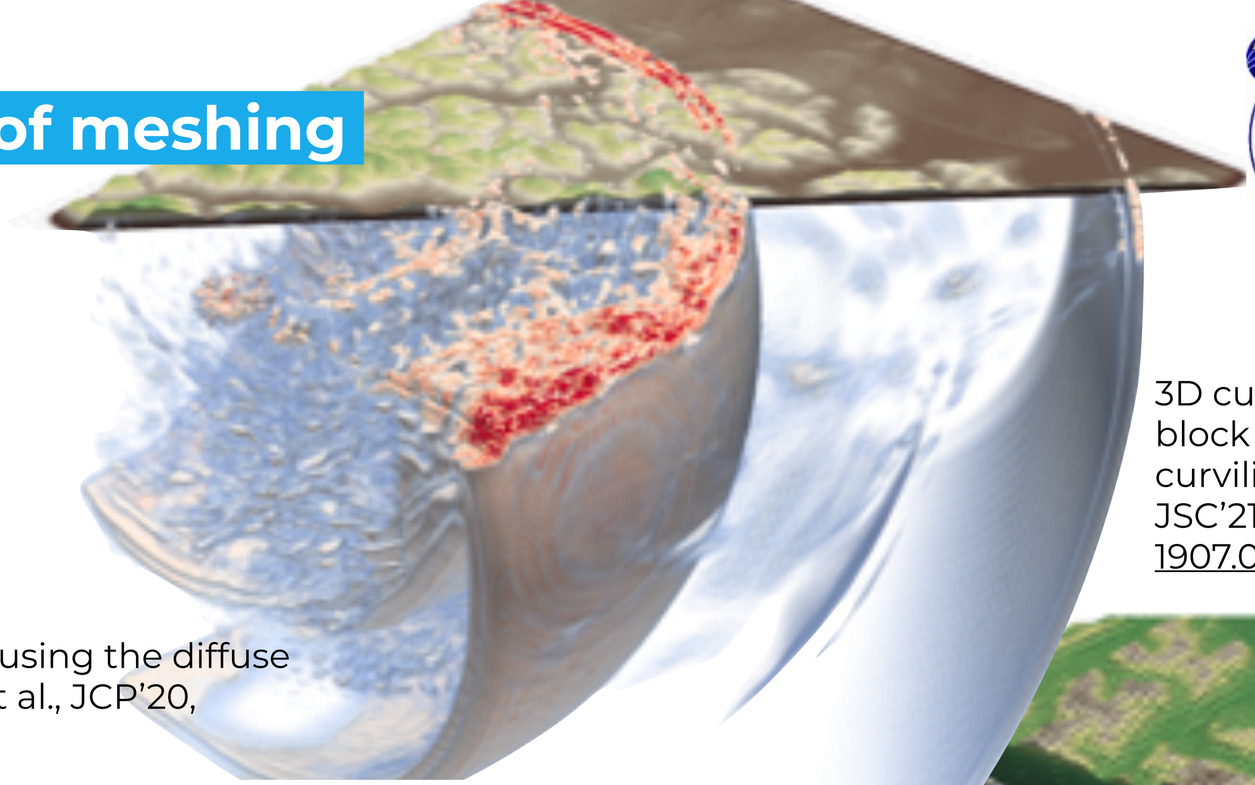

Reinarz et al., CPC, 2020

3D curvilinear meshes via multi-block boundary conforming curvilinear meshes (Duru et al., JSC’21 & https://arxiv.org/abs/1907.02658

Propagation of an out-of-plane brittle crack using the diffuse interface GPR model and ExaHyPE [Tavelli et al., JCP’20, Gabriel et al. Proc. R. Soc. A, 2021].

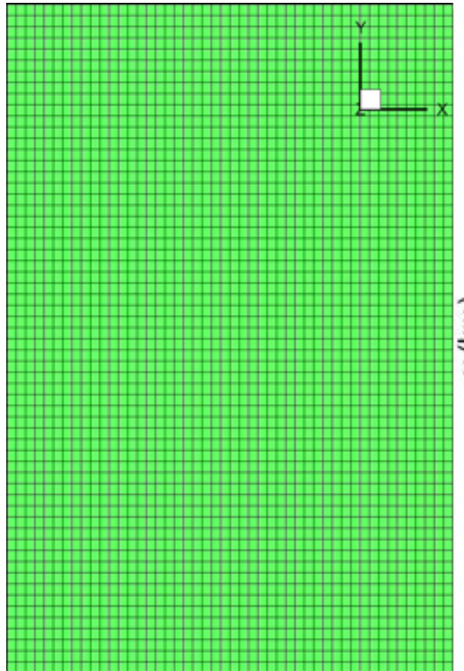

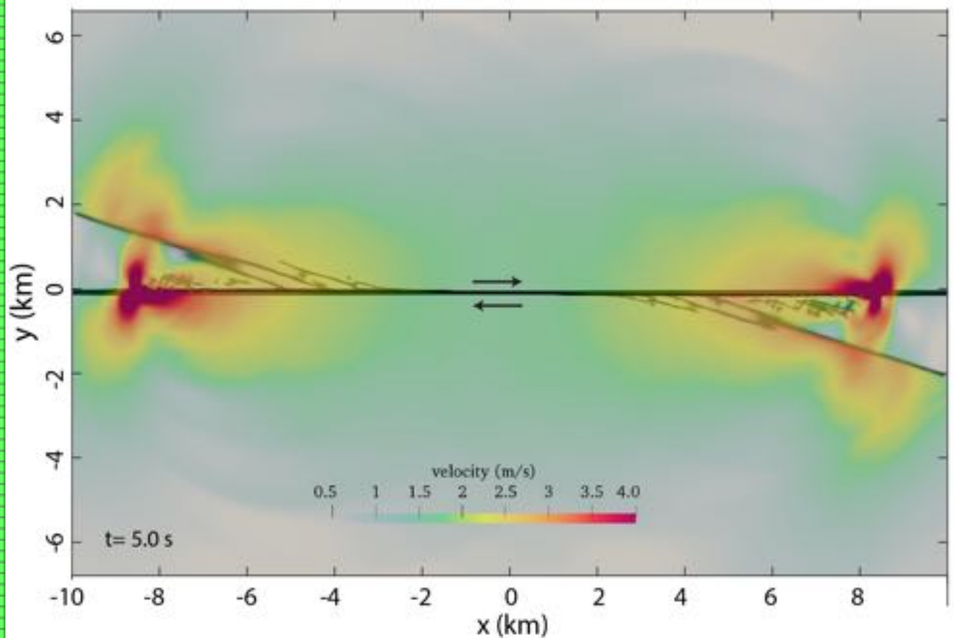

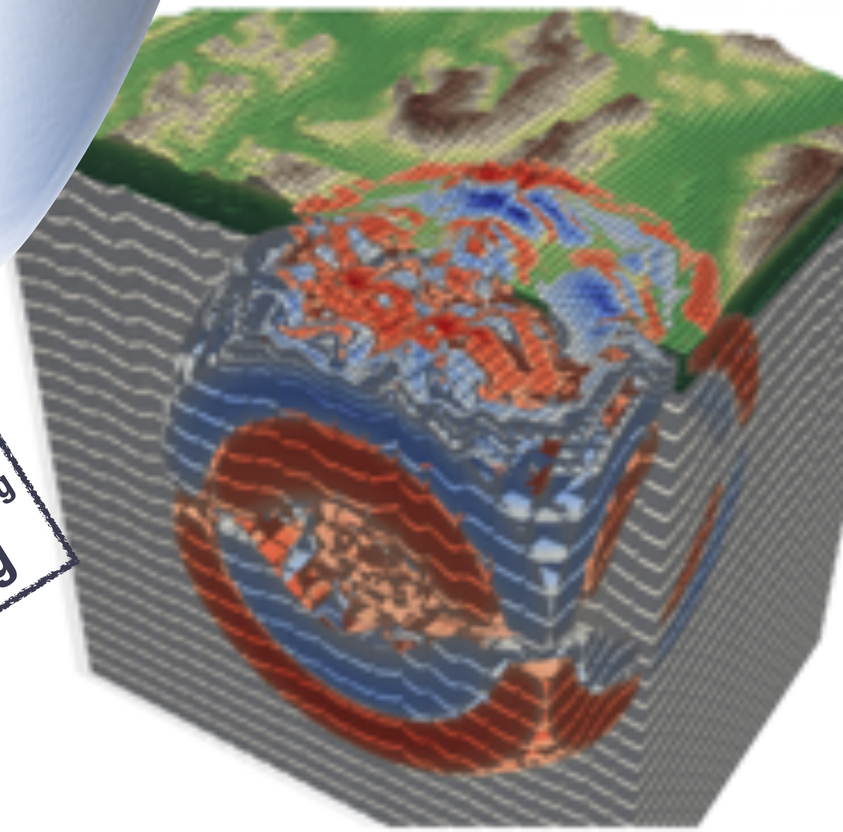

without feature-preserving meshing

Multi-physics
earthquake simulations

the ideal world

➡ **Many methods successfully solve (idealised) community benchmarks**

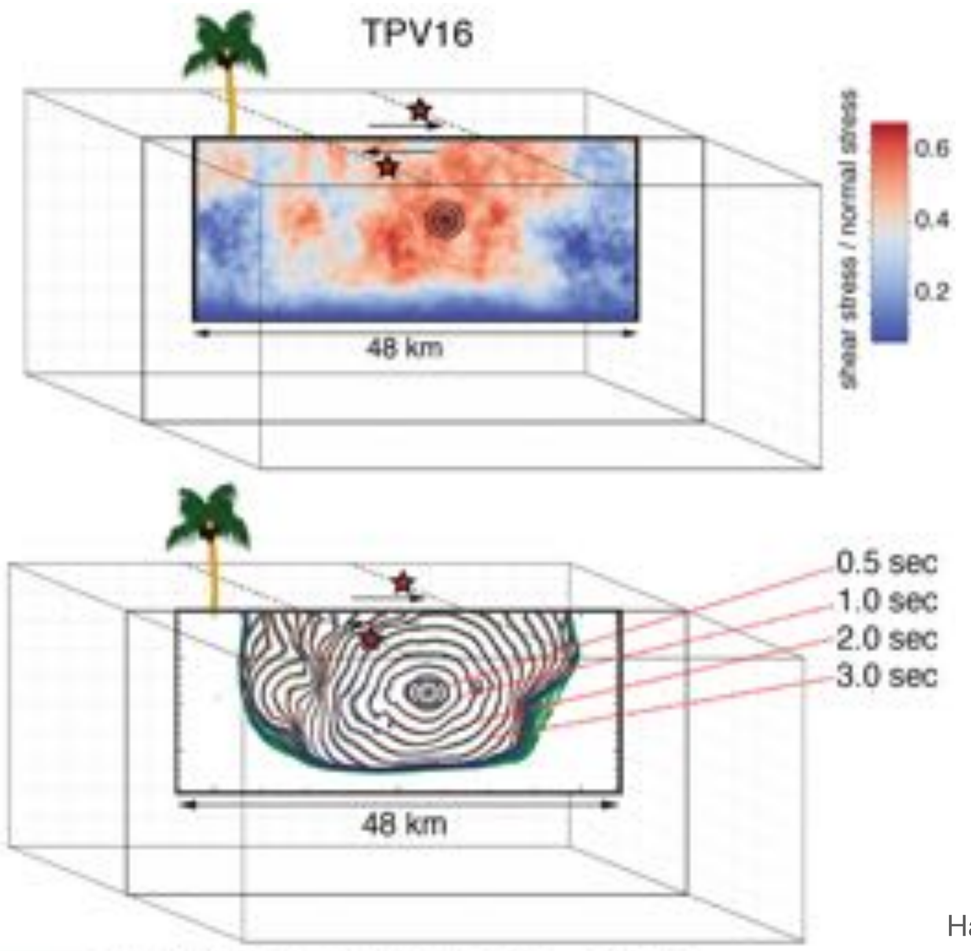

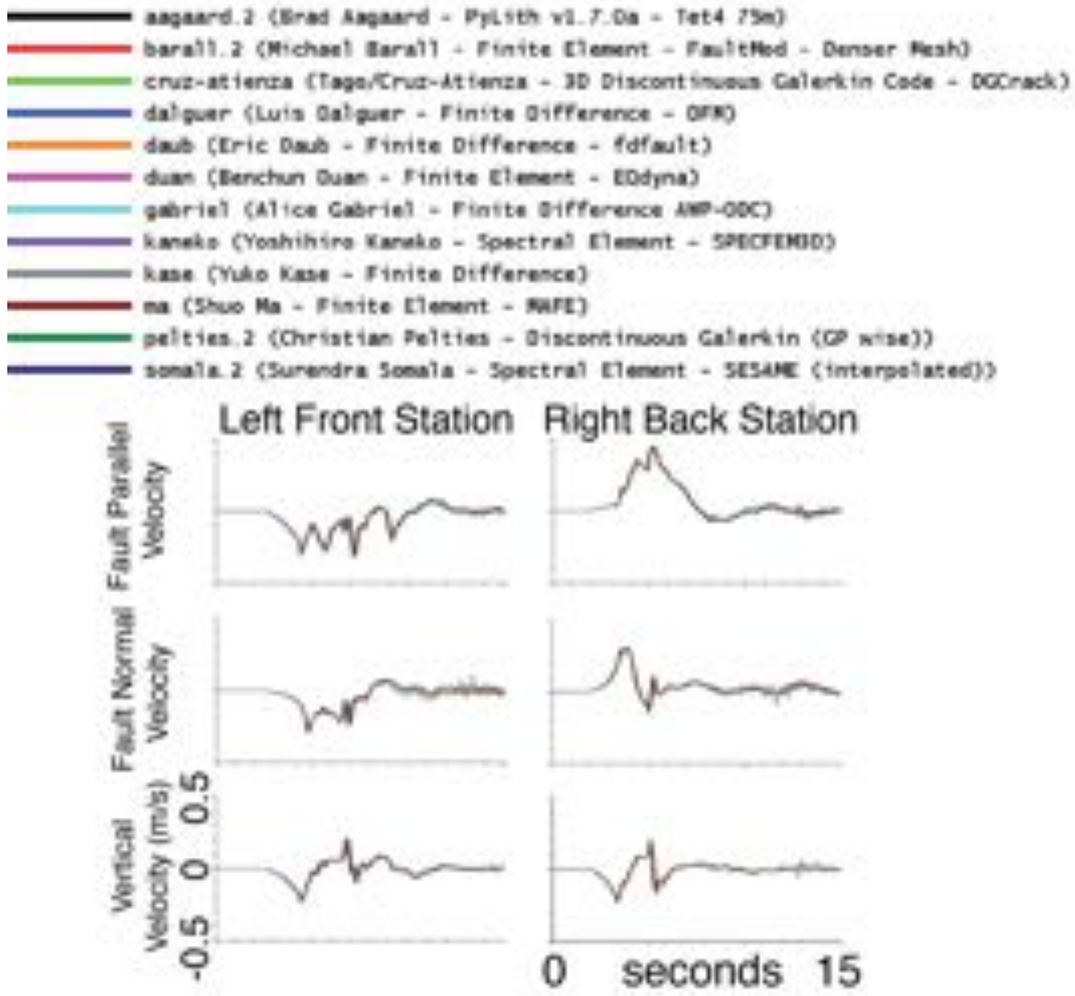

Harris et al., SRL 2018

Example

SCEC benchmark TPV3

http://web.gps.caltech.edu/~ampuero/fsem3d.html

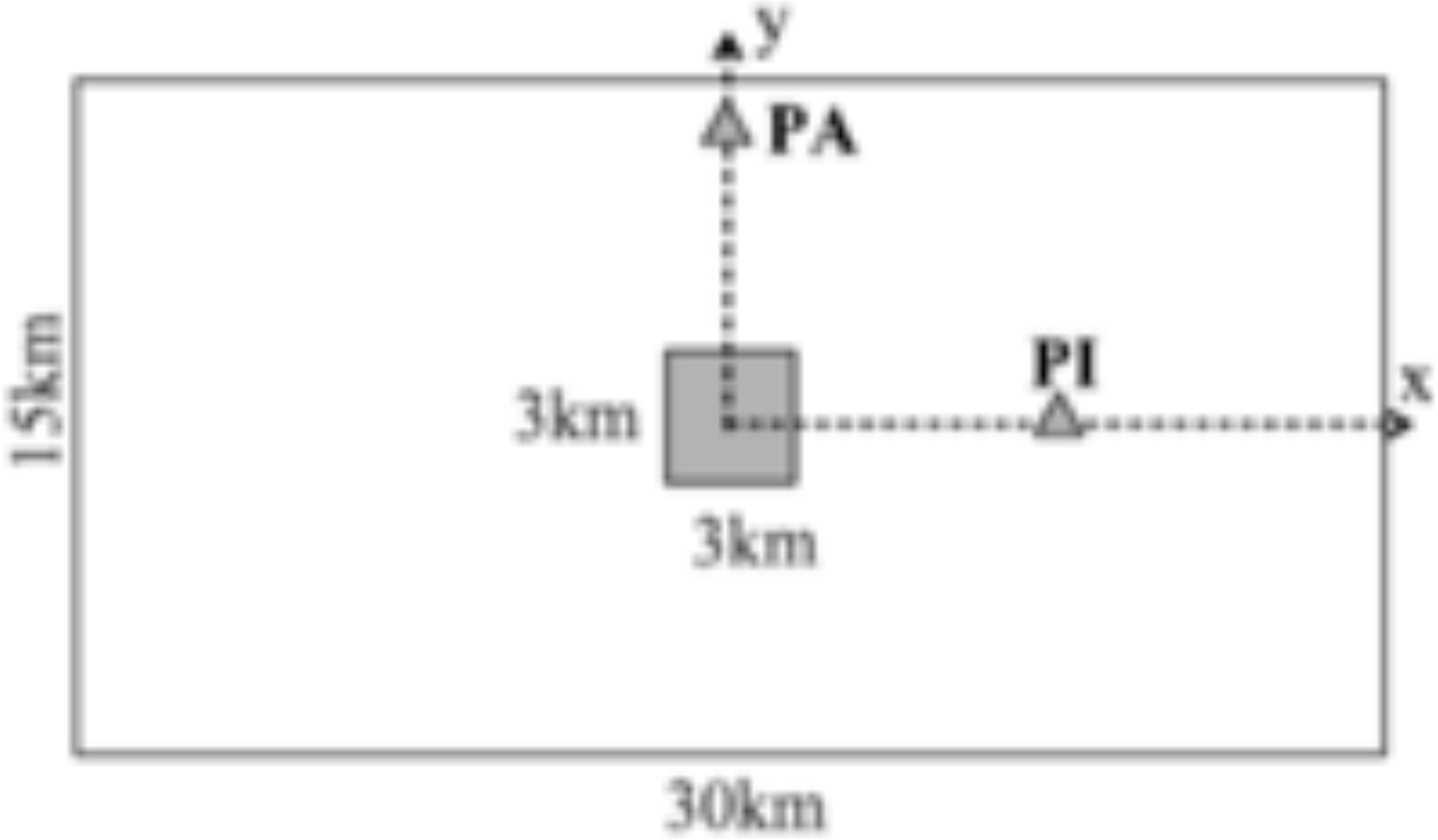

Example

SCEC benchmark TPV3

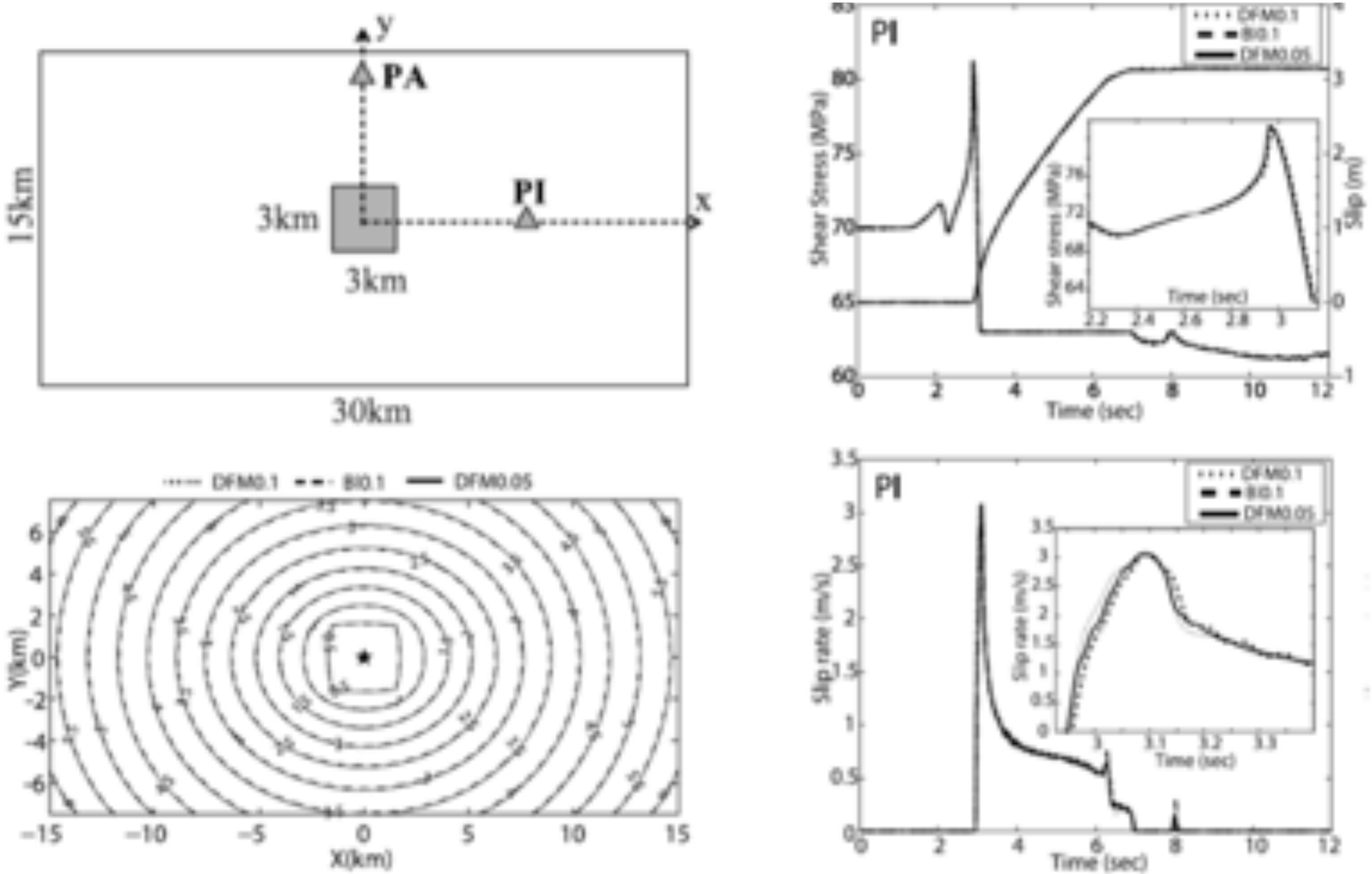

Day et al (2005)

Example

SCEC benchmark TPV3

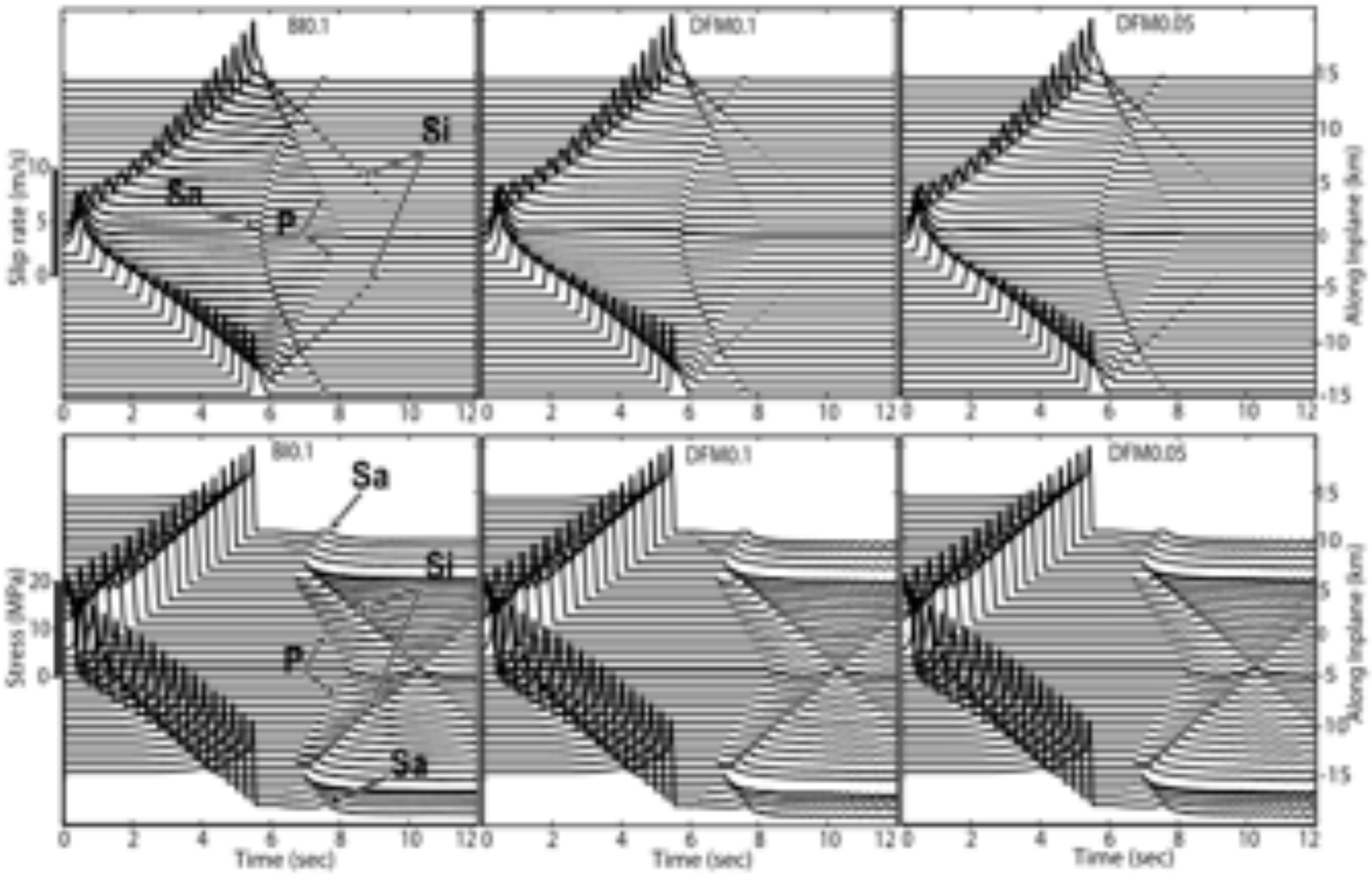

Figure 8. Time history of (top) slip rate and (bottom) shear stress for points along the axis of in-plane motion (*x* axis). The (left) BI0.1, (middle) DFM0.1, and (right) DFM0.05 solutions are shown. The labels P and Si correspond to the *P* and *S* waves, respectively, generated at the left and right edges of the fault (i.e., propagating predominantly along the axis of in-plane motion). The label Sa identifies the *S* waves generated at the top and bottom of the fault (propagating predominantly along the antiplane axis).

Example

SCEC benchmark TPV10

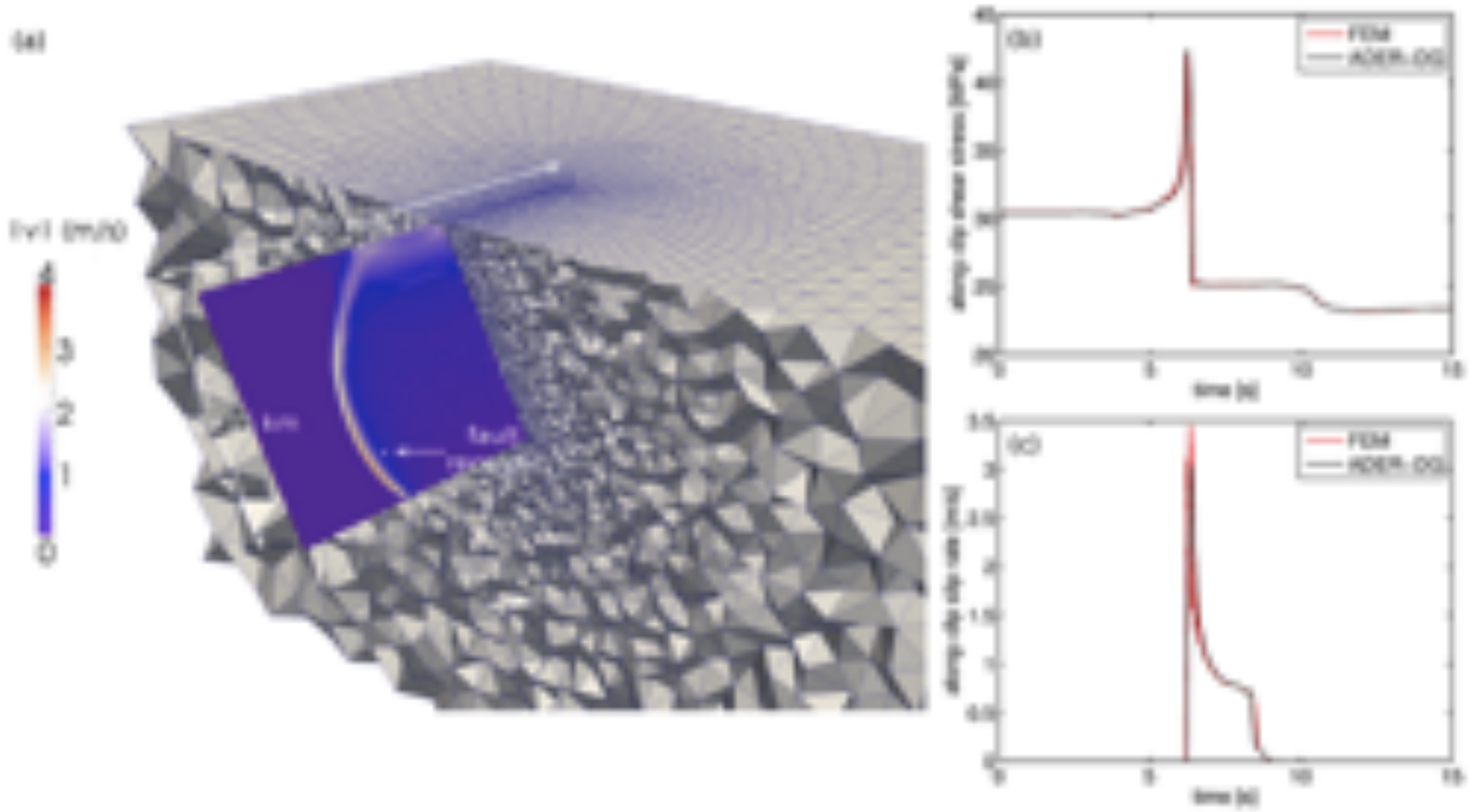

Fig. 1. **(a)** Asymmetric, unstructured mesh discretizing the dipping fault setup of benchmark problems TPV10 and TPV11 for SeisSol, and absolute slip rate $|v|$ on the fault plane at $t = 7.4$ s of TPV10 (subshear scenario). **(b)** Along-dip slip rate and **(c)** along-dip shear stress on a fault location at 7.5 km along-strike and 12 km along-dip in TPV10. The ADER-DG solution is shown in black, the FEM solution in red.

Example

SCEC benchmark TPV10

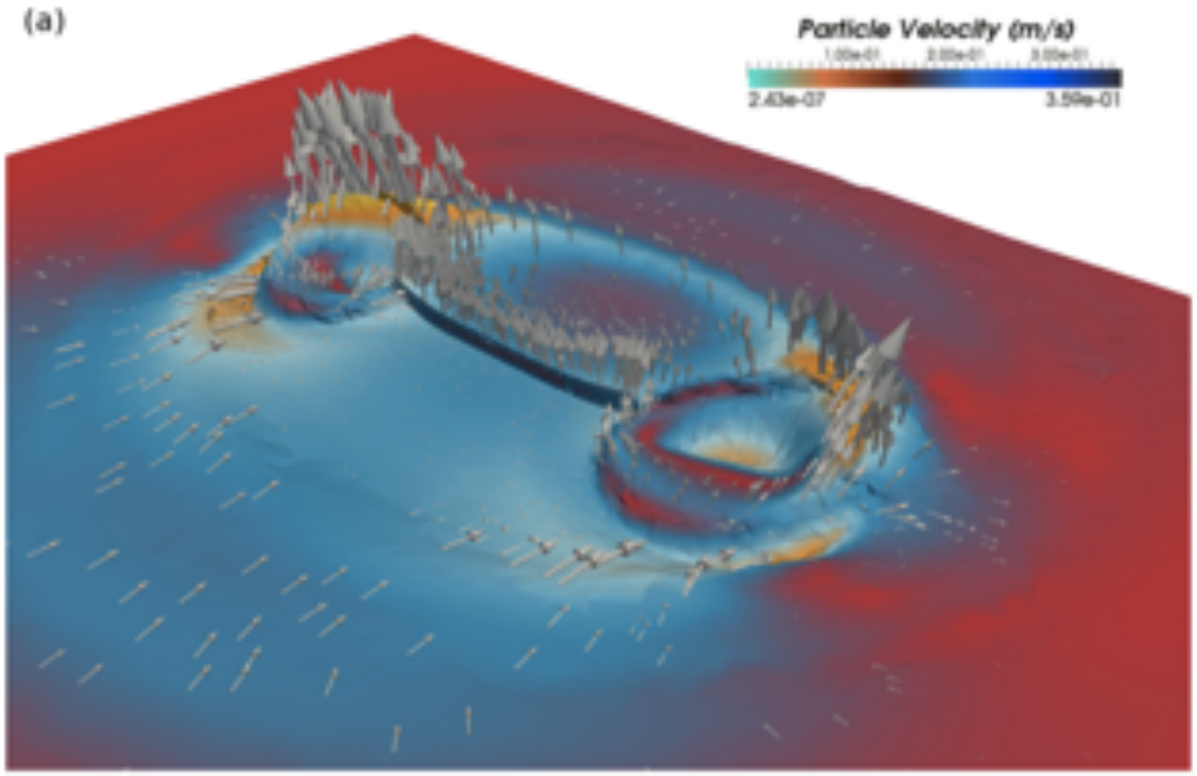

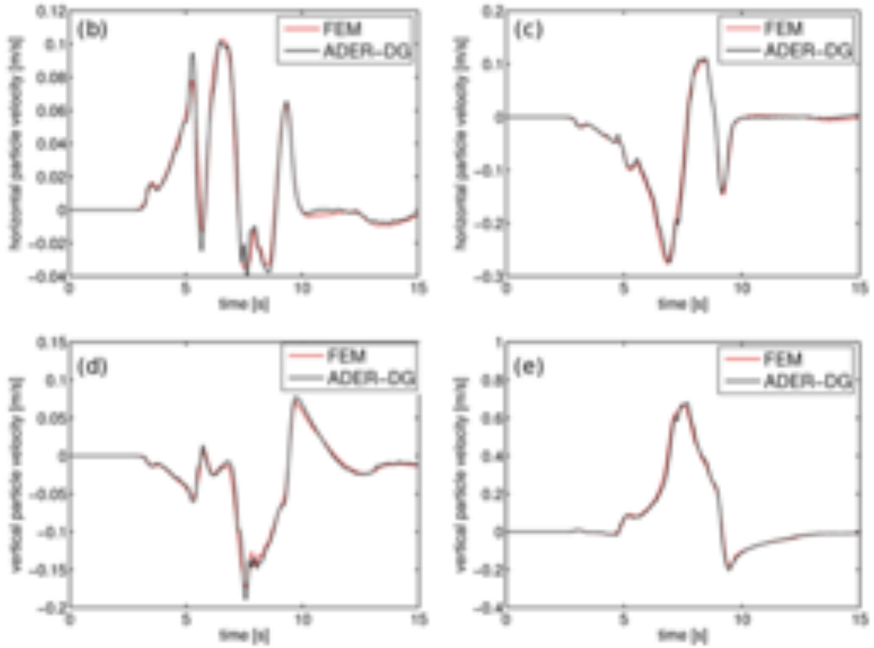

Fig. 3. (a) Asymmetric ground motion in the surrounding of the dipping fault at $t \approx 8$ s in TPV10. The color scale indicates the magni
absolute particle velocity at the surface, arrows and surface morphology reflect its direction. (b) and (c) are horizontal ground veloci
series at seismic stations located 3 km away from the fault trace and 12 km along-strike on the foot wall and hanging wall, respectiv
and (e) are the vertical ground velocities at the same stations. The ADER-DG solution is shown in black, the FEM comparison sol
red.

Example

SCEC benchmark TPV10

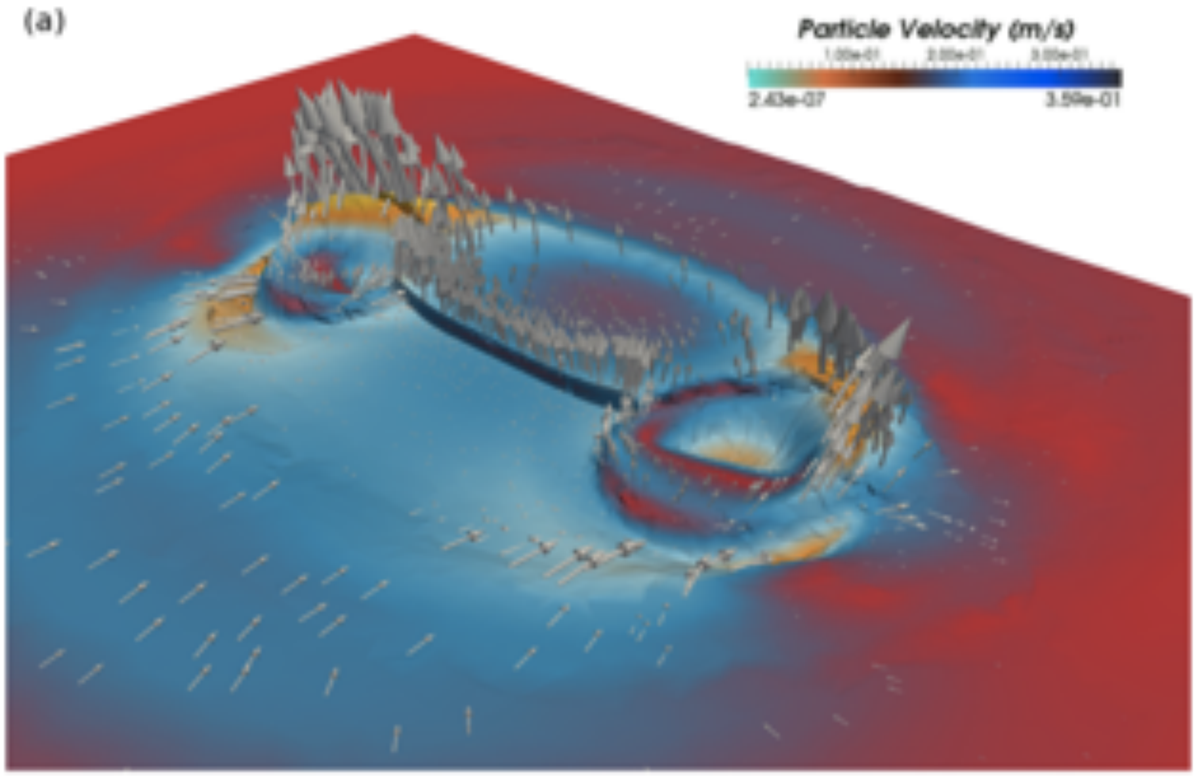

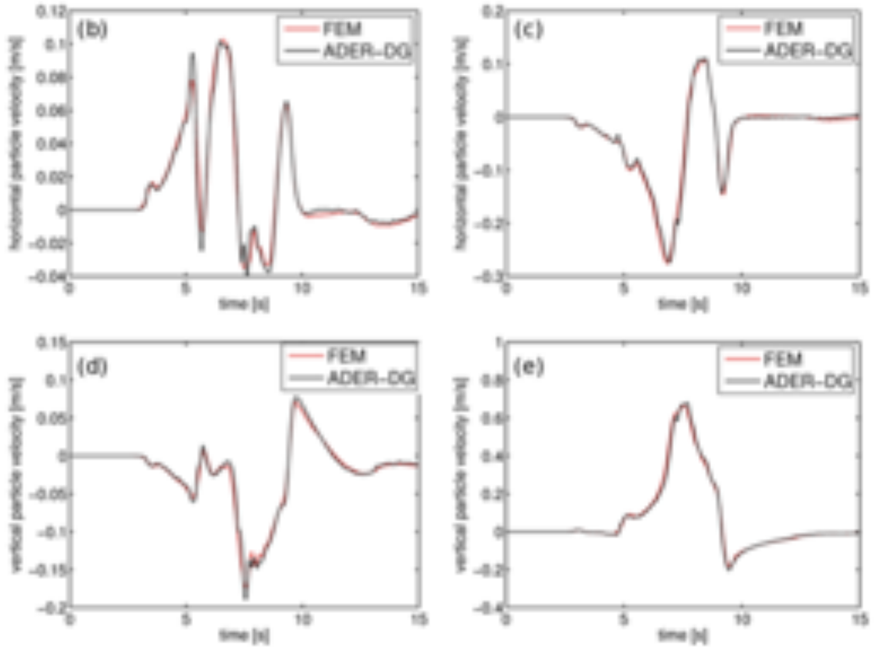

Fig. 3. (a) Asymmetric ground motion in the surrounding of the dipping fault at $t \approx 8$ s in TPV10. The color scale indicates the magni
absolute particle velocity at the surface, arrows and surface morphology reflect its direction. (b) and (c) are horizontal ground veloci
series at seismic stations located 3 km away from the fault trace and 12 km along-strike on the foot wall and hanging wall, respectiv
and (e) are the vertical ground velocities at the same stations. The ADER-DG solution is shown in black, the FEM comparison sol
red.

Rupture on a branched fault system

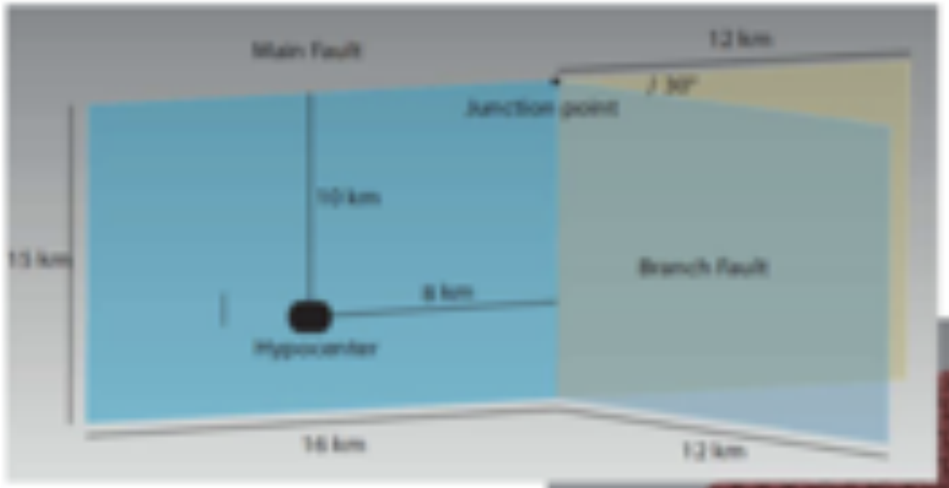

Spectral element mesh

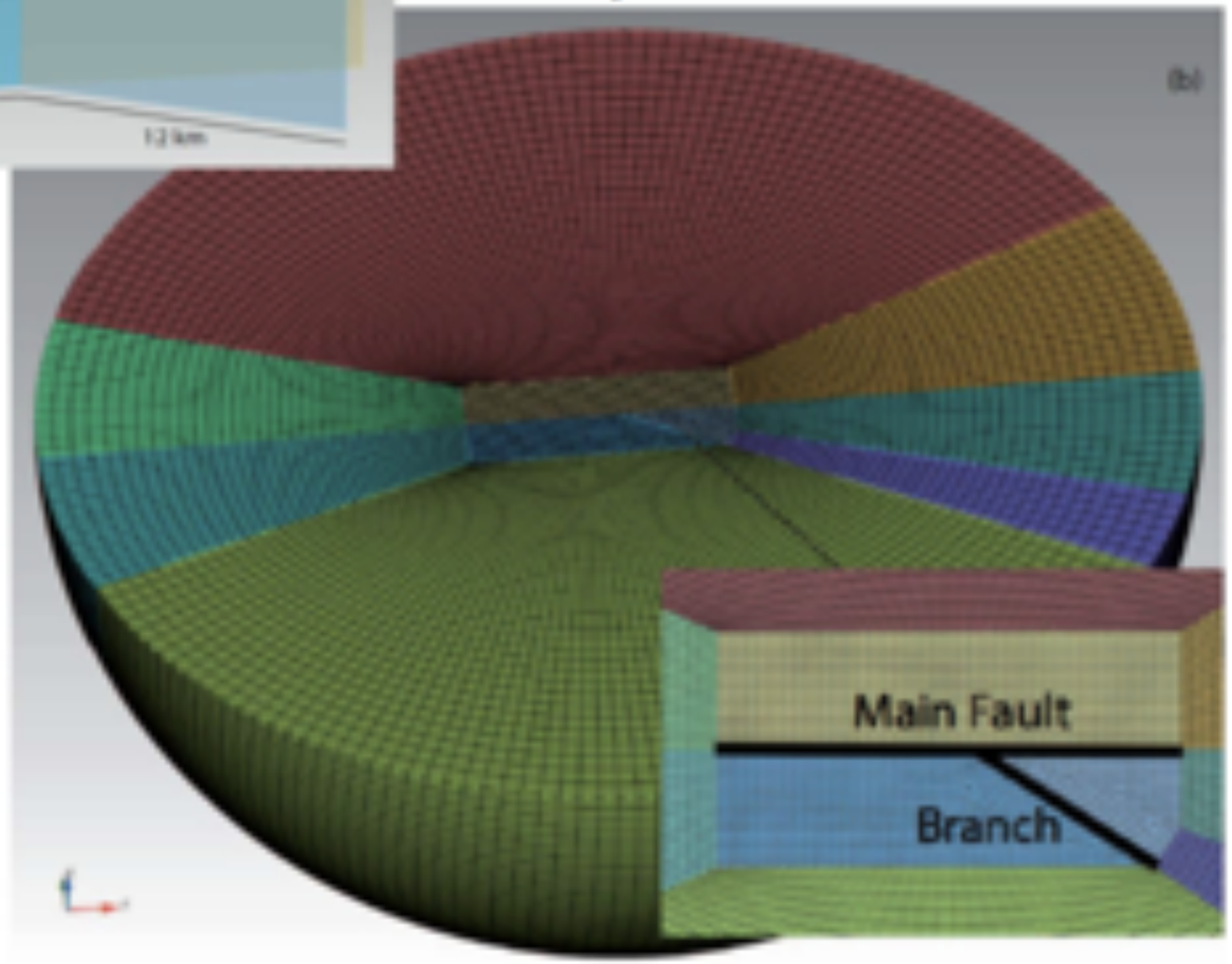

Galvez et al (2014)

Example

SCEC benchmark TPV24

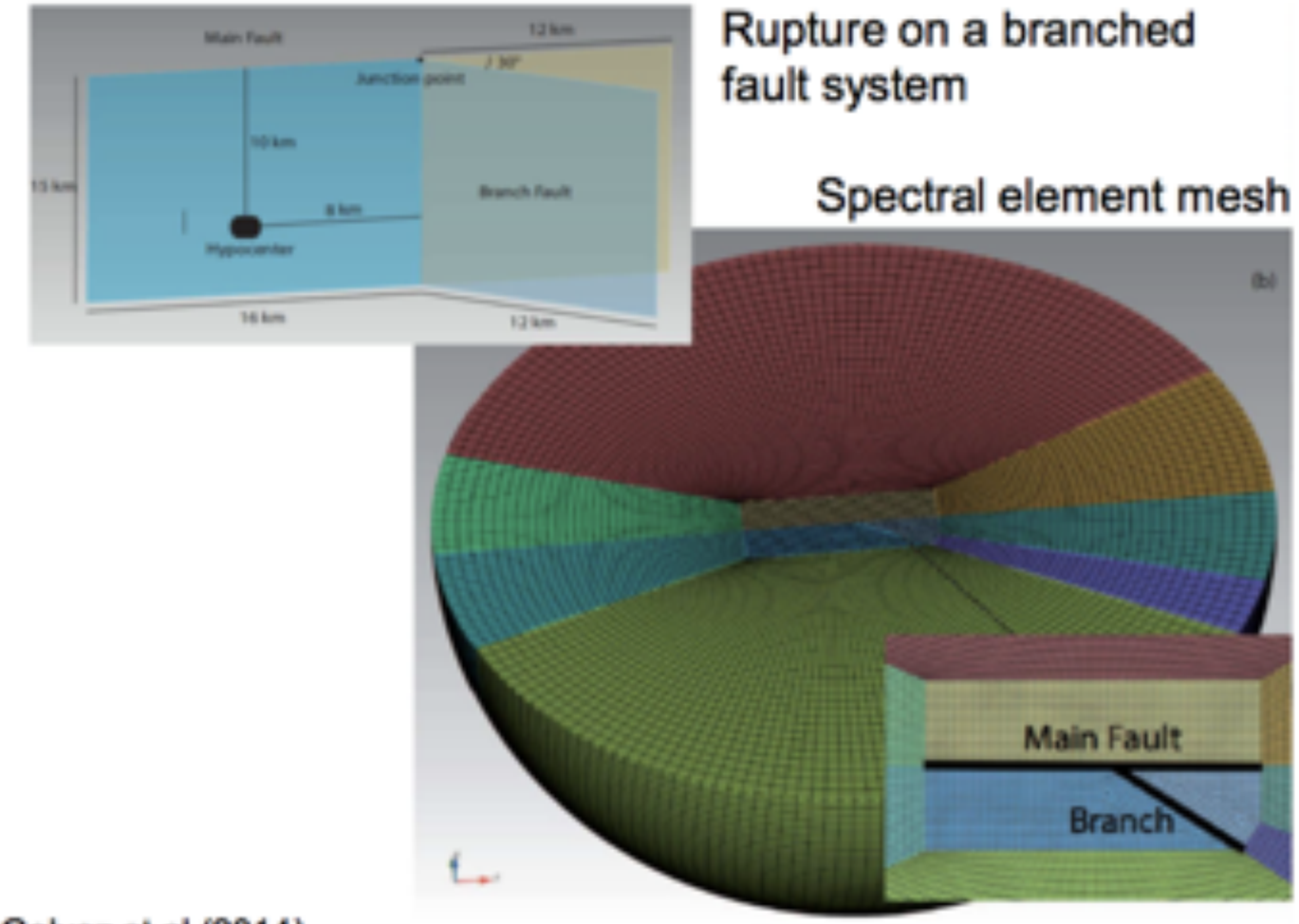

Rupture on a branched fault system

Spectral element mesh

Galvez et al (2014)

ruptures on rough faults

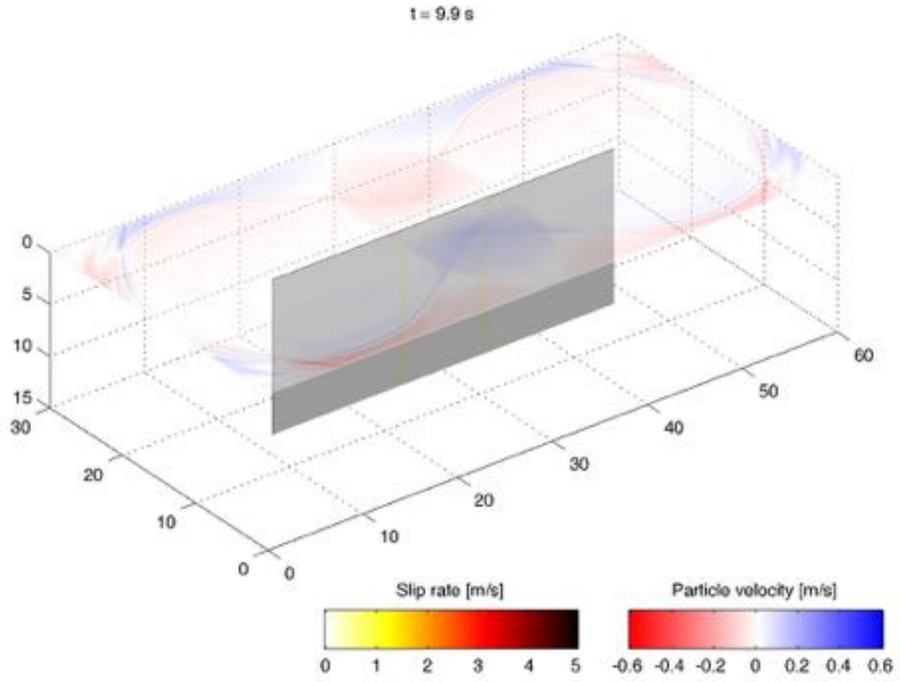

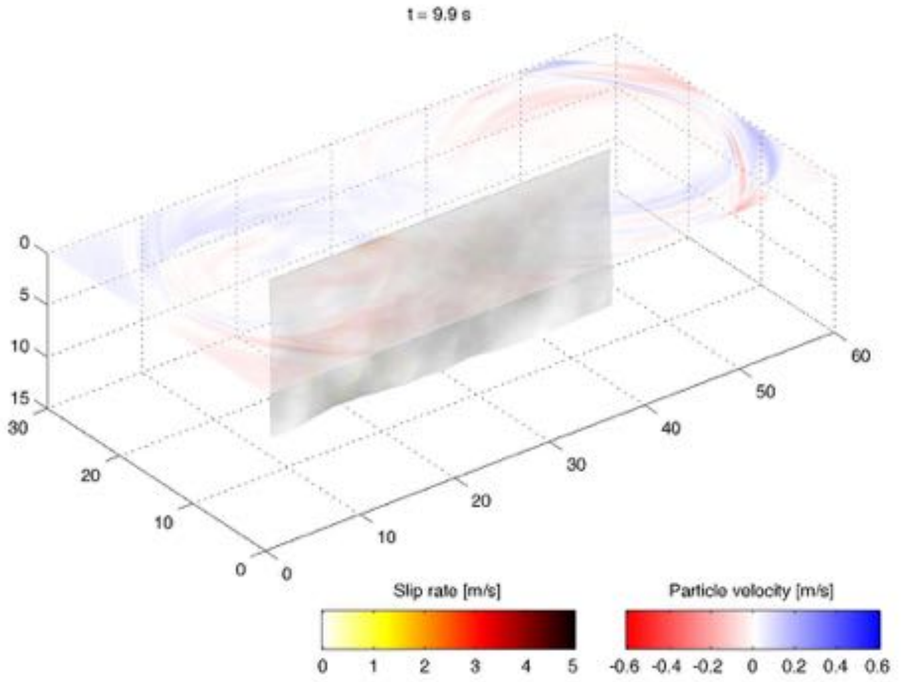

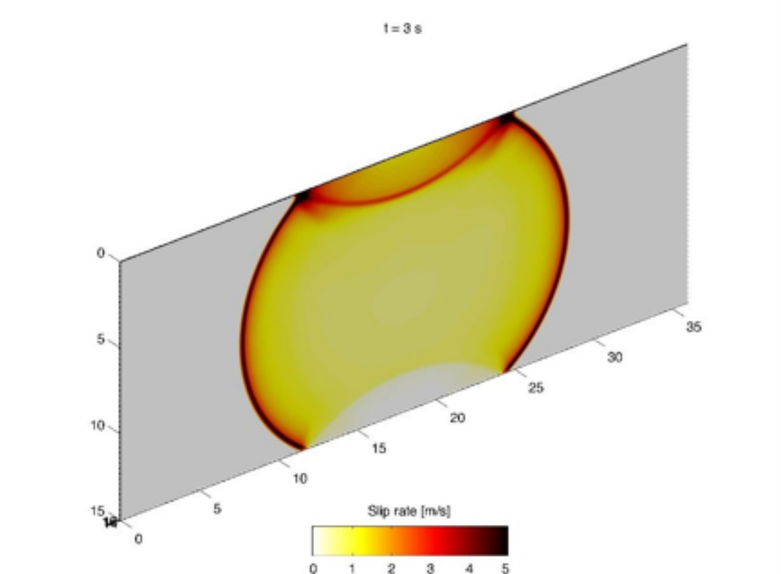

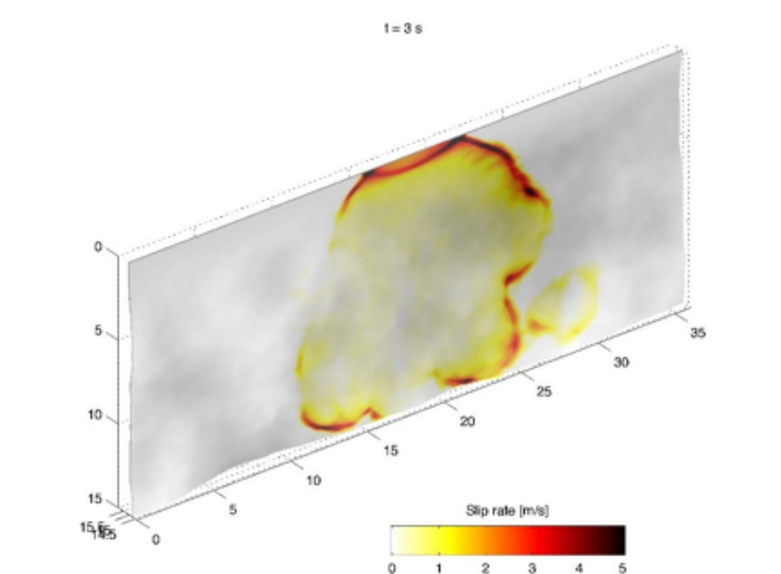

ruptures on rough faults

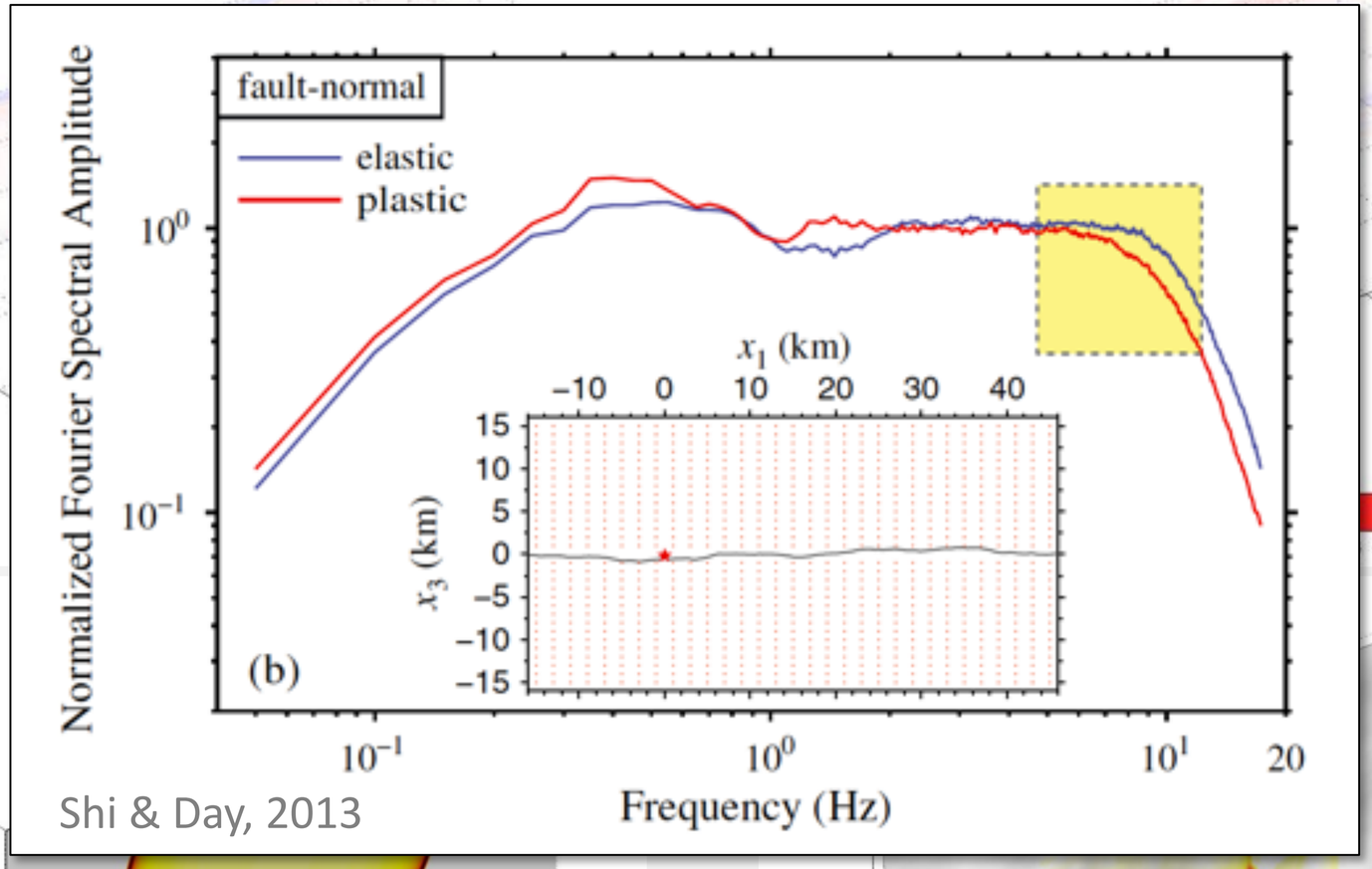

Shi & Day, 2013

ruptures on rough faults

uniform background stress tensor

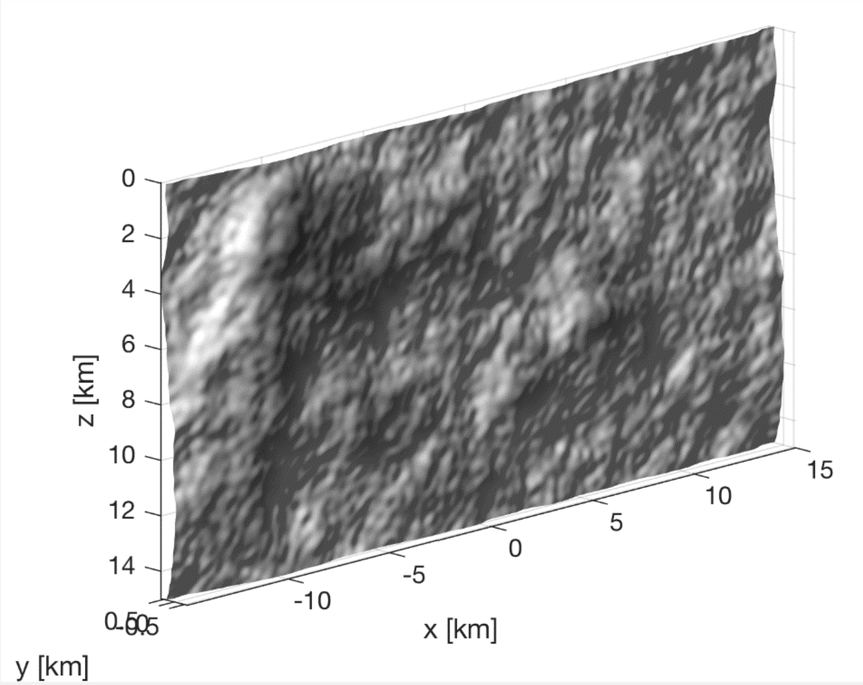

normal traction

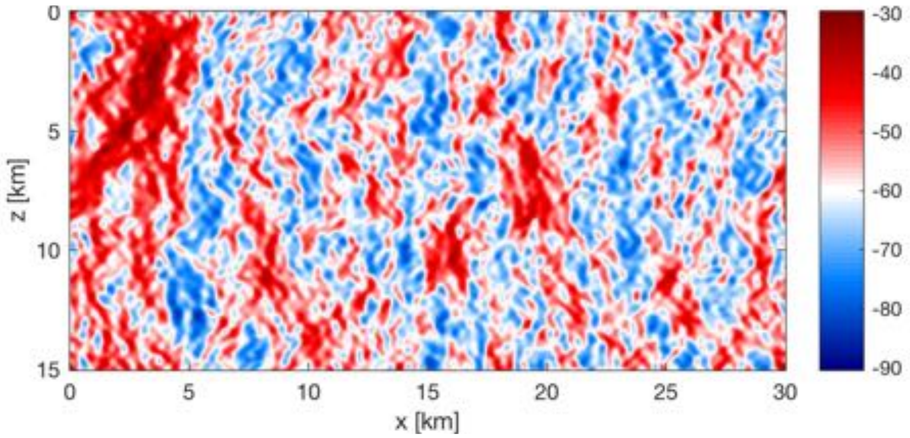

shear traction

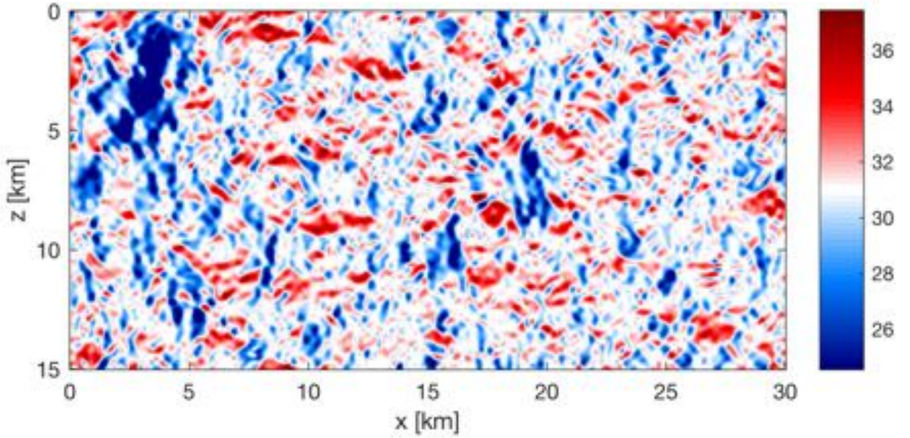

ruptures on rough faults

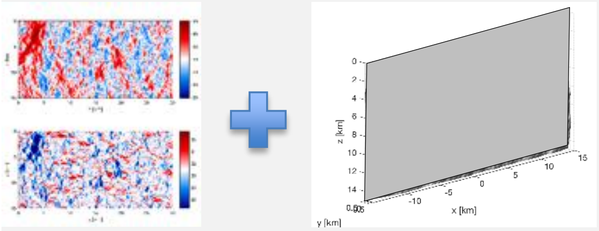

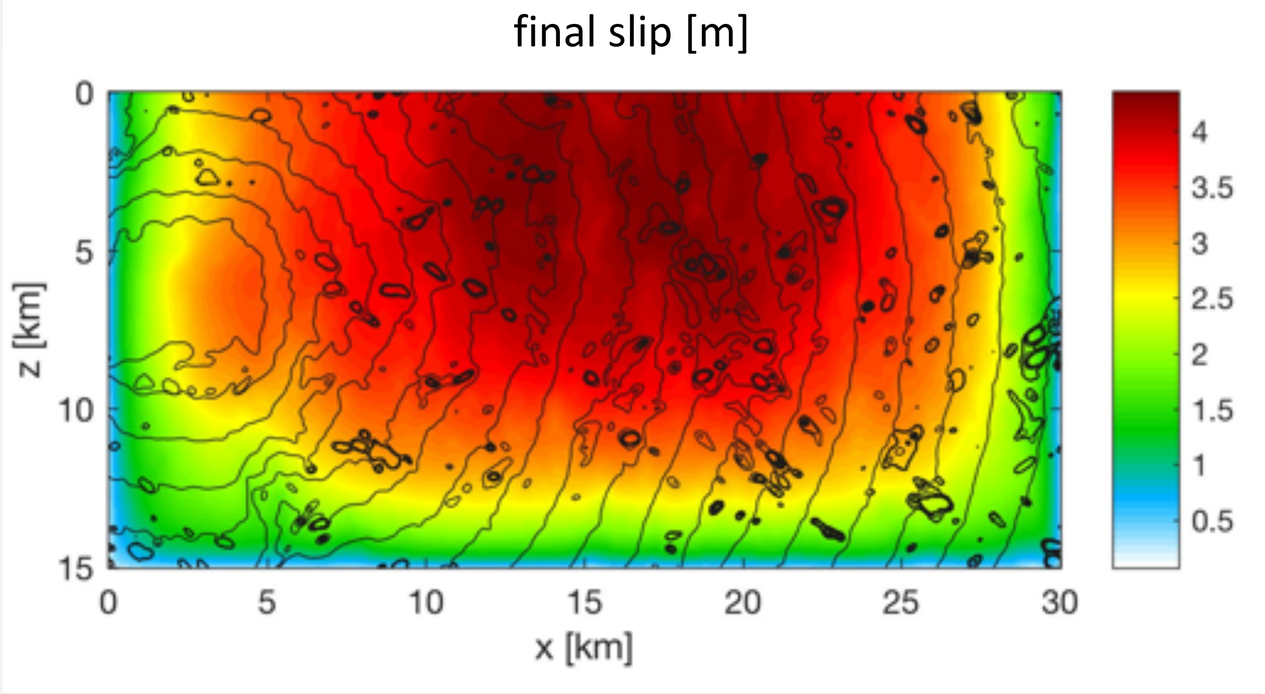

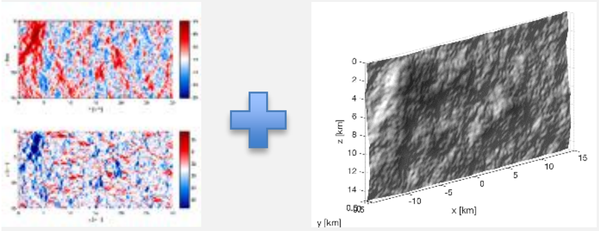

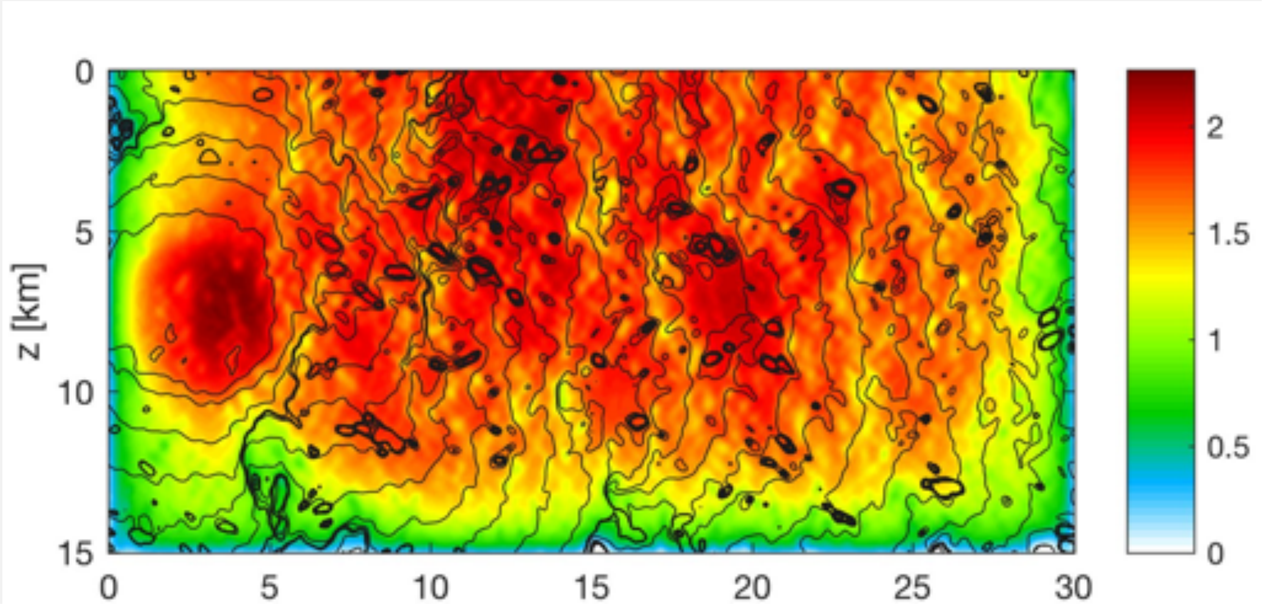

ruptures on rough faults

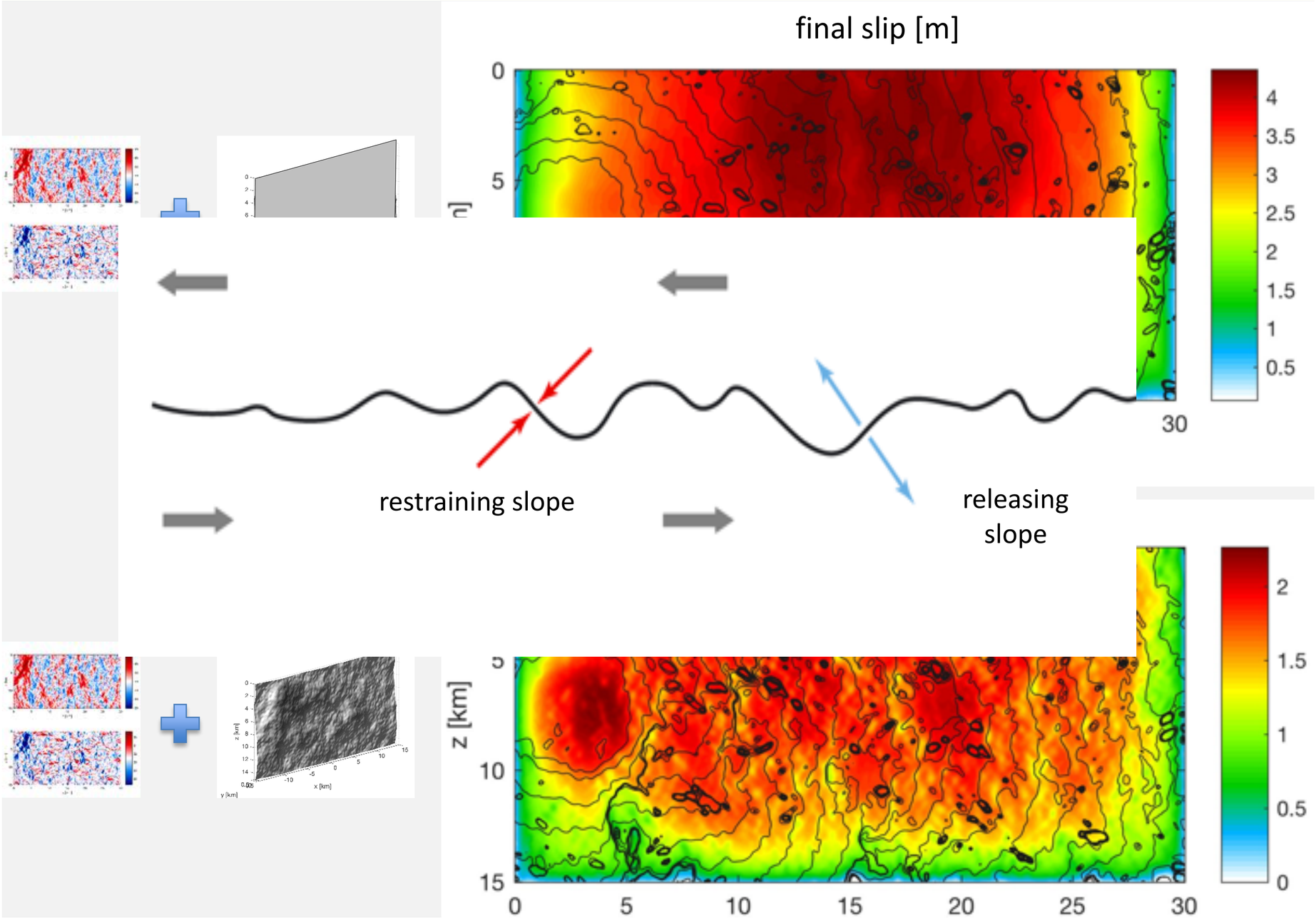

induced seismicity

Fluid injection creates overstressed patched,
i.e., zones weakened by increased pore pressure

Producers are obliged to report injected volumes to authorities

The conditions in such overstressed patch are better constrained
than for natural earthquakes

Induced seismicity provides a unique opportunity
to better understand earthquake ruptures

hydraulic fracturing (fracking)

- fluid is repeatedly injected into well under **high pressure** to stimulate flow of gas or oil and to enhance production
- fracking intentionally induces micro-earthquakes (vast majority with Mw < 1)
- involves both tensile and shear failures

Similar procedures during stimulation phase of EGS

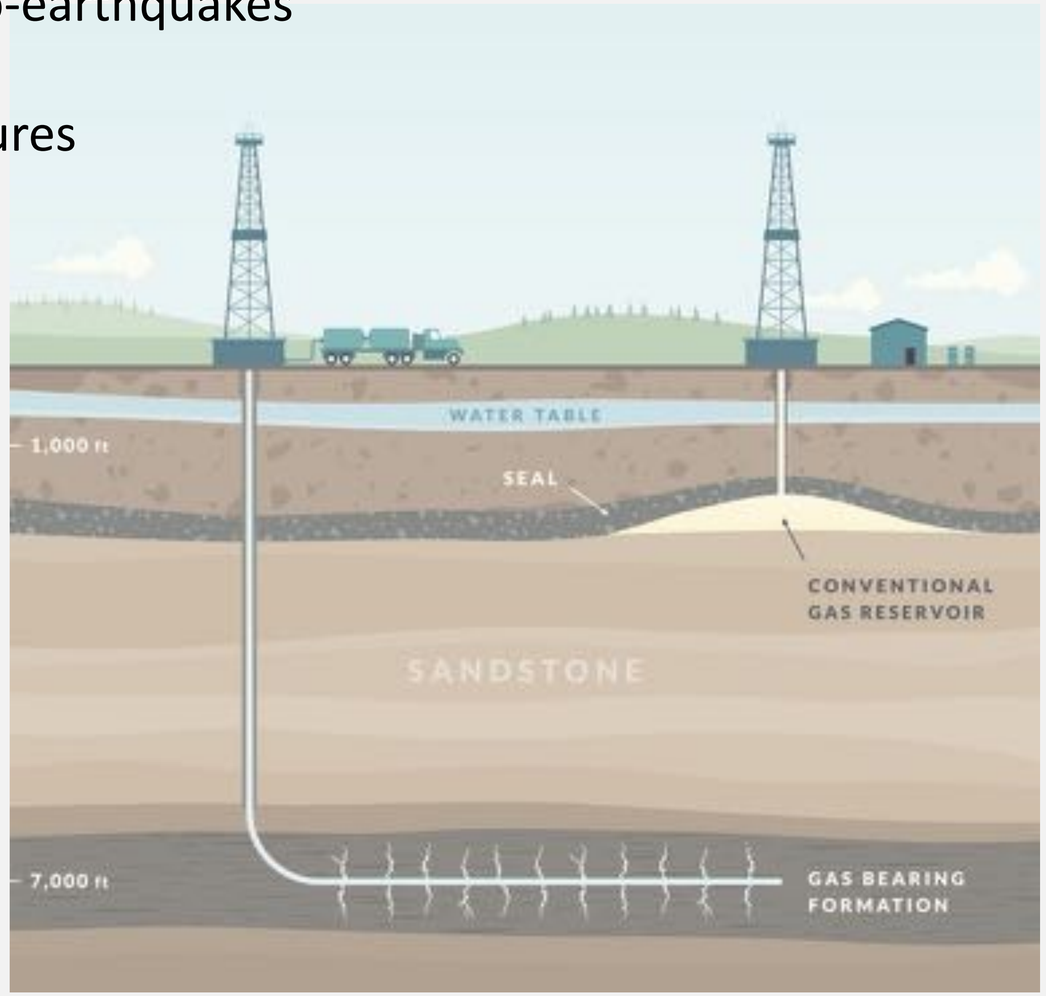

deep injection

- *wastewater disposal*
  into old/depleted oil/gas reservoirs
  or
  geothermal energy:
  (cold) water is injected into deep hot formations to produce hot water or steam

- stimulation/fracking may be used to improve flow in the reservoir, but generally, seismicity is not intentional and is usually quite low
- **the largest induced earthquakes are linked with deep injection**
- the earthquakes are triggered/induced by increased pore pressure

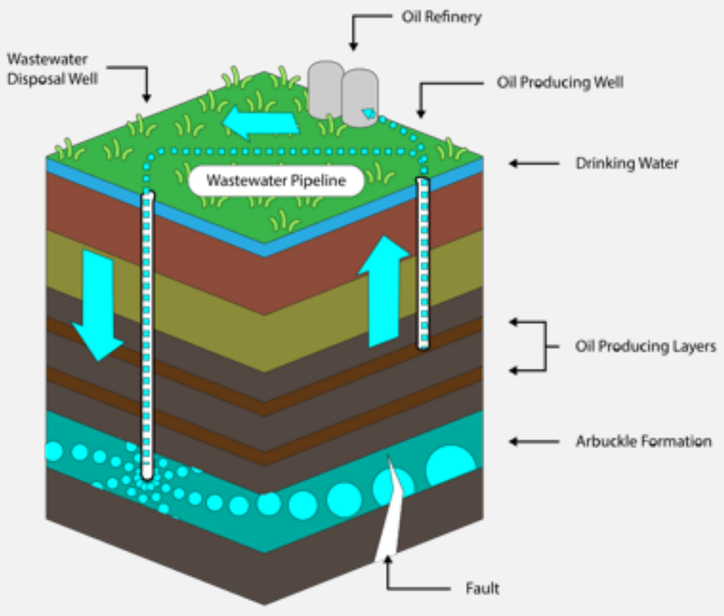

Based on original image by Steven Tian

Waste water disposal and hydro-frackinig in Oklahoma and Kansas

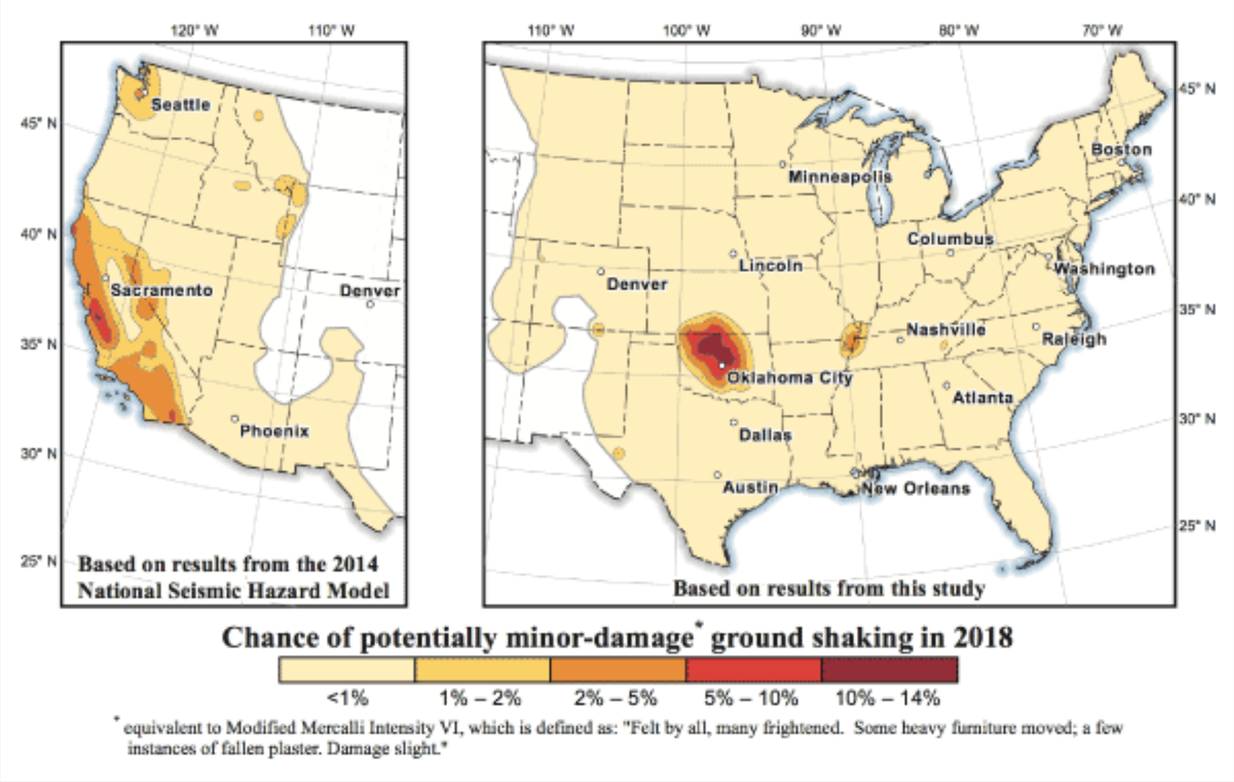

For 2018, due to extensive fluid-injection activities, the probability of inducing/triggering a minor-damage earhquake in Oklahoma and Kansas is higher than having a similar size natural earthquake in California

EGS Basel

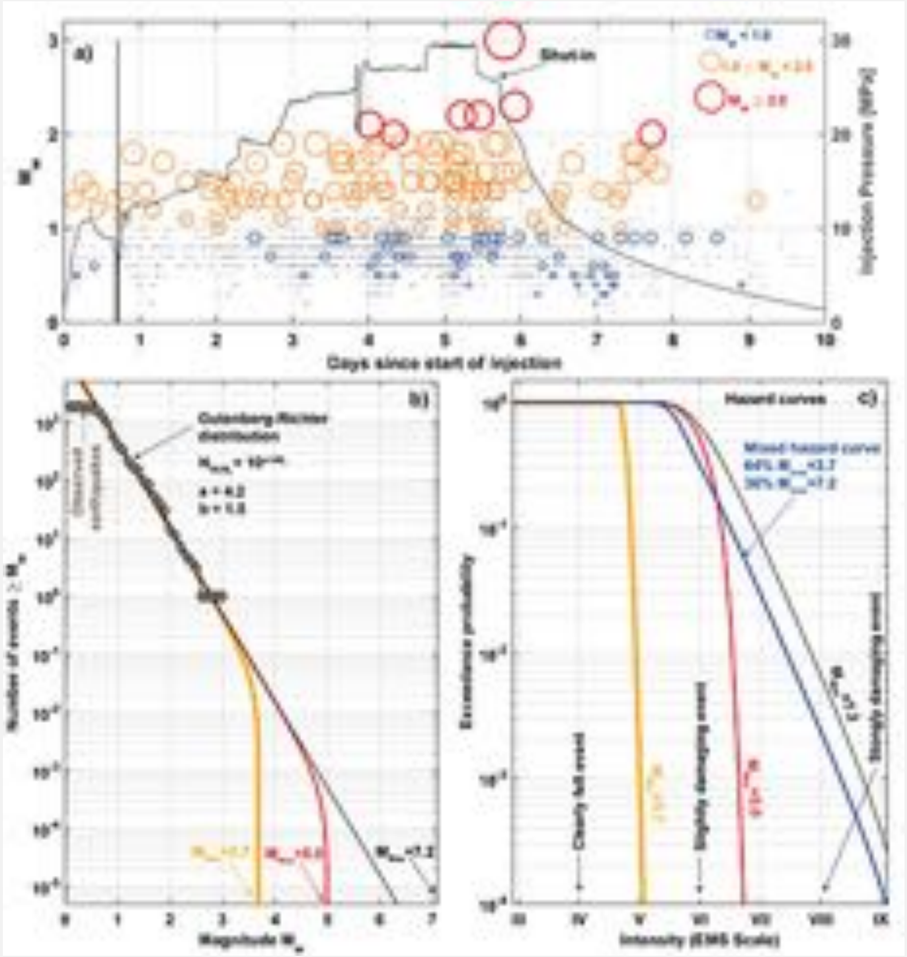

The stimulation of the reservoir has stopped only after 6days after Mw 3.4 event

arrested and runaway ruptures

laboratory experiments
revealing arrested ruptures

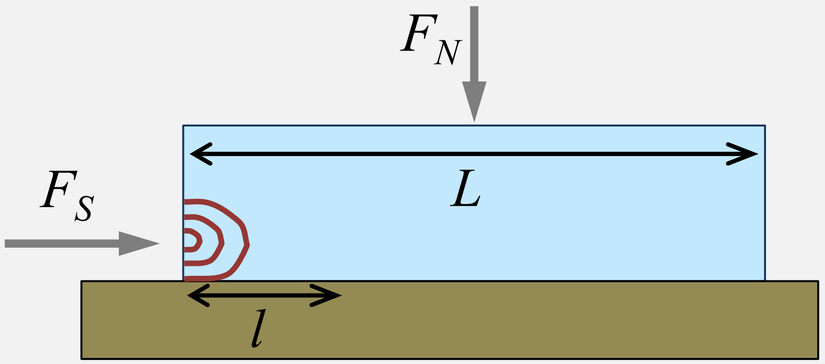

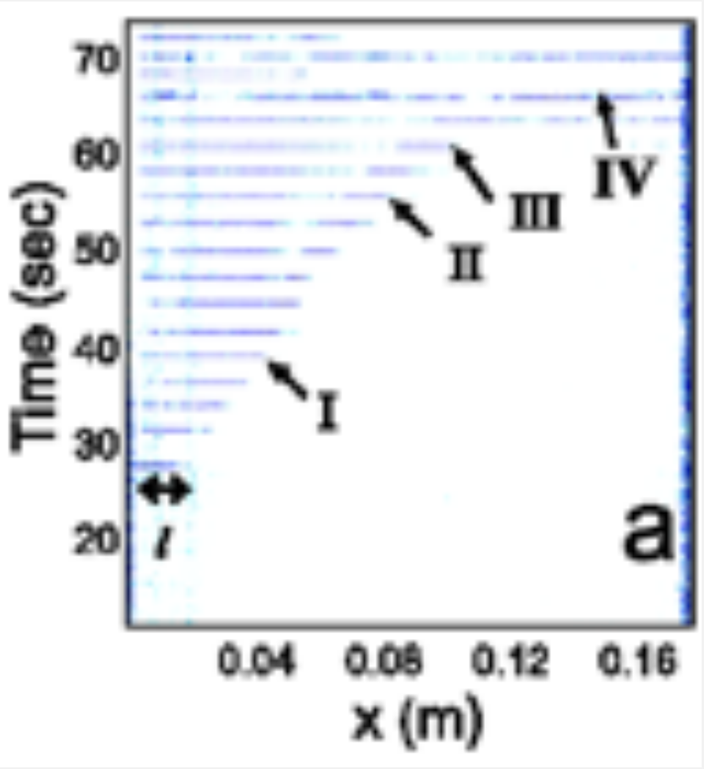

Rubinstein, Cohen and Fineberg (2007)

arrested and runaway ruptures

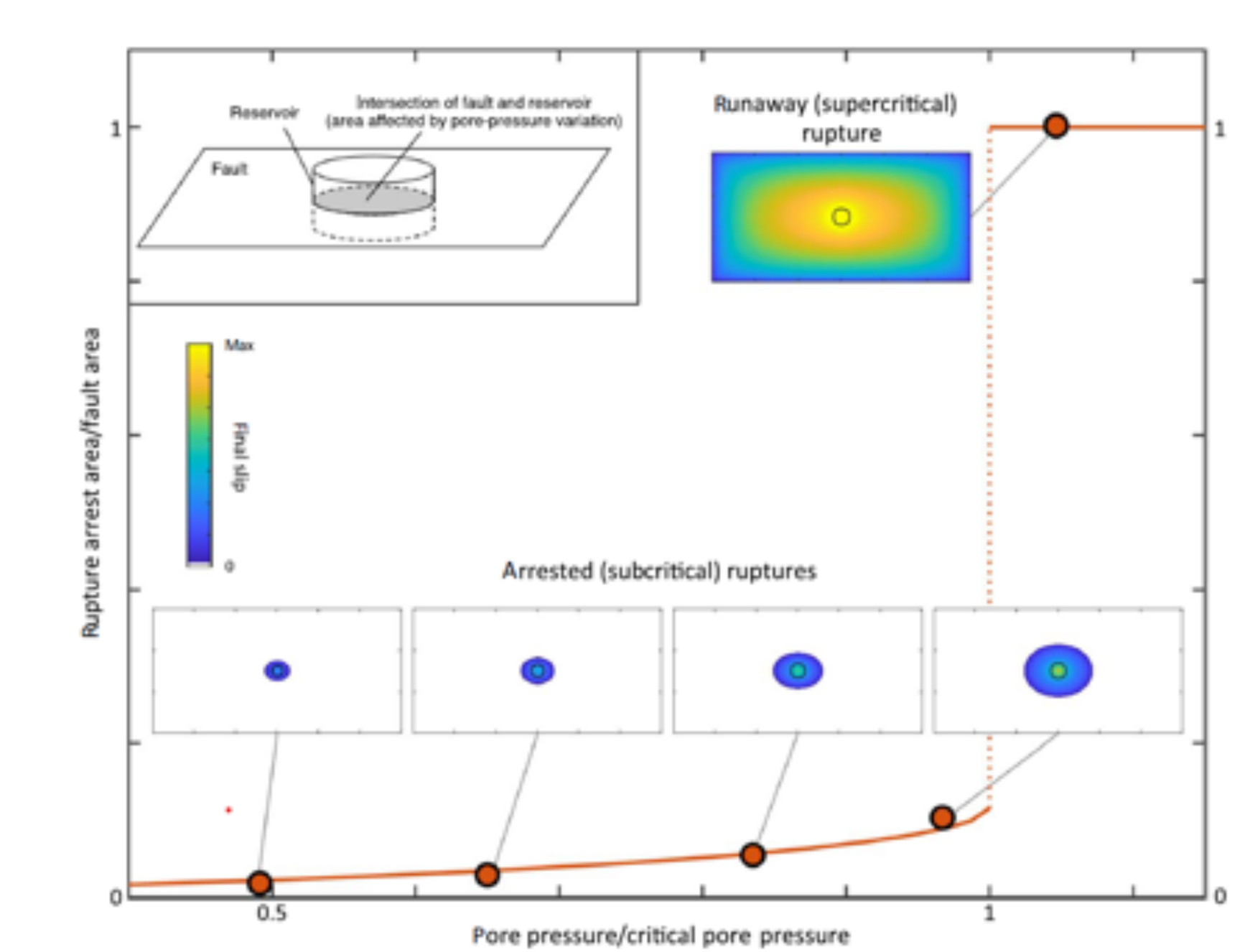

arrested and runaway ruptures

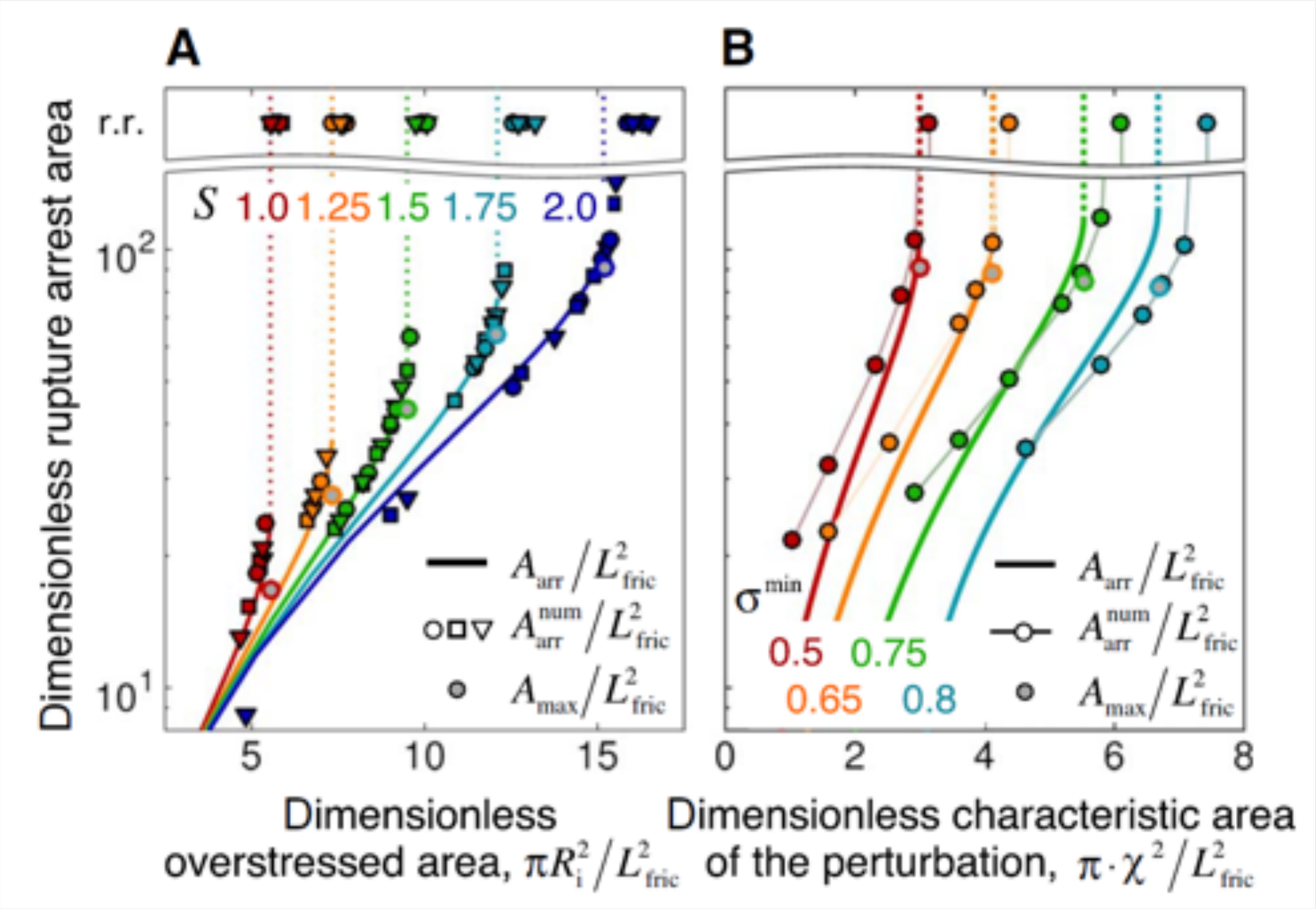

introduction: **arrested and runaway ruptures**

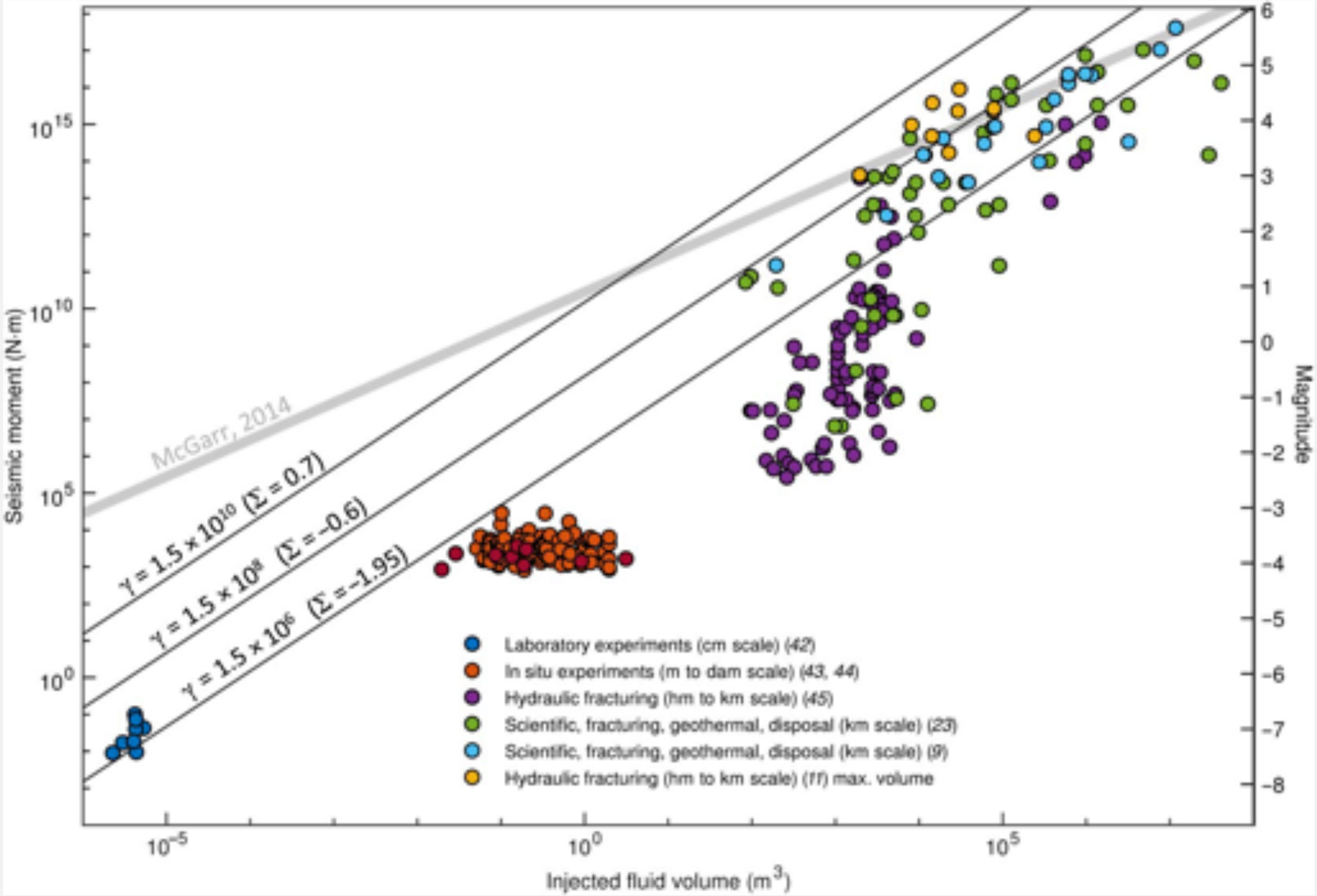

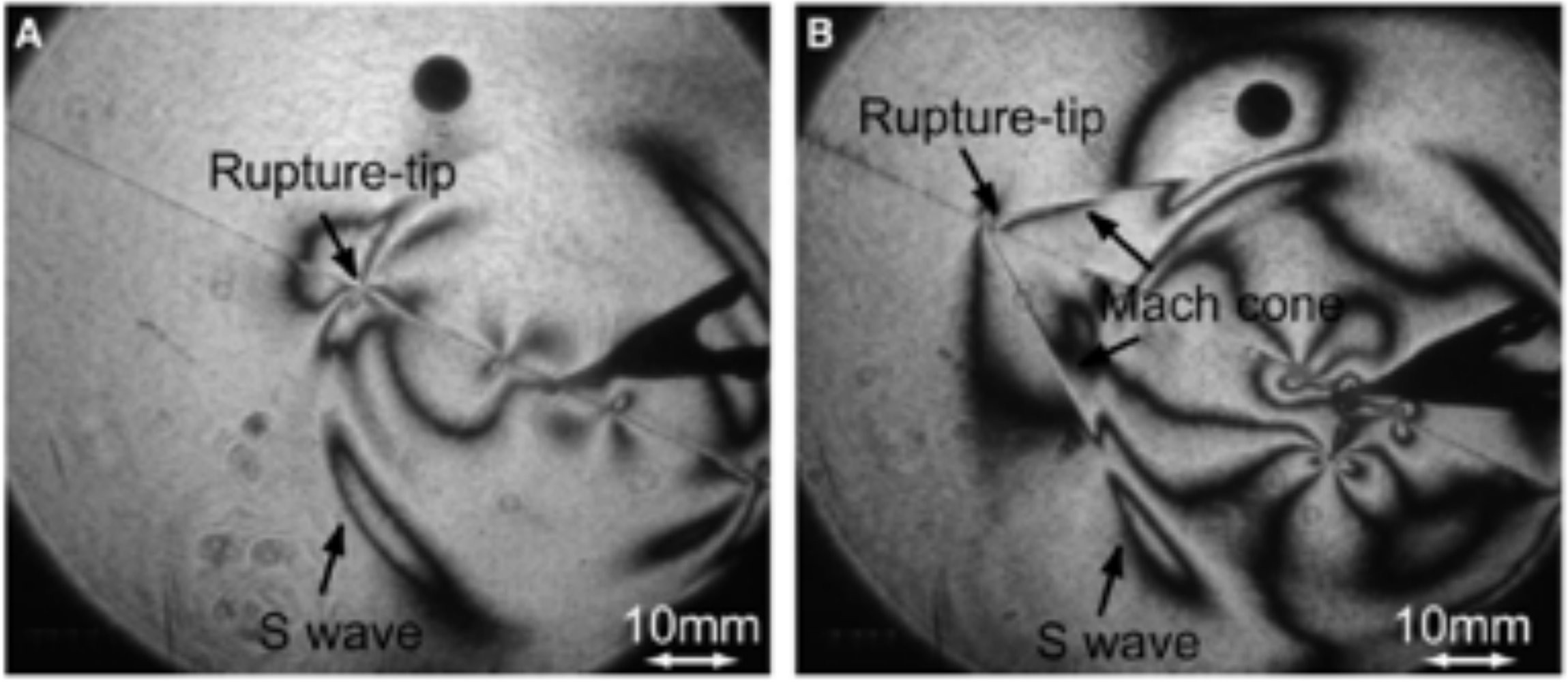

Fig. 2. Purely sub-Rayleigh ($\alpha = 25°$ and $P = 7$ MPa) (**A**) and purely supershear ($\alpha = 25°$ and $P = 15$ MPa (**B**) rupture at the same time (28 μs) after triggering.

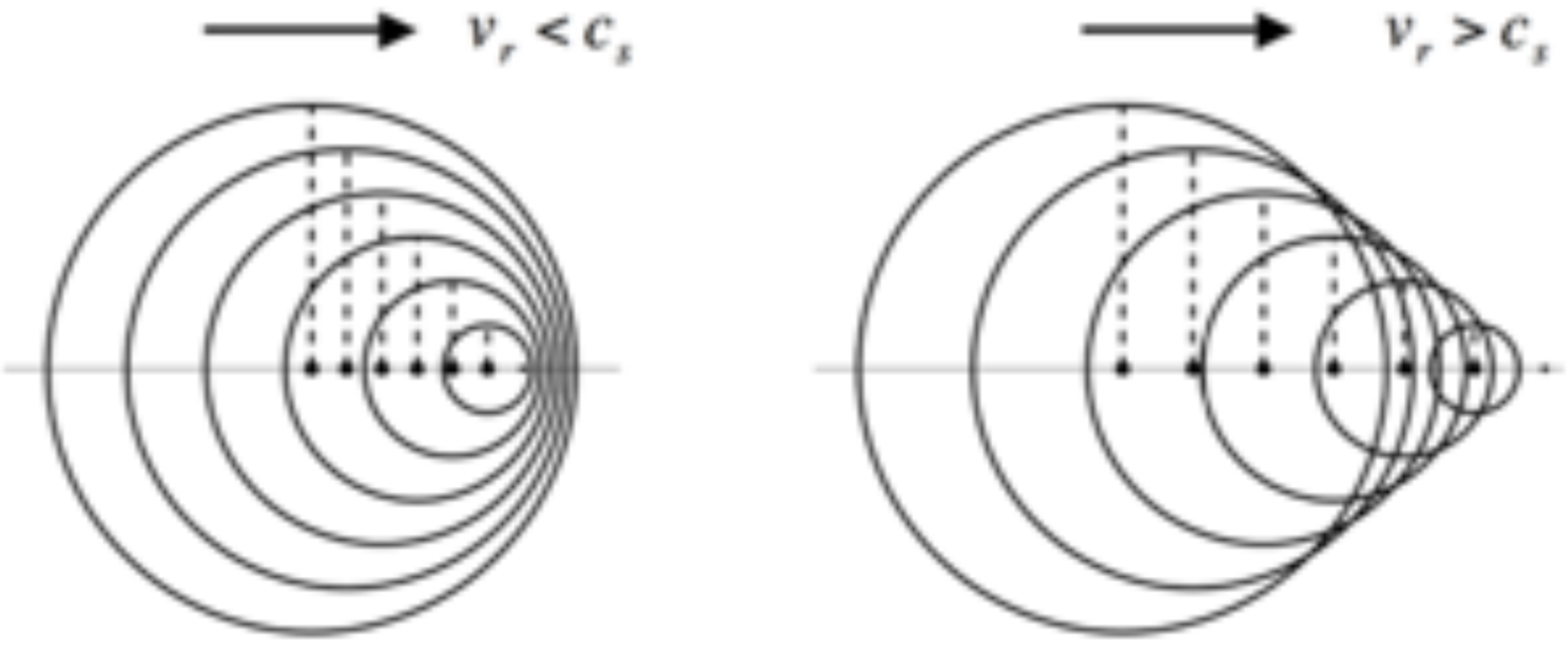
$v_r < c_s$
$v_r > c_s$

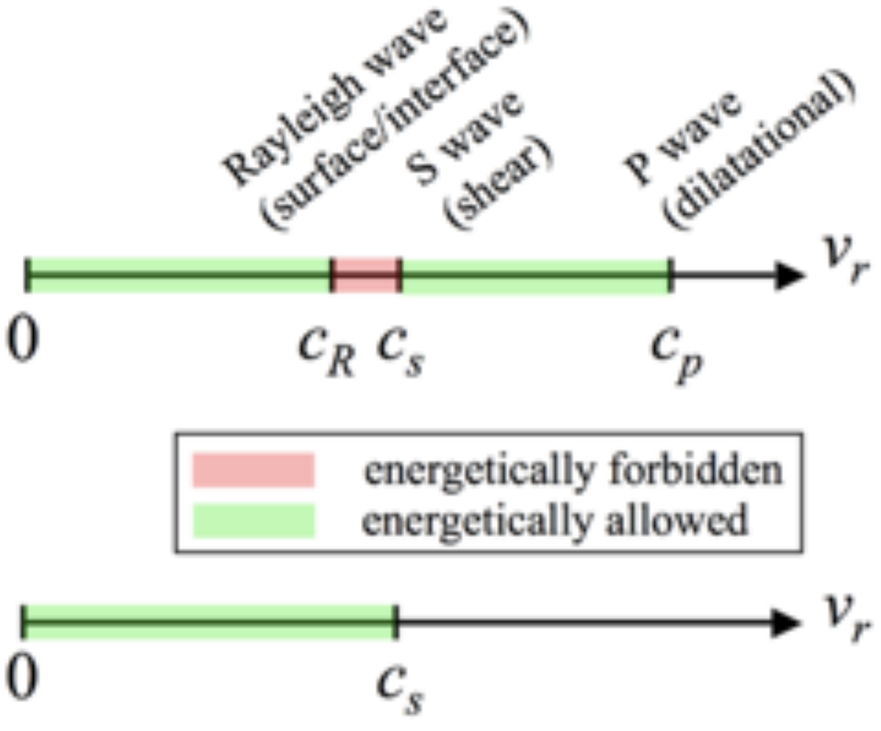
Rayleigh wave
(surface/interface)
S wave
(shear)
P wave
(dilatational)
v_r
0
c_R c_s
c_p
energetically forbidden
energetically allowed
v_r
0
c_s

Physics-based Coupled Models of the 2018 Sulawesi Earthquake and Tsunami

Large-scale, realistic model set-up

- Dynamic earthquake rupture coupled with seismic wave propagation, off-fault plasticity and fast-velocity weakening friction (μ_S=0.6, μ_d=0.1) is modeled with SeisSol. (https://github.com/SeisSol/SeisSol)
- Combines two **3D velocity models of the crust and at depth** (Awaliah et al.,2018; Fichtner et al.,2018) and high resolution **topography/bathymetry** (GEBCO, 30 arc seconds)
- Complex **fault geometries** are built from traces delineated by Sentinel-2 satellite data (De Michele, 2018, see right) and local fault maps.
- The faults **dip** according to regional focal mechanisms and field studies of faulting near Palu (Bellier et al., 2005; Watkinson and Hall, 2016).
- Faults are loaded by a **remote stress regime** in agreement with regional **transtension**.

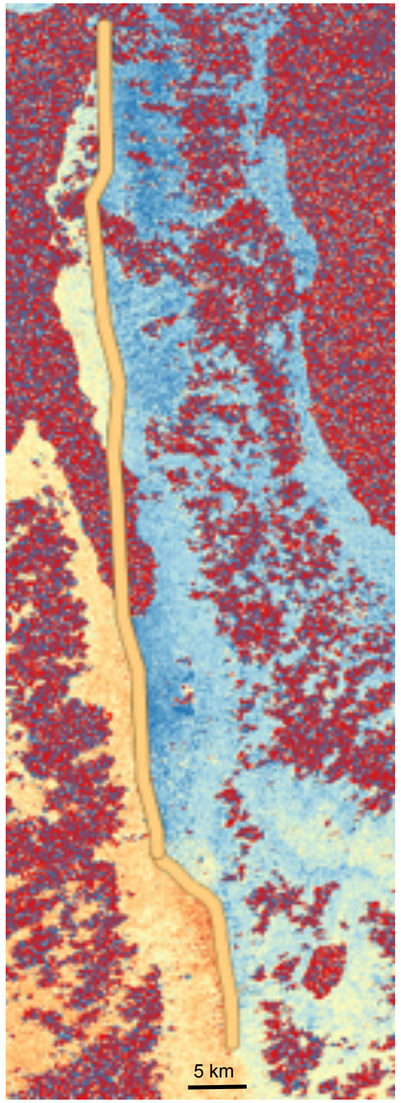

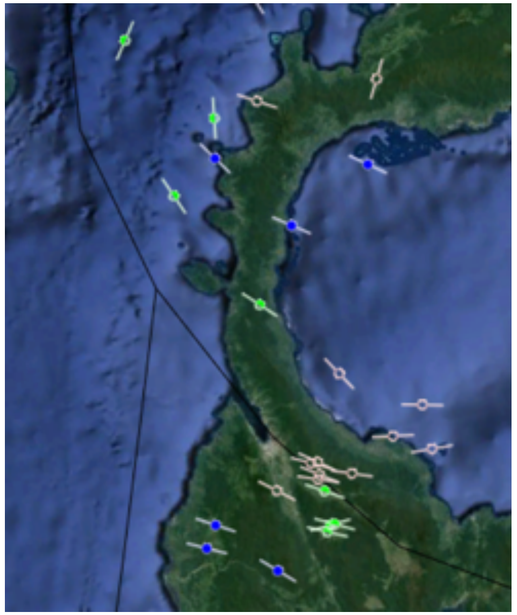

Above: Orientation of the maximum principal horizontal stress SH_{max} from the World Stress Map (Heidbach et al., 2018). The dataset shows regional variation, with SHmax constrained in the range of 105-135° from North. We use **SHmax=135°**, which allows for nucleation with less overstress than lower angles and generates ruptures with the expected slip orientations and magnitudes.

Left: fault trace considered for building the fault geometry, plotted over De Michele's data, which is processed from Sentinel-2 images (https://www.esa.int/spaceinimages/Images/2018/10/Indonesia_earthquake_displacement_data)

Physics-based Coupled Models of the 2018 Sulawesi Earthquake and Tsunami

Sustained supershear rupture

- **Widespread supershear rupture velocity (5 km/s) across geometric fault complexities is required to reproduce the teleseismic waveforms and the moment-rate function.**
- **Model results also match the moment magnitude, the overall duration and the inferred horizontal ground deformation.**

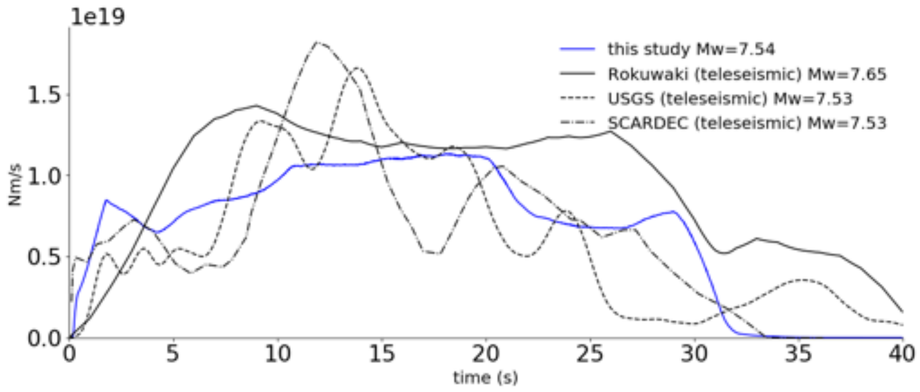

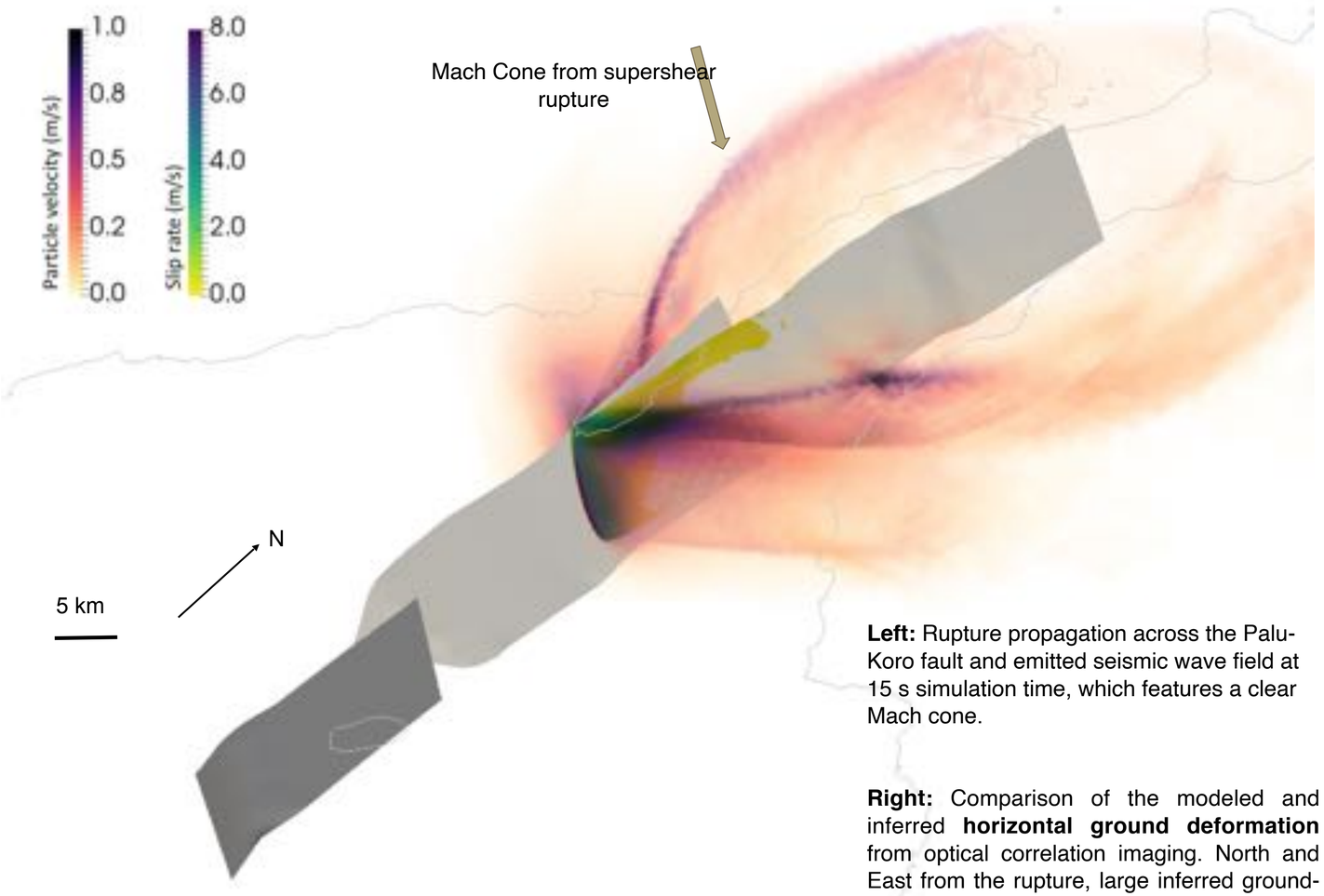

Left: Rupture propagation across the Palu-Koro fault and emitted seismic wave field at 15 s simulation time, which features a clear Mach cone.

Right: Comparison of the modeled and inferred **horizontal ground deformation** from optical correlation imaging. North and East from the rupture, large inferred ground-deformation are probably artifacts.

Below: Comparison of the modeled moment-rate function with inference from Rokuwaki et al. (2018), USGS and Scardec, all from teleseismic data.